Kamilla Arnesen

PAH Emissions from the Metallurgical Industry

Doktoravhandling

NTNU
Norwegian University of
Science and Technology

Kamilla Arnesen

PAH Emissions from the Metallurgical Industry

Thesis for the Degree of Philosophiae Doctor

Trondheim, September 2023

Norwegian University of Science and Technology
Faculty of Natural Sciences
Department of Materials Science and Engineering

NTNU
Norwegian University of
Science and Technology

Preface

This thesis is submitted in partial fulfilment of the requirements of the degree of Philosophiae Doctor (PhD) at the Norwegian University of Science and Technology (NTNU), Trondheim, Norway.

Abstract

Polycyclic aromatic hydrocarbons (PAHs) are a large group of organic molecules consisting of two or more fused aromatic rings. They can be created by incomplete combustion of organic materials and accumulate in nature. As a group, they are considered to be hazardous to human health as some PAH molecules are proven to be carcinogenic. Reduced PAH exposure is therefore recommended by the Norwegian government, among others. Through the use of carbon materials, the metallurgical industry emits PAH from different sources. Emissions in Norway have been reduced over the last decades, with the airborne persistent organic pollutant PAH emissions being 5.14 tonnes in 2020. Due to PAHs ability to accumulate in the environment further emission reduction is needed.

The main objective of this work has therefore been to contribute to the current knowledge on the influence of process conditions on PAH behaviour in metallurgical systems through laboratory and pilot-scale experiments. Special attention was given to investigating an extended range of PAH species, outside the standard list of PAH-16, and processes related to aluminium electrolysis and the production of metallurgical-grade silicon. During laboratory experiments, varying atmospheres and temperatures were used to investigate the variations of PAH emissions from green anode paste, a mixture used to produce pre-baked anodes for aluminium electrolysis. In the pilot-scale campaign for silicon production with flue gas recirculation (FGR), the influence of FGR on PAH formation and destruction was in focus. The last activity looked into the existence and formation of substituted PAHs from silicon and aluminium-related processes, where oxygenated and nitrated PAHs were of interest for the silicon process and sulfonated PAHs for the aluminium industry.

It was concluded from the laboratory study with green anode paste that the O_2 atmosphere showed the most influence on the emission levels, compared to argon and CO_2 atmospheres and emissions being at the highest level at temperatures close to 500 °C (with 750 °C being the maximum temperature tested). Four and five-ringed PAH dominated the emissions profile and even though the total emission level was reduced by the oxygen atmosphere, the level of four-ring PAHs was stable for all atmospheres as a result of varying molecular reactivity.

Through the silicon pilot-scale study, the PAH emissions were influenced by the changing process conditions caused by FGR. Both the level of FGR and oxygen correlated with the PAH emissions, causing the emission level to rise with increased FGR and decreased oxygen concentration. The measurements showed increased emissions of PAHs with lower molecular weight (bicyclic species), species of high thermal stability and the presence of substituted PAHs, where both oxy- and nitro-PAH species were found in greater amounts than their parent PAHs at elevated FGR levels. In addition, through combined characterisation and analytical methods related to sulfonated PAHs, the work concluded by finding the presence of polar polycyclic aromatic compounds, containing sulfate and sulfonated species, which previously have not been reported for PAH-related industry emissions.

Acknowledgements

During the work with this thesis, I have received help and support from a great number of people and some of you deserve a special mention.

First of all, I would like to express my sincere gratitude to my supervisor Gabriella Tranell. You have been a source of support, guidance and encouragement throughout the project. I would also like to show appreciation for my co-supervisors, Kristian Etienne Einarsrud and Thor Anders Aarhaug, who have shared their knowledge and insight. Thank you all for your valuable help and good discussions.

I would like to extend my gratitude towards my co-authors and collaborators. Thank you for your time and valuable contribution to this work. To Heiko Gaertner for sharing your experience and knowledge. To Vegar Andersen for our close collaboration and many discussions. To Katarina Jakovljevic, for your much-appreciated help and our time together in the lab.

I also appreciate the support of the SFI Metal Production Centre and partners, SINTEF, Hydro AS, Elkem AS and Eramet AS, for including me in discussions, giving valuable input to this project and welcoming me to visit.

Many thanks to my colleagues at the Department of Materials Science and Engineering for helping with technical issues and contributing to the social environment at work. To Cathrine, Marit, Sindre, Erlend, Alicia and Ece, to mention a few, for making this a more enjoyable journey.

And finally, I would like to thank my friends and family for all your support. I will be forever grateful. To my grandmother, you have meant the world to me. Thank you for all you have given me. And to my nephew, you are the best distraction an aunt could have. I very much enjoy getting to know you.

Contents

List of Tables

List of Figures

Nomenclature

Abbreviation	Description
^{13}C-NMR	Carbon-13 nuclear magnetic resonance
ATD	Analytical thermal desorption
CFD	Computational fluid dynamics
ECNI	Electron capture negative ion
EMEP	European monitoring and evaluation programme
FGR	Flue gas recirculation
FS	Fluorescence spectroscopy
FTIR	Fourier transformed infrared spectroscopy
GAP	Green anode paste
GC	Gas chromatograph
GC-MS	Gas chromatography mass spectrometry
HACA	Hydrogen abstraction and carbon addition
HAVA	Hydrogen abstraction vinyl acetylene addition
HMW	High molecular weight
HPLC	High performance liquid chromatography
HRMS	High resolution mass spectrometry
IARC	International agency for research on cancer
ICP-MS	Inductively coupled plasma mass spectrometry
LMW	Low molecular weight
LRMS	Low-resolution mass spectrometry
MAC	Methyl addition cyclisation
MG-Si	Metallurgical grade silicon
Nitro-PAH	Nitrated polycyclic aromatic hydrocarbons
NTS	Non-targeted screening
Oxy-PAH	Oxygenated polycyclic aromatic hydrocarbons
PAC	Polycyclic aromatic compounds
PAH	Polycyclic aromatic hydrocarbons
PASH	Polycyclic aromatic sulfur heterocycles

Table cont.	
PM	Particulate matter
POP	Persistent organic pollutant
PSR	Perfectly stirred reactor
qTOF	Quadruple time-of-flight
RSR	Resonantly stabilised radicals
RTO	Regenerative thermal oxidiser
SAF	Submerged arc furnace
TCD	Thermal conductivity detector
TD	Thermal desorption
TEF	Toxicity equivalence factors
UHPLC	Ultra high performance liquid chromatography
USEPA	United states environmental protection agency
UV	Ultra violet
VOC	Volatile organic compound
XAD-2	2-hydroxymethyl piperidine

Chemical Symbol	Description
Ar	Argon
C	Carbon
$CH_3^{\cdot}$	Methyl radical
CH_4	Methyl
$C_2H^{\cdot}$	Ethynyl radical
C_2H_2	Acetylene
$C_2H_3^{\cdot}$	Vinyl radical
C_4H_4	Vinylacetylene
C_6H_5	Phenyl
$C_6H_5^{\cdot}$	Phenyl radical
C_6H_6	Benzene
$C_{10}H_8$	Naphthalene
$C_{12}H_8$	Acenaphthylene
$C_{12}H_{10}$	Acenaphthene
$C_{14}H_{10}$	Anthracene/ Phenanthrene
$C_{16}H_{10}$	Fluoranthene/ Pyrene
$C_{18}H_{12}$	Benzo(a)anthracene/ Chrysene
$C_{20}H_{12}$	Benzo(a)pyrene

Table cont.	
CO	Carbon monoxide
CO_2	Carbon dioxide
H_2	Hydrogen
H_2O	Dihydrogen oxide
HSO_4	Hydrogen Sulfate
NaOH	Sodium hydroxide
N_2	Nitrogen
NO	Nitrogen monoxide
NO_2	Nitrogen dioxide
NO_2^+	Nitronium ion
$NO_3^{\cdot}$	Nitrate radical
NO_x	Nitrogen oxides
O_2	Oxygen
O_3	Ozone
$OH^{\cdot}$	Hydroxyl radical
Si	Silicon
SiO	Silicon monoxide
SiO_2	Silicon dioxide
SO_2	Sulfur dioxide
SO_3	Sulfur trioxide
SO_4^{2-}	Sulfate
SO_x	Sulfur oxides

Chapter 1

Introduction

1.1 Background

Polycyclic aromatic hydrocarbons (PAHs) are a group of organic molecules consisting of two or more fused aromatic rings. They occur naturally in petroleum and resin products and can be produced by incomplete combustion of organic matter. Natural sources of PAHs are forest fires and volcanic activity, and anthropogenic sources can be burning of biomass and oil, production of coke and the use of carbon in industrial processes. Some PAHs are classified as persistent organic pollutants (POPs), which are chemicals recognised as persistent, bio-accumulative, toxic, susceptible to long-range atmospheric transport, and can cause a risk to human health and the environment [1]. EUs Environmental Action Plan for 2020 state the need to decrease human PAH exposure as it is a global interest and concern to reduce PAH formation and distribution caused by human activity [2, 3].

The estimated global emission of the PAHs in 2007 was 504000 tonnes, where biomass fuels (firewood and crop residues consumed in the residential and commercial sectors) contribute to 60.5 % of the total emissions followed by petroleum consumption in the transportation sector (12.8 %) [4]. The primary sources can be separated into categories such as residential heating, industrial processes, incineration, open burning, power generation, and mobile sources. Non-combustion sources of PAH can be the production and use of coal-tar and creosote, which both are products made from distilling carbonaceous material formed by pyrolysis, and release of petroleum products. Even though burning of organic material is the main source of PAH emissions, any incomplete combustion process containing carbon and hydrogen can be a source of PAH [5]. PAHs are prone to long-range transport because of their physicochemical properties, and storage in environmental sinks

can therefore be a source of secondary PAH emissions. PAHs with three or more rings tend to accumulate in organic matter by dry or wet deposition to vegetation, soil, and aquatic sediments. Here the PAH may remain, be decomposed, or act as a secondary source of emission. Lower molecular weight PAHs have increased mobility as they are more volatile and can easier be recycled back into the environment [5].

In Norway, the POP PAH (Benzo(a)pyrene, Benzo(b)fluoranthene, Benzo(k) fluoranthene, Indeno(1,2,3-cd)pyrene) emissions are reported to the European Monitoring and Evaluation Programme (EMEP), and the USEPA PAH-16 are reported to the Norwegian Environmental Agency by the industry. Both POP and PAH-16 are reported as the total emission to air and water. The reported POP PAH emissions in 2005 was 17.5 tonnes, where process emissions from primary aluminium production, residential wood combustion and passenger cars were the main contributors [6]. In 2020, the airborne emission was reduced to 5.14 tonnes, mainly due to phasing out the use of Söderberg anodes in aluminium production [7]. Figure 1.1 shows the total POP emissions in Norway between 1990 and 2020, as well as distribution between different sectors, where industry emissions is the major contributor [6].
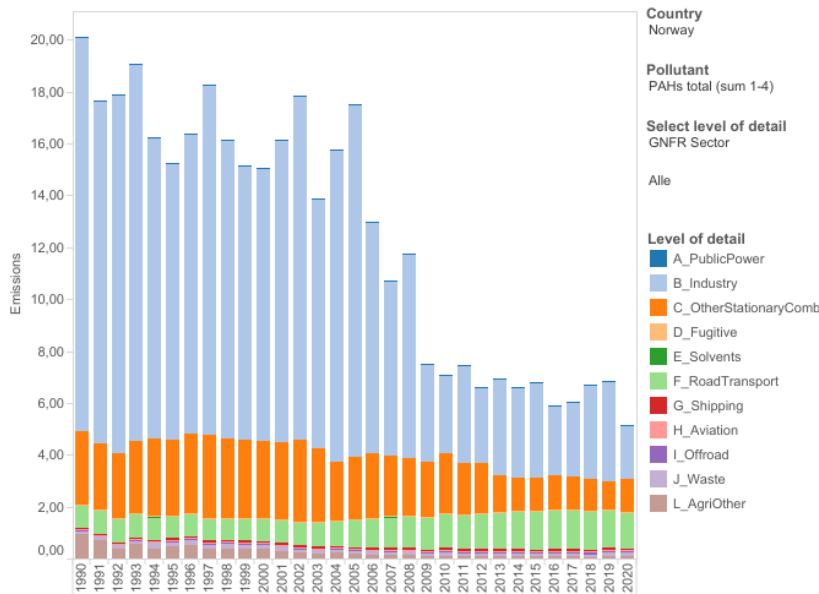
Figure 1.1: Norwegian emissions of POP PAHs from 1990 to 2020 reported to the European Monitoring and Evaluation Programme (EMEP). Emissions are reported in tonnes as the sum of Benzo(a)pyrene, Benzo(b)fluoranthene, Benzo(k)fluoranthene, Indeno(1,2,3-cd)pyrene emissions to air and water. Source: EMEP [6]

Table 1.1: PAH-16 Priority pollutants defined by the US Environmental Protection Agency.

Name	Rings	MW [g/mol]
Naphthalene	2	128.17
Acenaphthylene	3	152.19
Acenaphthene	3	154.21
Fluorene	3	166.22
Phenanthrene	3	178.23
Anthracene	3	178.23
Fluoranthene	4	202.26
Pyrene	4	202.26
Benzo[a]anthracene	4	228.29
Chrysene	4	228.29
Benzo[b]fluoranthene	5	253.32
Benzo[k]fluoranthene	5	253.32
Benzo[a]pyrene	5	253.32
Dibenzo[a,h]anthracene	6	287.35
Benzo[g,h,i]perylene	6	276.34
Indeno[1,2,3-cd]pyrene	6	276.34

In the 1970s the United States Environmental Protection Agency (USEPA) selected 16 PAHs as priority pollutants that still act as the global standard for monitoring and reporting. The priority was based on available knowledge at the time, toxicity, analysis method, and environmental occurrence. The priority PAHs are typical products of pyrosynthesis, where high-molecular weight PAHs dominate the emission profile [8]. The EPA-16 PAHs is a list with components consisting solely of aromatic rings (Table 1.1). By continued monitoring of the PAH in this list, keeping track of changes and trends over time has become more convenient. Some argue that the EPA-16 list is not optimal when measuring the exposure of toxic emissions, as some compounds have a short life span and decompose quickly when exposed to sunlight while other more stable compounds are not included, such as alkylated or substituted PAH [9].

Reported emissions of USEPA PAH-16 from aluminium plants in Norway (2021) ranges from 0.11 kg to 18.6 tonnes per year, depending on the plant technology and activity [10]. Major emission points are the anode baking furnaces producing prebaked anodes and aluminium electrolysis plants with Söderberg technology. The anodes are made from petroleum coke and coal tar pitch, where the latter is a well known source of PAHs [7].

The origin of PAH emissions from Norwegian silicon and ferro-silicon industry are the carbon raw materials, electrodes, and carbon paste. The source locations are the submerged arc-furnace and the metal tapping process. Reported emissions of USEPA PAH-16 from Norwegian silicon alloy plants in 2021 are reported to be between 19 and 121 kg per site per year [10]. The situation is similar for the production of manganese ferro-alloys, as the carbon raw materials used as reductants and electrode are the main source of emissions. Unlike in production of silicon, a manganese submerged arc-furnace is closed, leading to reduced available oxygen, causing incomplete combustion and higher PAH levels in the off gas [11]. Reported PAH emissions from Manganese ferro-alloy production plants in Norway can be up to 809 kg per year (2021) [10]. Common for all the reported emissions is that the majority of the emissions is to air.

1.2   Motivation and Thesis Objective

Through the use of carbon materials as reductants in the metal-producing industries PAHs are formed which need to be reported to environmental authorities and emissions must be limited. Currently, the methods for measuring PAHs produce varying results and together with the limited scope of the analysis and available standards, the mechanisms for PAH formation and decomposition are poorly understood. The variations between raw materials used and the process conditions for combustion and pyrolysis influence the reaction mechanisms and stability of the PAH emissions making monitoring for further understanding a major challenge. This work initially set out to investigate the correlation between carbon raw material types and properties and process parameters such as temperature and gas composition in a controlled laboratory setting to investigate its effect on PAH formation and destruction and connect them to industrial phenomena.

With the opportunity to participate in a pilot Silicon production campaign with flue gas recirculation and by having access to industrial raw materials relevant for aluminium anode production and samples of residues from anode production gas cleaning, the work expanded to increase focus on the effect of industrial conditions and PAHs. To expand the scientific impact, the decision was made to include a greater number of polycyclic aromatic hydrocarbons and to investigate substitution mechanisms relevant for the different metal production processes, sulfonation for the aluminium industry and nitration and oxygenation for the silicon process. This work aims to aid in achieving greater emission control and reduction by expanding the current knowledge of the influence of process conditions and treatment on PAH behaviour in metallurgical systems through laboratory and pilot-scale experiments. Figure 1.2 illustrate the project structure and activities with the objectives and scientific outcomes.
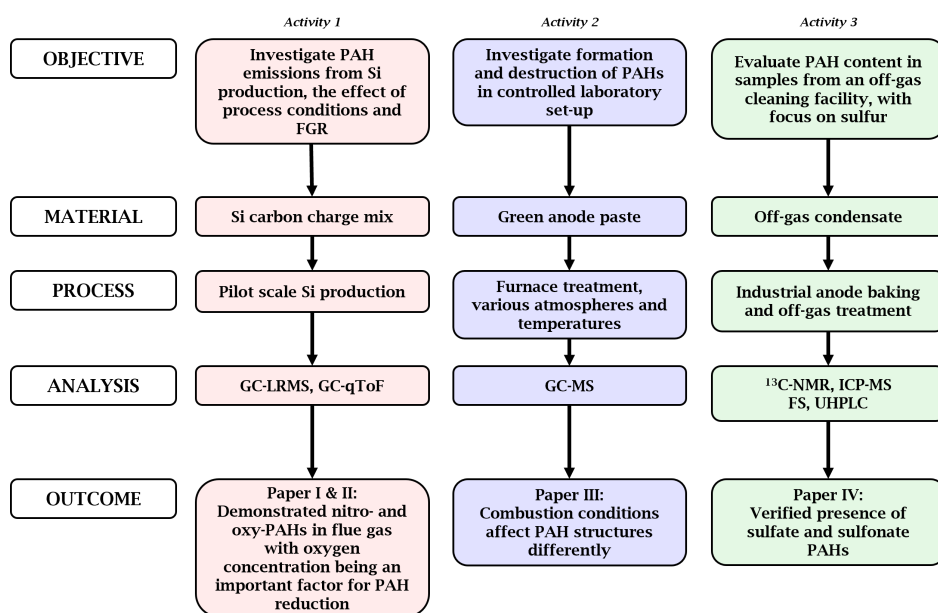
Figure 1.2: Outline of the thesis activities.

1.3   Thesis Outline

This thesis gives a literature survey in Chapter 2 presenting general information about PAH, mechanisms for formation, substitution and destruction, as well as the metal producing processes of aluminium and silicon with relevant information on off-gas cleaning, PAH sampling and analysis. Further, Chapter 3 to 5 presents the work of papers I - IV with summaries and extended discussions. Papers I and II will cover the findings from the work on flue gas recirculation for the pilot scale silicon alloy production and how the varying process conditions affected the evolution of PAHs, nitro- and oxy-PAHs. Paper III presents the work performed in a laboratory furnace where PAH emissions from materials used in the production of anodes for aluminium electrolysis were tested using varying temperatures and atmospheres. Lastly, paper IV presents the characterisation work performed on samples collected from an anode baking off-gas treatment facility where sulfur containing aromatic species originating from the raw materials are in focus.

Chapter 6 lists the main conclusions from the project work, followed by Chapter 7 which proposes possible future work to understand and mitigate PAH emissions from the metallurgical industry.

1.4   List of Publications

1.4.1   Primary Publications

This thesis was based on the work which resulted in four articles. Paper IV was a conference contribution, Paper I and III were published in scientific journals, and paper II is, at the date of writing this, submitted to a scientific journal. Copies of the papers can be found in the Appendix.

Paper I

K. Arnesen, K.J. Vachaparambil, V. Andersen, B. Panjwani, K. Jakovljevic, E.K. Enge, H. Gaertner, T.A. Aarhaug, K.E. Einarsrud, G. Tranell, **Analysis of Polycyclic Aromatic Hydrocarbon Emissions from a Pilot Scale Silicon Process with Flue Gas Recirculation**, Industrial & Engineering Chemistry Research, 2023, Doi: 10.1021/acs.iecr.2c04578

Statement of contribution:

Arnesen	Conducted experimental planning and work, performed data analysis, designed figures, formulation of manuscript. Submission and review of the manuscript.
Vachaparambil	Conducted modelling planning and work, performed data analysis, designed figures, formulation of manuscript and review.
Andersen	Conducted experimental planning for the Si pilot, data analysis, discussed results and gave scientific feedback.
Panjwani	Participated in modelling planning and work. Gave scientific feedback.
Jakovljevic	Conducted experimental planning and work and participated in data analysis and discussion.
Enge	Participated in GC/LRMS analysis of all samples with identification and quantification of PAH components and formulation of the analysis method.
Gaertner	Conducted experimental work, performed gas analysis by micro-GC and LaserGas instruments and gave scientific input.
Aarhaug	Co-supervisor of the project. Contributed to the experimental planning, discussed results, and gave scientific feedback during writing.
Einarsrud	Co-supervisor of the project. Contributed to the experimental planning, discussed results, and gave scientific feedback during writing.
Tranell	Supervisor of the project. Contributed to the experimental planning, discussed results, and gave scientific feedback during writing.

Paper II

[Submitted]K. Arnesen, V. Andersen, K. Jakovljevic, E.K. Enge, H. Gaertner, T.A. Aarhaug, K.E. Einarsrud, G. Tranell, **Analysis of Nitro- and Oxy-PAH Emissions from a Pilot Scale Silicon Process with Flue Gas Recirculation**, Environmental Science: Advances

Statement of contribution:

Arnesen	Conducted experimental planning and work, performed data analysis, designed figures, formulation of manuscript. Submission and review of the manuscript
Andersen	Conducted experimental planning for the Si pilot, data analysis, discussed results and gave scientific feedback.
Jakovljevic	Conducted experimental planning and work and participated in data analysis and discussion.
Enge	Participated in GC-qToF analysis of all samples with identification and quantification of PAH components and formulation of the analysis method.
Gaertner	Conducted experimental work, performed gas analysis and gave scientific input.
Aarhaug	Co-supervisor of the project. Contributed to the experimental planning, discussed results, and gave scientific feedback during writing.
Einarsrud	Co-supervisor of the project. Contributed to the experimental planning, discussed results, and gave scientific feedback during writing.
Tranell	Supervisor of the project. Contributed to the experimental planning, discussed results, and gave scientific feedback during writing.

Paper III

K. Arnesen, T.A. Aarhaug, K.E. Einarsrud, G. Tranell, **Influence of Atmosphere and Temperature on Polycyclic Aromatic Hydrocarbon Emissions from Green Anode Paste Baking**, ACS Omega, 2023, Doi: 10.1021/acsomega.3c01411

Statement of contribution:

Arnesen	Conducted experimental planning and work, performed data analysis, designed figures, formulation of manuscript. Submission and review of the manuscript.
Aarhaug	Co-supervisor of the project. Contributed to the experimental planning, discussed results, and gave scientific feedback during writing.
Einarsrud	Co-supervisor of the project. Contributed to the experimental planning, discussed results, and gave scientific feedback during writing.
Tranell	Supervisor of the project. Contributed to the experimental planning, discussed results, and gave scientific feedback during writing.

Paper IV

K. Arnesen, A. Albinet, C. Chatellier, N. Huyng, T.A. Aarhaug, K.E. Einarsrud, G. Tranell, **Characterization of Industrial Hydrocarbon Samples from Anode Baking Furnace Off-Gas Treatment Facility**, Light Metals 2023, p.680-687, Doi: 10.1007/978-3-031-22532-1_91

Statement of contribution:

Arnesen	Conducted experimental planning and work, performed data analysis, designed figures, formulation of manuscript. Submission and review of the manuscript.
Albinet	Participated in UHPLC and HRMS analysis of all samples with identification of substituted and native PAH components, formulation of PAH analysis method, contributed to the manuscript and gave scientific feedback.
Chatellier	Participated in UHPLC and HRMS analysis of all samples with identification of substituted and native PAH components, formulation of the analysis method and designed figures.
Huynh	Participated in UHPLC and HRMS analysis of all samples with identification of substituted and native PAH components, formulation of the analysis method and designed figures.
Aarhaug	Co-supervisor of the project. Contributed to the experimental planning, discussed results, and gave scientific feedback during writing.
Einarsrud	Co-supervisor of the project. Contributed to the experimental planning, discussed results, and gave scientific feedback during writing.
Tranell	Supervisor of the project. Contributed to the experimental planning, discussed results, and gave scientific feedback during writing.

1.4.2   Other Publications

K. Jakovljevic, T.A. Aarhaug, K. Arnesen, H. Gaertner, I. Kero, G.M. Tranell, **Influence of temperature and atmosphere on PAH emissions from carbonaceous materials used in industrial processes: Method development**, To be published

Chapter 2

Literature Survey

2.1 Structure and Properties of PAHs

Polycyclic aromatic hydrocarbons (PAHs) are one of the most structurally diverse classes of organic compounds. The term "PAH" refers to a compound containing two or more fused aromatic rings made only of carbon and hydrogen [12]. The different structural configurations of polycyclic aromatic hydrocarbons lead to different physicochemical properties of these compounds. Important characteristics of these compounds are high melting and boiling points, low vapour pressure, and relatively poor solubility in water. The last two characteristics represent the main physicochemical factors that control the distribution between soluble and particulate components of the atmosphere, hydrosphere, and biosphere. Vapour pressures range from highly volatile (naphthalene) to relatively non-volatile (dibenzo[a,h]anthracene). Water solubility decreases for each additional ring system, i.e., water solubility decreases with increasing molecular weight [13]. Low molecular weight PAHs, with 2-4 rings, exist in the vapour phase in the atmosphere, while higher molecular weight PAHs, with more than four rings, can exist both in the vapour and particle phase [14, 15]. Examples of PAHs of low and high molecular weight, Naphthalene and Benzo[a]Pyrene, are shown in Figure 2.1 as line-angle structures, where the carbon atoms are located at the corners of the structure, and bonds to hydrogen are not present.

2.1.1 Organic Structure

Aromatic molecules, such as benzene, are planar, cyclic structures with delocalised π-electrons above and below the plane of the carbon ring. The delocalised electrons ensure identical C-C bondlengths and the delocalisation energy provides
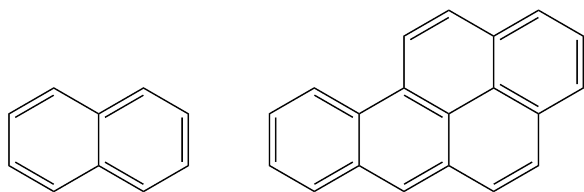
Figure 2.1: PAH line-angle structures. Left: Naphthalene Right: Benz[a]Pyrene.

stability. This is often referred to as aromaticity. The compounds were originally called aromatic because of the fragrance they emit and today, the term identifies a specific chemical structure. The aromatic compounds have structural traits in common, such as a continuous cyclic cloud of π-electrons, an odd number of π-electron pairs and sp^2 hybridised carbon atoms. The criteria is the same for mono- and polycyclic hydrocarbons, meaning multiring systems such as naphthalene (two benzene rings) and chrysene (four benzene rings) are also aromatic [16].

PAH molecules are a stable form of hydrocarbons and are naturally present in the atmosphere. They are often formed by hydrocarbon combustion in low oxygen partial pressure. The combustion of coal is a source of PAH due to the low hydrogen - carbon ratio. The low vapour pressure contributes to PAH absorption on particular matter [17].

The different structures of PAHs, linear, angular and cluster, influence the reactivity and stability of the molecules [18]. Angular structures are more stable than linear as studies show is due to a greater level of π-interactions, based on Clar's model, and interactions between hydrogen atoms in the bay region (e.g. u-shape of an aromatic structure where carbon and hydrogen atoms are closest to each other) resulting in increased armoaticity. An example is the three ring isomers, anthracene and phenanthrene (Figure 2.2), where the structural differences result in phenanthrene having higher thermodynamic stability [19].
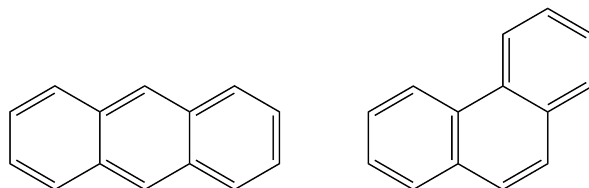
Figure 2.2: PAH line-angle structures. Left: Anthracene Right: Phenanthrene.

The bay region is found to increase the molecules mutagenic and carcinogenic activity [20]. Another influencing factor on PAH stability is the number of rings. Larger PAH molecules have a greater resistance to degradation at ambient conditions, due to increased aromaticity [21].

2.1.2 Health Risk

PAHs are the largest group of known chemical compounds that can cause cancer. Although some PAHs are not carcinogenic, they may act as co-carcinogens and can have low acute toxicity to humans. In addition to carcinogenicity, which poses perhaps the most significant health risk, some compounds also show genotoxic, immunotoxic, cardiovascular, and neurological effects. Because of their toxicological relevance, biological monitoring of exposure to PAHs is of primary interest to human health. Exposure to individual PAHs is rare because these compounds almost always exist in complex mixtures. Since the composition of these mixtures is not always constant, assessing the health risk of individual compounds can be difficult. However, individual compounds, for which a link to the incidence of cancer is known, can be used as markers to study the effects of the whole mixture [22, 23].

Because of their effects on human health, persistence in the environment, and ability to convert to more reactive species, the United States Environmental Protection Agency (US EPA) in 1976 classified 16 PAHs as priority pollutants. These 16 priority compounds were chosen among the numerous PAHs because of the high possibility of human exposure as they are typical products from pyrosynthesis, where high-molecular weight PAHs dominate the emission profile. Seven of the 16 PAHs are listed as potential carcinogens for humans and include Benzo[a]anthracene, Benzo[a]pyrene, Benzo[b]fluoranthene, Benzo[k]fluoranthene, Dibenzo[a,h]anthracene, Chrysene, and Indeno[1,2,3-cd]pyrene, with the exception of Benzo[a]pyrene which is listed as a known human carcinogen [22].

Benzo[a]pyrene is the most studied PAH where metabolites are know to cause cancer. Metabolites form adducts with DNA, which can lead to damage in the DNA strands, causing mutations [24].

2.2 PAH Formation

PAHs and derivatives are usually formed through thermal processes (e.g. pyrolysis) and incomplete combustion reactions of hydrocarbons. These reactions can occur from natural processes such as forest fires and volcanic activity. Usually anthrospheric processes are the root of the formation of PAH with the greatest environmental impact, e.g. through a process where hydrocarbons of low molecular mass, such as methane, act as precursors for PAH at temperatures greater than
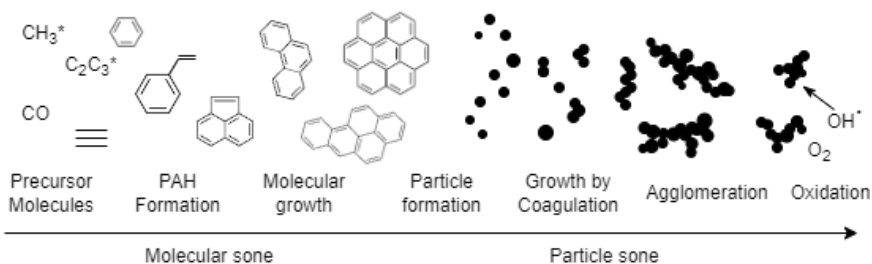
Figure 2.3: Sketch of PAH formation from precursor molecules and molecular growth to soot and destruction by oxidation. Inspired by Obaidullah et al.[27].

500 °C. This is also called pyrosynthesis. Free radicals can break C-C and C-H bonds and by dehydrogenation, formation and addition of aryl ring structures (e.g. C_6H_5), result in aromatic ring structures and molecular growth. High molecular weight alkanes present in fuels and plant material can form PAHs by pyrolysis, where the hydrocarbon chains are broken to form smaller, unstable molecules or radicals, before undergoing pyrosynthesis [25].

PAH evolution can be summarised into formation of the first aromatic ring (C_6H_6) during combustion of aliphatic species, growth into larger PAH and eventually soot formation, and oxidation of these species into smaller aromatic rings and carbon dioxide, which is illustrated in Figure 2.3. The main formation mechanisms are based on different reactants, where acetylene additions (e.g. HACA), vinyl acetylene additions (HAVA), and radical reactions with C1 - C6 are usually in focus. [26]

2.2.1 Mechanisms

Acetylene Addition - HACA

The hydrogen abstraction and acetylene/ carbon addition (HACA) PAH formation mechanism originates from work by Frenklach et al.[28] in 1985, where kinetic modelling of soot formation was performed. Hydrocarbon pyrolysis by the way of acetylene (C_2H_2) addition was investigated, and the fusing of aromatic rings and PAHs was found to have an important role in the formation of soot at elevated temperatures (> 600 K). The work describes the formation of the initial aromatic ring through a two-step mechanism, combining acetylene radicals and hydrogen abstraction resulting in cyclisation and further growth. The mechanism is illustrated in Figure 2.4 with an example of naphthalene formation from benzene. The mechanism is described to have a high reaction affinity towards PAH growth caused by the reactive nature of the hydrogen radical and low energy barriers of the addition
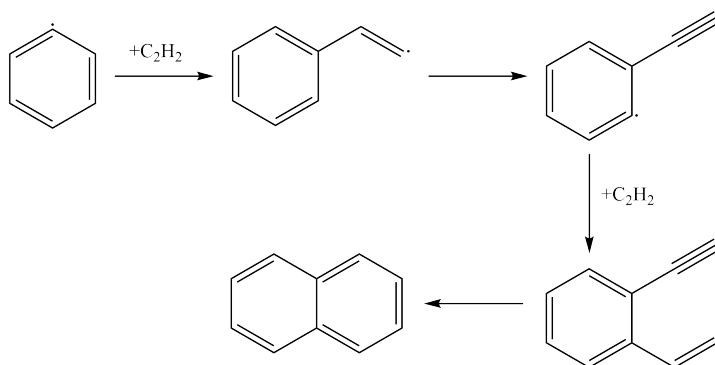
Figure 2.4: Illustration of Naphthalene formation from Benzene through the Acetylene addition mechanism (HACA).

reactions leading to the low reversibility. The HACA mechanism is still under development, especially for larger PAH molecules, and is summarised in a review by Reizer et al. [26].

Vinyl acetylene Addition - HAVA

Vinyl acetylene (C_4H_4) is an abundant hydrocarbon species in flame combustion and has therefore been investigated as an intermediate in tar formation, called the vinyl acetylene addition (HAVA) mechanism. The mechanism describes the reaction between vinyl acetylene and a PAH radical to form a new PAH molecule of increased molecular weight in two steps [26]. PAH formation and growth through the HAVA mechanism has been investigated in both high temperature pyrolytic conditions (1600 K) [29, 30].

Radical Additions

The last main mechanism for PAH formation and growth is the addition of hydrocarbon radicals. Polymerisation of methane was investigated by Weissman and Benson in 1984[31], and has later developed into the methyl addition cyclisation mechanism (MAC), where PAH molecules are created or grow by methyl radicals ($CH_3\cdot$) forming a chain, or is added to an existing aromatic structure, and the chain eventually stabilises by forming a five or six carbon ring [32]. Similar mechanisms have been investigated for ethynyl ($C_2H\cdot$), vinyl ($C_2H_3\cdot$) and phenyl ($C_6H_5\cdot$). Resonantly stabilised radicals (RSR) are temporary stable molecules found to be a cause of PAH radical recombination in combustion processes [26].
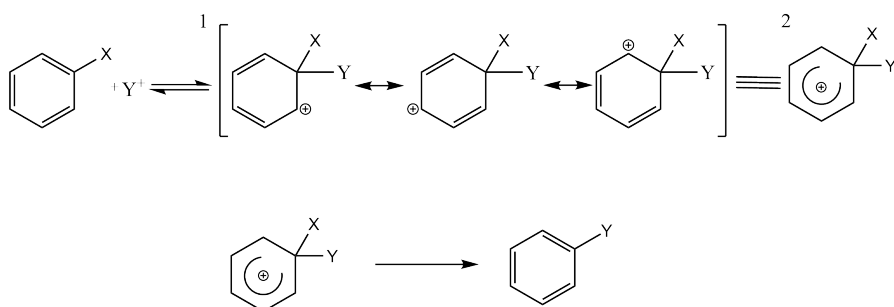
Figure 2.5: Arenium ion mechanism of electrophilic aromatic substitution. © Tetrahedron, Katritzky et al.[33]. Reproduced with permission from Elsevier.

2.2.2 PAH Substitution

PAHs and other aromatic compounds are nucleophiles due to the cloud of π electrons. PAHs will therefore be reactive with electrophile compounds, such as sulfur and nitrogen oxides. An electrophilic aromatic substitution reaction (Figure 2.5), create carbocation intermediates (1) (often described as (2)) and the reaction pathway will be compelled to preserve the aromaticity, as they are stable with a low free energy. An electrophilic aromatic substitution reaction such as nitration, sulfonation or Friedel-Crafts acylation will mostly occur by the arenium ion mechanism and produce intermediate arenium ions and radical carbocation. Creation of the arenium ion is usually the rate-determining step and will initiate the reaction pathway [16].

Examples of electrophiles found in industrial processes are the nitronium ion (NO_2^+) and sulfur trioxide (SO_3). The nitronium ion can be created through protonation of nitric acid by sulfuric acid, which will activate the nitration reaction and create nitro-PAHs. Sulfonation of PAHs create aromatic sulfonic acids and can be performed when SO_3 is created from fuming sulfuric acid (oleum) [34]. PAH can also be oxygenated, and an oxy-PAH contain at least one carbonylic oxygen attached to an aromatic ring [35]. These electrophilic aromatic substitution reactions can occur both in gas and solid phase and produce various substituted PAHs [33, 36, 37].

The substitution reaction results in property changes compared to the original PAH, meaning the product substance can have different health effects. The new structure will most likely have an increased polarity, resulting in the substituted PAHs having an increased affinity towards water. An example is naphthalene sulfonates, which are highly water-soluble as opposed to the origin PAH, naphthalene, and are used as a flow tracers in geoethermal reservoirs [38].
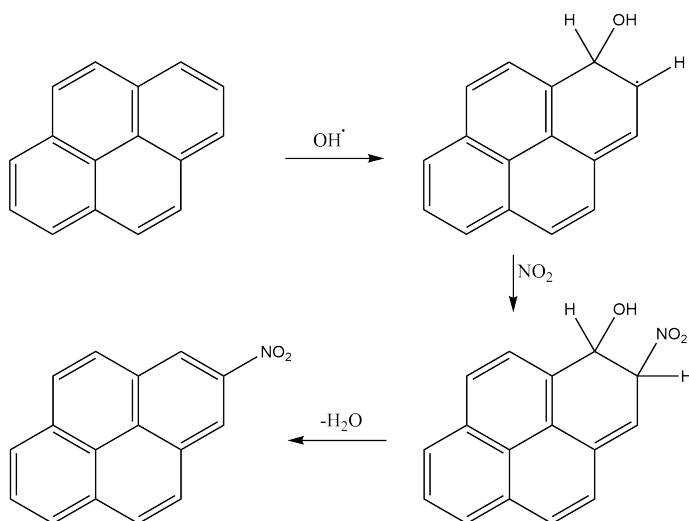
Figure 2.6: An example of a nitration mechanism of pyrene with OH· initiating the substitution reaction. © Arey et al.[40]. Reproduced with permission from Elsevier.

In the work by Hrdina et al.[39], parent PAH transformation through atmospheric oxidation is described, recognising key atmospheric oxidants of PAHs to include ozone (O_3), hydroxyl radical (OH·), nitrogen dioxide (NO_2), and nitrate radical (NO_3·). An example of a possible mechanism for nitration of pyrene is presented in Figure 2.6.

The concentration of substituted PAHs is often low compared to native PAHs, but studies indicate these PAH species have a potent role as environmental toxins. Toxicity studies indicate that substituted PAH species potentially have mutagenic and carcinogenic properties and the International Agency for Research on Cancer (IARC) classify 1-nitropyrene as "probably carcinogenic to humans", with PAH derivatives recognised as mutagens [22].

Substituted PAHs are also recognised as being bio-accumulative which is described in the study by Gimeno et al.[41], where accumulation of polycyclic aromatic sulfur heterocycles (PASHs) in waste water and sediment is found as a result of human activity. Witter and Nguyen [42], analysed oxygen, nitrogen and sulfur-containing PAHs in sediments found in urban streams and found, compared to rural areas, human activity contributing to accumulated concentration of substituted PAHs. In addition, the substituted PAHs were traced back to sources of similar petrogenic and pyrogenic PAH sources and suggest including ONS-PAH measurements to traditional PAH analysis can contribute to greater understanding of pollutant source identification.

Sulfonated, nitrated and oxygenated PAHs have all been found as part of emissions from various high temperature pyrolytic processes. In research on emissions from diesel engines, oxy- and nitro-PAH compounds are detected, where NO_x is known to be a considerable part of the exhaust [43]. Heeb et al.[44], investigated how diesel engine filters influenced PAH and nitro-PAH profiles in diesel exhaust and found the filter to promote formation of some nitro-PAH, and enhanced the degradation of others depending on the operating conditions of the engine. Hayakawa [45], investigated the formation of nitro-PAH compared to their parent PAH with increasing combustion temperatures, representing diesel-engines, coal and wood burning stoves. The nitro-PAH/PAH ratio was observed to increase with temperature for compounds such as 1-nitropyrene, 6-nitrochrysene and 7-nitrobenz[a]anthracene. Drotikova et al.[46], measured PAH in ambient air in Longyearbyen, Svalbard, and found coal-fired power plants to be one of the main sources of PAHs, with 9-fluorenone and 9,10-anthraquinone to be the dominating oxy-PAH speices.

In a study by Adánez-Rubio et al.[47], oxy-PAH and thiophene (sulfur heterocycles) emission was monitored from pyrolysis of ethylene and SO_2 with varying sulfur concentrations. Both formation of oxy-PAHs and thiophenes increased with pyrolysis temperature (max. at 1375 K and 1275 K) and with the concentration of SO_2. The addition of sulfur to combustion processes is described by Streibel et al.[48], where sulfur, in various forms, alter the oxidation chemistry by providing alternative interactions and routes for radicals and by inhibiting catalytic activity and resulting in decreasing native PAH emissions. The authors also question the interactions between sulfur oxides and the combustion intermediates and radicals, suggesting further studies are needed.

2.3 PAH Degradation

PAHs in the environment may undergo photo-oxidation, chemical oxidation, adsorption on soil particles and leaching or transformation by microorganisms. They are difficult to degrade in natural environments and their persistence increases with molecular weight. With bio-accumulation, the hazardous risk of PAH exposure can increase when residing in contaminated areas [49].

2.3.1 Chemical Degradation

Oxidative Degradation

PAH decompose to water and carbon dioxide at complete combustion. At low temperature and/or when not enough oxygen is present, such as with rich fuel mixtures, competing reactions occur between PAH formation and degradation [50]. Thomas and Wornat [51] described the importance of oxygen and temperature in the formation and destruction of PAH in a high temperature reactor using catechol as a model fuel. By investigating the effect of varying oxygen levels and temperatures up to 1000 °C, oxygen was recognised to have an important role both in creating free radicals that lead to increased PAH formation at T < 850 °C, and also increased PAH destruction at T > 850 °C at high levels of oxygen. Degradation is dependent on temperature, and Gai et al.[52], found the decomposition temperatures of naphthalene and anthracene to range from 700 °C to 900 °C during pyrolysis in argon atmosphere, with naphthalene being easier to decompose. The main decomposition products was found to be ethylene and propane with smaller amounts of methane and hydrogen. Degradation mechanisms of large PAH through thermal treatment and chemical oxidation can produce PAH of smaller size as intermediates if enough energy is not supplied [21]. Sun [53] observed temperature as being a great influence on radical and PAH formation by the way of intermolecular reorganisation to increase molecular stability and aromaticity, at conditions where complete oxidation is not achieved. Liu et al.[54] investigated PAH emissions from coal combustion in a fluidized bed combustor. In this study, incomplete combustion of PAHs was found at temperatures up to 900 °C, being strongly influenced by the level of excess air in the reactor.

Catalytic Degradation

Catalytic systems are known to promote the decomposition of PAH and are investigated for several purposes such as reduced emissions from vehicles, remediating contaminated soil and water and conversion of hydrocarbon feedstock. Catalysts such as transition metals, metal oxides and zeolites are used depending on the process and conditions [55]. Using a copper and vanadium-based catalyst for NO_x and VOC, including PAH, emission reduction on diesel engine exhaust is commonly done by selective catalytic oxidation and reduction. The catalyst will promote hydrogen abstraction by weakening the C-H bonds leading to oxidation with the sufficient air/fuel ratio and temperature [56]. Through catalytic cracking, an acidic zeolite catalyst was found to show activity for reactions such as hydrogen transfer and scission of C-C and C-H bonds [57]. The work of Pujro et al. [58], investigated the use of a zeolite catalyst for decomposition of aromatic hydrocarbons and found it to promote ring-opening reactions at 450 °C and the decomposition was
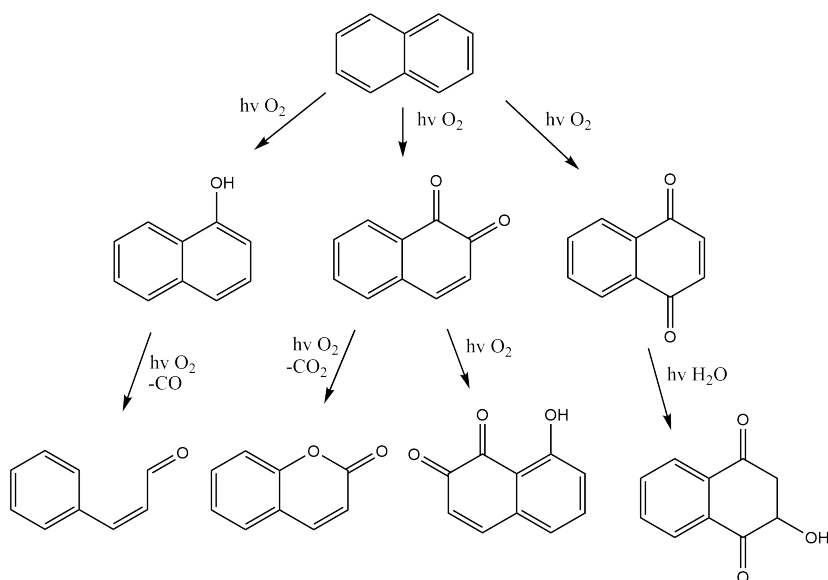
Figure 2.7: Various photolysis degradation routes for naphthalene with oxygen present. © McConkey et al. [61]. Reproduced with permission from Springer Nature.

shown to increase with an increasing number of carbon molecules in the aromatic structure. Purification of water and soil of PAH and other organic compounds are often done by generation of hydroxyl radicals. This can occur through the Fenton reaction where the radicals are produced by decomposition of hydrogen peroxide over catalytic ferrous ions [59].

Photolysis Degradation

Photolysis degradation of PAHs can occur when photons are absorbed by the PAH structure, and the light causes electrons to become exited and the structure becomes unstable. The mechanism is more effective for species in the vapour phase (as solid particles can act as a shield from the photons), where at atmospheric conditions, molecules such as ozone and hydroxyl radicals can continue the degradation process. The general properties of the PAH molecule influence the efficacy of the degradation reaction, as small linear molecules are more easily affected then larger angular molecules with greater stability. Suggested photolysis degradation routes for naphthalene are shown in Figure 2.7 [1, 60].

2.3.2 Biodegradation

Microorganisms can be used to reduce the concentrations of hazardous PAHs by conversion and bio-transformation to less hazardous/non-hazardous molecules.

The use of algae, bacteria and fungi have been investigated both individually and in combination. The rate of degradation is dependent of several factors. These include the PAH chemical structure, available oxygen, microbial population, and nutrients and factors influencing the microorganism condition, such as pH and temperature [62].

2.4   Metallurgical Industry

2.4.1   Aluminium Production

Primary aluminium is produced by electrolysis of alumina with carbon anodes in the Hall-Héroult process. Most modern production lines use prebaked carbon anodes which are a mixture of petroleum coke, anode butts and coal tar pitch [63]. Prebaked anodes are produced in an open or closed top baking furnace, where green anodes are stacked in pits, covered with packing coke and, heated to 1200 °C through a cycle up to 20 days (Figure 2.8) [64].
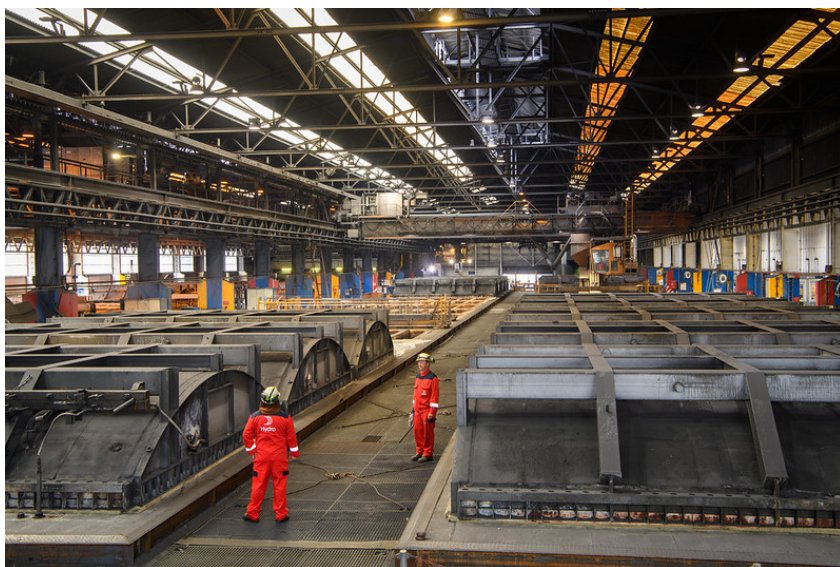
Figure 2.8: Anode baking furnace at Årdal Carbon, Årdalstangen in Norway. Photo: Halvor Molland/Hydro

Coal tar pitch is a well-known source of PAHs. The pitch serves a purpose as binder for the coke particles, and as an energy source for the baking through combustion of volatile organic compounds (VOCs) [65]. Coal tar pitch has a composition of about 97 % aromatic and hetero-aromatic compounds, with great variety of structures from 128 to > 2500 Daltons. The presence of derivatives such as phen-

ols, ketones, amides, and amines are also reported, contributing to the complexity of the mixture. Petroleum coke originates from a crude oil refinery feedstock which will define the coke quality and structural properties. A typical anode grade calcined petroleum coke has a "sponge" structure, with up to 60 % aromatic structures, containing 1.5 – 3.5 wt% sulfur, and traces of vanadium, nickel and iron [66, 67]. The sulfur is usually present as organic sulfur such as five-membered heterocyclic rings named thiophenes, on their own, as a part of thiophene-containing PAHs structures, as described by Xiao et al.[68], as metal sulfides or substituted sulfur oxide groups on PACs structures [69, 70].

Conditions during anode baking have been measured at 3 and 11 % oxygen, which could facilitate incomplete combustion conditions for PAHs [71]. The off-gas from a baking furnace has been analysed and is reported to contain CO_2, CO, CH_4, H_2, SO_x and other volatile organic compounds, which originate from the coke and the coal tar pitch [71, 72]. Off-gas treatment plants clean the gas to reduce emissions. An schematic of the smelting process and gas treatment centre is shown in Figure 2.9. Typical equipment to reduce airborne industry emissions are regenerative thermal oxidisers (RTO), which reduce organic matter using combustion chambers operated at about 900 °C. Other technologies used for volatile organic compounds, particulate matter and SO_2 are bag house filters, wet scrubbers and electrostatic precipitators, often in combination [73].
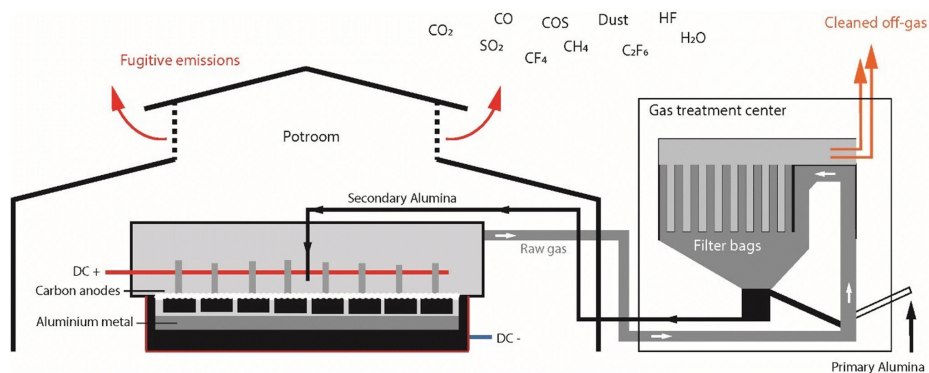
Figure 2.9: Illustration of the aluminium smelting process and gas treatment centre. From Aarhaug and Ratvik [74], under the terms of the Creative Commons Attribution 4.0 International License.

Currently in Norway, emissions from industrial plants to air and water, are reported to the government and the priority EPA-16 PAH emissions in 2019 were 57 metric tons, where production of prebaked anodes for aluminium production is one of the main contributors, typically in the range of 0.5 kg to 18 tones per Al plant per year

(2022) [75]. While the reported PAH-16 emissions are effectively reduced in the gas phase though gas cleaning, some condensed hydrocarbon residues from anode baking furnaces build up in the off-gas treatment plants and are observed in the pipes and filters.

2.4.2 Silicon Production

The semi-closed submerged arc furnace (SAF) is commonly used to produce metallurgical grade silicon (MG-Si) through carbothermal reduction, using a mix of coal, coke, charcoal and woodchips as the reductants (Figure 2.10) [76]. The carbon materials reduce the quartz to silicon alloy, by the overall reaction shown in Eq. 2.1, where σ is the Si-yield, which gives the distribution between tapped Si and SiO leaving the furnace to react to SiO_2 (silica fume) [77].

$$SiO_2 + (1 + \sigma)C = \sigma Si + (1 - \sigma)SiO_{(g)} + (1 + \sigma)CO_{(g)} \qquad (2.1)$$
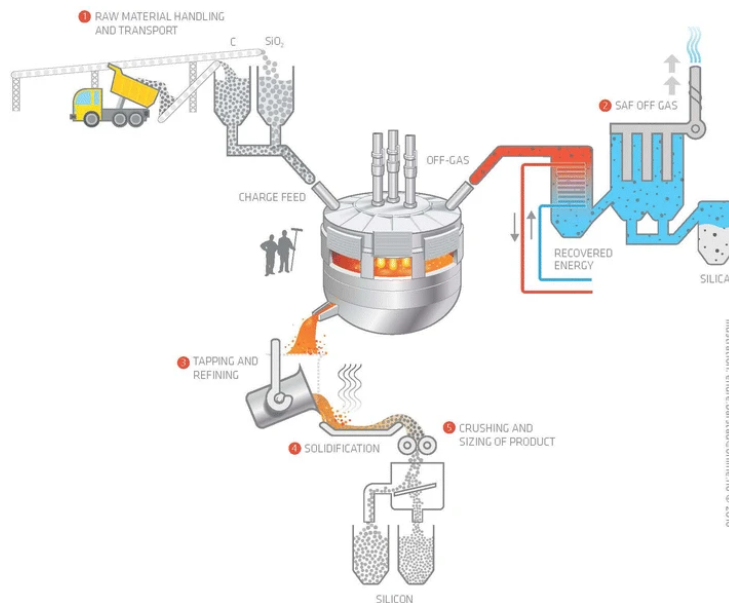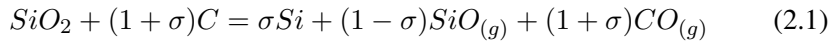
Figure 2.10: Illustration of a submerged arc furnace used for silicon production marked with the various process steps. From Kero et al.[78], under the terms of the Creative Commons Attribution 4.0 International License.

Silicon oxide (SiO) and carbon monoxide (CO) that reach the top of the furnace react with air, to form silica fume and carbon dioxide (CO_2), respectively, in the furnace hood [77]. This affects the temperature at the charge surface in the furnace

which can reach 700 to 1300 °C. Because the SAF is semi-closed, the under-pressure in the furnace drives the surrounding air into the furnace hood diluting the furnace off-gas, which consist mainly of air. The excess of air combined with the high temperature produce thermal NO_x through combustion, the so called Zel-dovich mechanism, of nitrogen and oxygen in the air by radical formation, shown in Equations 2.2 - 2.4. As described by Kamfjord [79], the SiO and CO combustion produce high temperature hot spots at the top of the furnace charge, where also VOCs and moisture evaporate, creating conditions for fuel, prompt and thermal NO_x formation.

$$O + N_2 \leftrightarrow NO + N \tag{2.2}$$
$$N + O_2 \leftrightarrow NO + O \tag{2.3}$$
$$N + OH \leftrightarrow NO + H \tag{2.4}$$

Off-gas temperatures can be 400 to 700 °C above the crust of the charge materials in contact with air, and the silica fume is typically captured using a bag-house filter at moderate temperatures of approximately 60 to 220 °C, depending on the filter type and the composition of the fume. PAHs are emitted from the furnace, either from the top of the gas permeable furnace charge material or through gas released during the tapping process. Typically these PAHs originate from pyrolysis and combustion of the carbon raw materials, electrodes and carbon paste. Reported emission values from Norwegian silicon alloy plants are estimated to be in the range of 10 to 70 kg per site per year, using emission factors [78]. Efficient pyrolysis of coal should result in the breakdown of large organic molecules to smaller hydrocarbons and in efficient combustion the only products should be small gaseous molecules such as CO_2, H_2O, CO etc. However, such complete degradation of coal rarely occurs and organic compounds, including PAHs, are released during the reduction process. Work is being done to develop PAH reduced or PAH-free binder products to reduce emissions [80]. Apart from the PAH evolution driven by fuel containing PAH, combustion of aliphatic fuels (like methane or acetylene) can also generate PAH. Fuel bounded PAH as well as the aliphatic fuels evolving from the carbon material in the furnaces are not well understood. A study by Gaertner et al.[81] report EPA-16 PAH emission from the flue gas stack at a silicon plant in Norway to be 2 $\mu g/Nm^3$ in the off-gas and 1.81 ng/g EPA16-PAH on the dust (PM). Increased levels of PAH emissions were observed after a furnace re-start. Reported emission levels vary between plants, and in 2020 Norwegian silicon and ferro-silicon producers reported between 0.35 kg/y and 296.39 kg/y EPA-16 PAH emission to air and water from different plants to the Norwegian Environmental Agency[75].

2.4.3   Off-Gas Cleaning

Process gas streams are cleaned to avoid contamination, equipment damage and pollution. The off-gas is cleaned in accordance with regulations of emission control to remove toxins and hazardous components. Primarily, a gas - solid separation is performed for the gas cleaning, removing fine dust particles and liquid mist using equipment such as impingement, filtering, washing, combustion and electrostatic precipitation. Factors like particle size, capacity, gas velocity and pressure drop are important for cleaning process [82]. Complete removal of organic pollutants such as PAH and polychlorinated dioxins and furanes can be particularly challenging as destruction methods can also lead to reformation at unfavourable destruction conditions [83].

Impingement separators use baffles to obstruct the path of the solid particles in the gas flow, before they are collected. The restricted gas flow can lead to a higher pressure drop compered to other techniques, but have the ability to separate smaller particles then some other dry collectors. This is an important step in removing organic pollutants from the gas stream as they adsorb on particles and ash [83]. Filters combine the techniques of impingement and filtration to separate gas and solids. A fabric, such as cotton, fibre glass or paper is coated to obtain the filtration size, and using the fibres to obstruct the particles in the gas flow. A bag filter is a typical application where multiple bags are fitted in a rectangular chamber and solids are removed mechanically by vibration or by varying the gas flow. Filters can also be used for air cleaning. This differs from cleaning process gas mainly by the fact that the separated material must not be collected and treated [82]. Catalytic filter bags are described by Neuwahl et al.[84], as a "Best available Technique" for reducing VOC emission to air, where the filter bags are impregnated with a catalyst or the catalyst is mixed directly with the organic material during production of the fibres. Several catalysts are used depending on the process conditions such as temperature and off-gas composition, such as manganese, copper, vanadium and iron based materials [85]. Carbon-containing adsorbents are also an effective method to remove organic content from the exhaust gas [83].

A combustion chamber can be used to reduce organic volatile content in the flue gas. They typically operate at temperatures between 900 °C and 1200 °C, and the gas flow and chamber size can be specified to achieve optimal residence time, together with secondary injection of air and sufficient air mixing. A regenerative thermal oxidiser (TRO) is an example of a combustion chamber and is illustrated in Figure 2.11 [84].

Wet scrubbers are used when the off-gas is cleaned by washing, often using water. Gas and water move in counter-current and the solids are removed as a slurry.
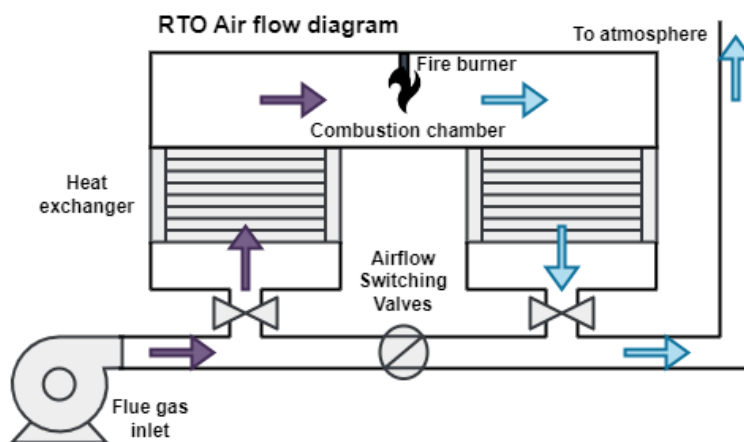
Figure 2.11: Illustration of a combustion chamber, regenerative thermal oxidiser (RTO), used for gas cleaning to reduce emission of organic volatiles. Recreated from Catalytic Products International [86].

This application can also be used to cool the gas flow, as well as neutralise other components in the stream. The scrubbers are often equipped with spray nozzles, plates and or packing material to increase efficiency. Venturi scrubbers is a type of wet scrubber where the inlet turbulence is used to atomise the water to increase the contact area between the cleaning liquid and pollutant. The slurry is often collected and treated using a cyclone separator. A Venturi scrubber can also be adapted to be used to remove gaseous pollutants by gas - liquid absorption [82].

Electrostatic precipitators collect fine particles by ionising the gas when it passes through high voltage electrodes. The charged particles attach to the earthed electrode and are removed mechanically or by washing. The technique is effective, at high cost [82].

2.5   PAH Sampling and Analysis

A challenge in measuring PAHs stem from PAH being a complex mixture of compounds with different physical properties. In industrial off-gasses, a distinction between light, heavy and soot/ particle bound PAHs is often made. Light PAHs, 2-3 aromatic rings, are typically found in the gas phase, and in terms of emissions will be airborne or in an aqueous phase (due to small PAHs being more water soluble). Heavy PAH, 4 rings or larger, will more often be found as solids, or condensed on dust particles. Heavy PAH are therefore more likely to be found among dust and scale deposits which can clog off-gas systems. This challenge is reflected in the methods used for sampling, which usually take place in the industrial stacks

and take into account that PAHs will exist both in gas and solid form. In addition, condition such as off-gas temperature, particulate concentration and humidity can affect the sampling procedure [87].

PAH sampling from stationary sources follow a standard (ISO 11338-1:2003), where three different strategies for sampling is proposed. The strategies suggest using filters and absorbents to collect solid and gaseous PAHs, respectively, with variations on handling moisture, condensation and the temperature and flow control [88]. An example of what such a sampling setup could look like is shown in Figure 2.12.
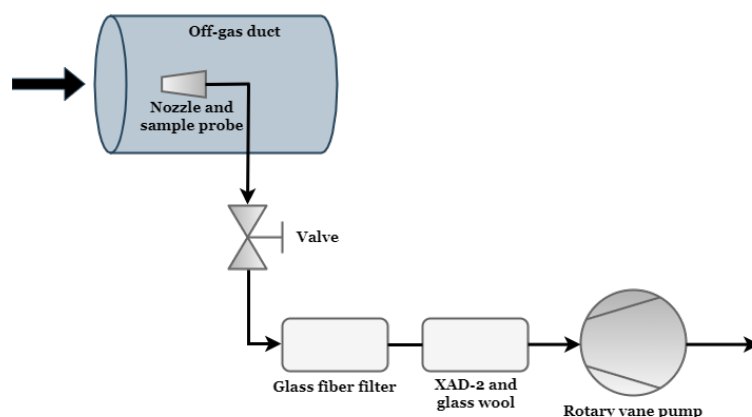
Figure 2.12: PAH sampling line, including glass fibre filter, XAD-2 cartridge with glass wool and pump with silica drying town for moisture removal. From Arnesen et al.[89], under the terms of the Creative Commons Attribution 4.0 International License.

A nozzle and probe with a gas-sampler pump to maintain stable gas flow is used to extract the gas from an off-gas duct. A glass fibre thimble filter is used to collect particles and PAH in condensed phase, followed by cartridges with glass wool and an absorbent materiel for gas phase PAHs. XAD-2 (2-hydroxymethyl piperidine) is a porous hydrophobic organic polymer resin which is a commonly used absorbent. When performing sampling on a gas stream that contain large amounts of dust or water, additional elements with a coarser filter and a silica unit, respectively, can be used. Such samples need further treatment and analysis. Pre-treatment often involve desorption of the PAHs from filter and/or absorbent to liquid phase using an organic solvent, a cleaning procedure to remove impurities, concentrate the sample by purging evaporation and finally analysis using a gas chromatography coupled with a mass spectrometry detector (GC-MS) [90]. The off-gas sampling time can be up to 6 hours, and samples are normally collected from plants a couple times each year. Variations and correlation between operational differences and pro-

cesses (ex. charging and tapping of metal) and PAH emissions are not taken into account as continuous sampling is not performed and the time between sampling and final results can take several weeks. In addition to general uncertainties connected to sampling and analysis, this results in large variations in reporting of total PAHs emissions [87].

To be able to adjust and connect changes in process parameters and operations other analysis methods and combinations of methods have been investigated. Kjos et al.[91] (2014), investigated the use of Fourier Transformed Infrared Spectroscopy (FTIR) and GC-MS as a potential procedure to analyse a large range of organic compounds online and on-site and study the dynamic gas composition from an aluminium anode baking furnace. In this work, both methods were found to be suitable technologies for PAH monitoring, where the FTIR analysis was found to be suitable for the gas phase VOCs and the lighter PAH fraction by the GC-MS. In later work by Kjos et al.[92] (2022), the use of thermal desorption (TD) tubes (steel tubes containing an absorbent material) in addition to GC was used to document the VOC distribution during a firing cycle for a anode baking process. Also VOC loss, breakthrough, of the TD tube absorbent material was tested to investigate the efficiency of the tube set-up by connecting several tubes in series. It was reported that the different measuring methods showed similar emission trends, such as signals for benzene observed to peak earlier in the firing cycle than naphthalene caused by the difference in boiling points, and the efficiency of the gas cleaning technology was greatest for the largest VOC and PAH molecules. Online monitoring using photo-ionisation detectors have been suggested by SINTEF as a possible solution to monitor volatile organic components in real-time [93].

Chapter 3

Summary of Paper I and II - PAH emissions from Pilot-Scale Experiment

3.1 Introduction and Motivation

In the silicon process, PAHs originate from pyrolysis and combustion of the carbon raw materials, electrodes and carbon paste [78]. Efficient pyrolysis of coal should result in the breakdown of large organic molecules to smaller hydrocarbons and in efficient combustion, the only products would be CO_2 and H_2O. However, such complete degradation of coal rarely occurs and organic compounds, including PAHs, are released during the reduction process. With an increasing focus on the environmental impact of the process industry, among others, reporting, handling and treating emissions will only be of greater importance in the future.

In the work by Gaertner et al.[81] EPA-16 PAH emissions from the flue gas stack at a silicon plant in Norway was studied. Emissions in the range of 2 $\mu g/Nm^3$ from gas phase measurements and 1.81 ng/g EPA-16 PAH measured on the particulate matter (PM) was found and increased levels of PAH emissions were observed after a furnace re-start. To investigate the necessary process conditions for complete combustion from ferroalloy plants, Panjwani et al.[94] used post processing techniques based on CFD modelling and reported that temperature should exceed 800 °C for optimal combustion of 1-methylnaphthalene in addition to having a longer residence time > 2s. Wittgens et al.[42], investigated the possibility of including a post-combustion chamber for increased energy recovery with reduced PAH and NO_x emissions in the ferroalloy industry with positive results. Together

27

with the thesis of Andersen (2023) [95], studying flue gas recirculation (FGR) for the silicon process, and Kamfjord (2012), [79], studying NO_x formation in the silicon process, these represent a body of work forming the basis for understanding the off-gas systems and the current status for emissions of PAHs from the SAF-based Si production process. They are however lacking a broader focus of PAHs seen in light of complex process interactions which is important to get a complete understanding of the challenge that is total emission reduction.

Paper I and II hence aim to investigate a broad range of PAH emissions from a pilot scale silicon submerged arc furnace operated continuous during a three-day campaign. The campaign was performed to investigate the implications of different process conditions such flue gas flow, and varying amounts of flue gas recirculated back to the furnace charge surface. A direct result of the recirculation was the increased concentration of CO_2 in the off-gas. Other indirect effects were due to the decreased levels of oxygen which affected combustion reactions such as SiO, NO_x and PAH formation and destruction.

Flue gas recirculation (FGR) is a known method used for emission control by recycling parts of the process off-gas as seen in diesel engines to reduce oxygen levels, temperature and NO_x formation, and as a way to concentrate off-gas species, such as CO_2, for further processing and CO_2 capture [96–98]. The method has also been found to increase the level of hydrocarbon species (including PAHs), when temperature and oxygen concentration reach a certain level due to reduced oxidation efficiency [99–101].

With the change in combustion conditions caused by FGR, investigating the presence of a larger range of PAHs (native, heterocyclic, alkylated, and subsituted PAHs) is of great value to gain a better understanding of the phenomena occurring in the Si furnace and off-gas system. An extended list of PAH EPA-16 was analysed, "PAH-42", which included heterocyclic and alkylated PAHs and was described and analysed in paper I. In paper II, the focus was on substituted PAH, oxy- and nitro-PAHs, specifically. In paper I, CFD modelling was performed by colleagues in SINTEF Industry as a supplement, and to verify trends seen in the experimental work by simulating PAH evolution (1 to 5 ring PAHs) in OpenFOAM by combustion of known PAH precursor molecules, C_2H_2 and hydrogen, in varying oxygen concentrations, to simulate FGR.

3.2   Experimental Method

The pilot furnace set-up used during the campaign was a one-phase submerged arc furnace with a graphite electrode at NTNU/SINTEF in Trondheim, Norway. The power was supplied to the furnace through a 6" graphite electrode (EG90, Tanso) at maximum 400 kVA, with a target of 160 kW load. The furnace and off-gas system is illustrated in Figure 3.1. More information about the campaign and furnace design can be found in the works of Andersen et al.[102, 103].

The furnace off-gas system was modified to achieve a semi-closed system, which included a furnace hood, recirculation and redistribution system. The level of FGR was controlled using a series of fans and valves to control the amount and direction of the off-gas.

A mix of coal, coke, charcoal, woodchips and quartz made up the raw materials and were supplied by an industrial partner. The materials were used as received, except for the woodchips, which were dried at 100 °C for 24 h. More information about the carbon raw materials is found in Table 3.1.

Table 3.1: Information about the carbon raw materials used in the FGR pilot experiments. Analysis performed by ALS Scandinavia, Luleå, Sweden

	Coal	Coke	Charcoal	Woodchips
Moisture (wt%)	10.8	11.7	4.7	4.8
Fix C (DB, wt%)	57.6	90.5	79.0	14.6
Ash (DB, wt%)	2.0	2.8	3.3	1.1
Volatiles (DB, wt%)	40.4	6.6	17.7	84.2
Share of C-mix (% Fix C)	40	15	30	15
Carbon (%DW)	78	90.8	83	50.7
Nitrogen (%DW)	1.58	1.68	0.39	0.2
Oxygen (%DW)	12	2.5	9.6	41.4
Hydrogen (%DW)	5.79	1.83	3.71	6.48
Sulfur (%DW)	0.05	0.42	0.05	0.11

The off-gas composition was analysed during the experiment using different techniques, both on the furnace outlet and inlet. Gas composition (e.g. H_2, O_2, N_2, CO_2 and CH_4) was analyzed using an Agilent 490-PRO Micro-GC with TCD detectors. The GC used two columns for separation, where column 1 was a 3m + 10m MS5A, RTS column with Ar carrier gas, and column 2 used a 10 m PPQ column with He carrier gas. In addition, LaserGas II and LaserDust instruments (NEO monitors) were used for measuring CO_2, O_2, NO_x, and dust analysis.
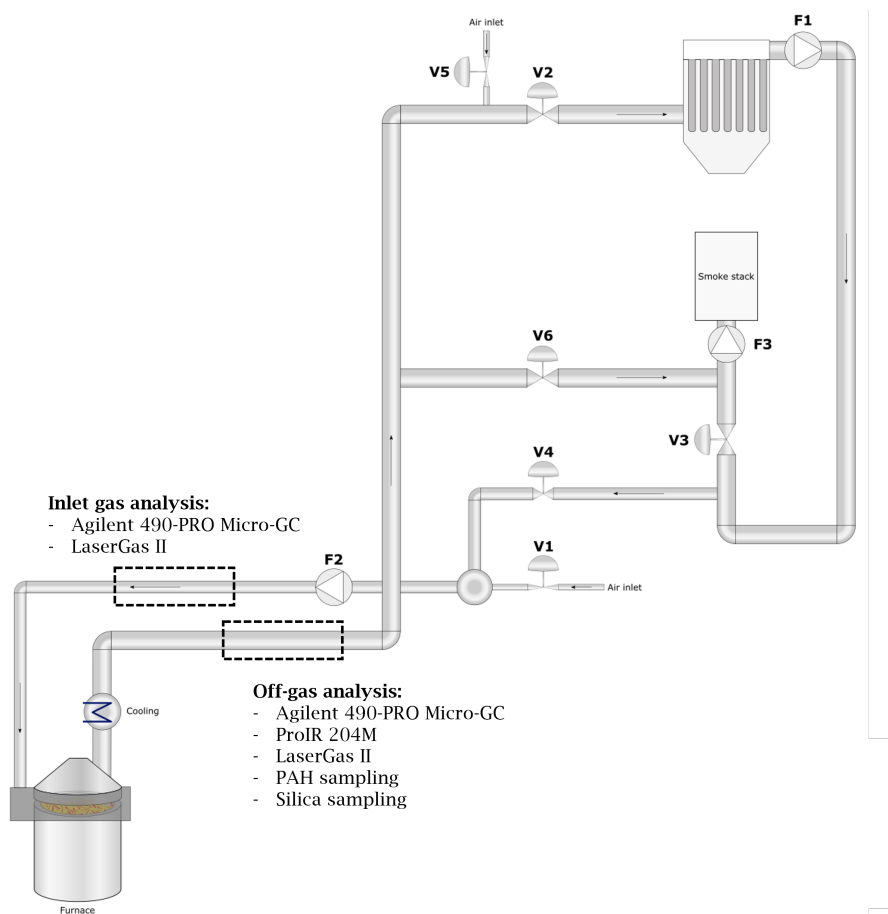
Figure 3.1: Silicon pilot SAF with a closed off-gas recirculating system. Placement of valves (V), fans (F) and location of various sampling systems are marked, from Andersen et al.[102], © 2022 The Minerals, Metals & Materials Society. Used with permission.

Figure 3.2: Picture showing the PAH sampling set-up for the pilot-scale experiments with the different elements of the sampling equipment; pipe with heating band, filter and XAD-2 housing, pump and exhaust gas line.

PAHs were sampled after the cooler using a sample collection system adapting from a standard set-up following isokinetic sampling principles, shown in Figure 3.2. A nozzle (4.16 mm) and probe (1/2", SS) were used to extract the gas from the off-gas duct. To ensure sampling of both PAHs in gas and particulate matter, both glass fibre thimble filters (22 Ø, Munktell/Ahlstrom, Sweden), and cartridges with glass wool and XAD-2 (30.0 g, Supelpak-2, Merck Life Science AS, Germany), were used as absorbents. A rotary vane gas-sampler pump (Paul Gothe GmbH, Germany) was used to maintain stable gas flow. By adjusting the pump extraction velocity to match the gas flow in the off-gas line, a representative sample extraction was achieved. This resulted in a set off three samples which together made up the result from each experimental cycle, the filter, XAD-2 and the acetone used to wash the filter house between samplings.

Samples for PAH analysis was obtained from specific experimental steps during the campaign, and the process parameters for each sample is shown in Table 3.2. Several measures were done to reduce uncertainty related to the PAH samples, with the off-gas variations in mind. Sampling was planned to be performed in duplicates, and triplicates when possible, for experimental cycles with similar process set points. In the end, this was not an option due to the complex nature of process control for the pilot furnace.

Sampling followed a procedure to be performed identically each time. This also included the preparation work which included steps such as drying the filters and

Table 3.2: Gas flow, recirculation ratio and oxygen set-points at PAH sampling in the FGR Pilot campaign.

Sample Number	Flow [Nm^3/h]	FGR [%]	Oxygen [vol%]
1	1000	0	20.7
8	1000	0	20.7
14	1000	0	20.7
5	1000	70	17.2
11	1000	70	17.2
4	1000	88	10.0
13	1000	88	10.0
2	500	0	20.7
9	500	0	20.7
12	500	0	20.7
3	500	60	16.2
7	500	60	16.2
6	500	78	10.1
10	500	78	10.1

packing of the XAD-2 containers. Other practical measures were: filters, XAD-2 and solvents used for sampling were part of the same batch to limit variations. Blank samples were treated in the same way as samples from the furnace gas and a heating band was used on the sampling probe between the off-gas duct and the first sample container to avoid PAH condensation in the nozzle and pipe. Samples were stored and shipped cooled, air tight and wrapped in aluminium foil to protected against degradation by UV light and heat.

Sampling was performed during 14 of the 27 experimental cycles in the pilot campaign. After analysis and evaluation, only 9 of the samples were redeemed to be reliable. During four sampling cycles, no PM was collected in the glass fibre filters even though the sampling pump registered gas flow, indicating a leak in the sampling line with only ambient air being sampled. One cause for this could be the choice of sampling equipment. Parts of the set-up was made from glass, in part to have visual control of the filter and XAD-2 during sampling and the ability to design a custom made sampling set-up. A downside which could cause a leak was the solution for glass-metal transitions in the equipment where vacuum fittings with Teflon o-ring seals was used. This connection is more sensitive to movements in the sampling line and need more visual adjustments during sampling, than for example a metal-metal connection. Result from the last of the five samples were determined to be an outlier, as comparing with experiments of similar FGR, where the result did not fit within a 90 % confidence interval.

Samples were analysed by NILU (Kjeller, Norway), and followed NS-EN ISO/IEC 17025 standard. In addition to extraction and clean up procedures, "PAH-42" was analysed by gas chromatography (GC) with a low-resolution mass spectrometer detector (LRMS), and nitro- and oxy-PAH analysis was performed by GC quadrupole time-of-flight (GC-qToF) in Electron Capture Negative Ion (ECNI) mode. The list of the PAH-42 components is shown in Table 3.3 and the substituted PAH components in Table 3.4.

3.3   PAH Evolution Model

To gain insight into the PAH evolution in such a complex system as a submerged arc furnace, a simplified geometry of a co-flow burner was used to model PAH formation. This work was performed by colleagues in SINTEF Industry. In the present study, only chemistry driven PAH was considered and the work assumed that the fuel consisted of C_2H_2, N_2 and H_2 and that these species are mainly responsible for the chemistry driven PAH [105]. These gases were injected in at 42.2 m/s at a constant temperature of 1000 ^oC with mass fraction (Y) of C_2H_2, N_2 and H_2 equal to 0.246, 0.708 and 0.046 respectively. The flue gases were assumed to consist (by mass fraction) of N_2 and Ar equal to 0.763 and 0.005, the mass fraction of O_2 was varied (the values used were 0.232, 0.203, 0.174, 0.145, 0.116 and 0.058), and the remaining fraction was CO_2. The decreasing O_2 content indicated higher levels of FGR.

The solver used to simulate the process is reactingFoam, a turbulent reacting flow solver available in the open source CFD framework OpenFOAM [106]. The reaction kinetics and thermodynamic data for combustion including PAH evolution proposed by Slavinskaya et al.[105] was used in this work. The reaction mechanism considers acetylene combustion with evolution of PAH until five ring aromatic species (like Benzo(a)pyrene) - consisting of 112 species and 939 reactions.

Table 3.3: List of 42 PAH components analysed in the FGR off-gas samples.

Compound	MW [g/mol]	T_b [°C]^a	# of rings
Naphtalene	128.1	218	2
2-Methylnaphtalene	142.2	241	2
1-Methylnaphtalene	142.2	245	2
Biphenyl	154.2	255	2
Acenaphthylene	152.2	279	3
Acenaphthene	152.2	279	3
Dibenzofuran	168.2		3
Fluorene	166.2	294	3
Dibenzothiophene	184.3		3
Phenanthrene	178.2	338	3
Anthracene	178.2	340	3
3-Methylphenanthrene	192.3	352	3
2-Methylphenanthrene	192.3	355	3
2-Methylanthracene	192.3	359	3
9-Methylphenanthrene	192.3	355	3
1-Methylphenanthrene	192.3	359	3
Retene	234.3		3
Fluoranthene	202.3	383	4
Pyrene	202.3	393	4
Benzo(a)fluorene	216.3	407	4
Benzo(b)fluorene	216.3	402	4
Benz(a)anthracene	228.3	435	4
Triphenylene	228.3	439	4
Chrysene	228.3	448	4
Benzo(ghi)fluoranthene	226.3	432	5
Cyclopenta(cd)pyrene	226.3		5
Benzo(b)fluoranthene	252.3	481	5
Benzo(k)fluoranthene	252.3	481	5
Benzo(j)fluoranthene	252.3	480	5
Benzo(a)fluoranthene	252.3		5
Benzo(e)pyrene	252.3	493	5
Benzo(a)pyrene	252.3	496	5
Perylene	252.3		5
Dibenzo(ac)anthracene	278.3		5
Dibenzo(ah)anthracene	278.3		5
Indeno(1,2,3-cd)pyrene	276.3	536	6
Benzo(ghi)perylene	276.3	550	6
Anthanthrene	276.3		6
Coronene	300.4	430	6
Dibenzo(ae)pyrene	302.4	414	6
Dibenzo(ai)pyrene	302.4		6
Dibenzo(ah)pyrene	302.4		6

^{a} PAH boiling point sources [90, 104]

Table 3.4: List of nitro- and oxy-PAH components analysed in the FGR off-gas samples.

Compound	MW [g/mol]^a	# of rings	IARC Classification^b
9-Nitroantheracene	223.2	3	Group 3
2+3-Nitrofluoranthene	247.3	4	Group 3
1-Nitropyrene	247.3	4	Group 2A
4-Nitropyrene	247.3	4	Group 2B
3-Nitrobenzanthrone	275.3	4	Group 2B
7-Nitrobenz[a]Antheracene	273.3	4	Group 3
1,3-DiNitropyrene	292.2	4	Group 2B
1,6-DiNitropyrene	292.2	4	Group 2B
9-Fluorenone	180.2	3	-
9,10-Anthraquinone	208.2	3	-
2-Methyl-9,10-Anthraquinone	222.2	3	-
6H-Benz[de]Anthracen-6-one	230.3	4	-
1,2-Benzanthraquinone	258.3	4	-
6H-Benzo[cd]Pyren-6-one	254.3	5	-

^{a} PAH MW [104]

^{b} PAH IARC status [22]

3.4 Results and Discussion

3.4.1 Experimental Results

Each sampling period started within a new experimental cycle for the pilot furnace, after stable process conditions were reached. A cycle lasted from feeding of the raw materials to charge material collapse in the furnace and the tapping of the metal, which lasted about 1.5 hour. This is unlike an industrial furnace process were the liquid Si is continuously tapped and the raw materials are added as needed during production [77]. The end of the cycle was often marked with a charge collapse and blowout in the furnace which lead to an increase in temperature due to the combustion caused by the addition of oxygen. This change in furnace conditions marked the end of a stable period and end of sampling. Flue gas recycling ratios, gas concentrations and flow values were calculated as an average over the stable sampling period. FGR rate was based on the ratio of in- and outlet CO_2 concentration measurements by the LaserGas instrument, and ambient CO_2 was set to 0.06 vol%. The measured flow, FGR and oxygen levels for each PAH sample is presented in Table 3.5.

The strategy for sampling was chosen so the samples should relate to the furnace conditions during a stable period. As consequence of this, the time it took from the raw materials where added to the set points for an experiment were reached could vary between each sample. As well as, the initial evaporation of VOCs from

Table 3.5: Measured gas flow, recirculation ratio and oxygen averages from PAH sampling in the FGR Pilot campaign, sorted by flow and decreasing oxygen levels.

Sample Number	Flow [Nm^3/h]	FGR [%]	Oxygen [vol%]	Flue Gas Temperature [°C]
1	965	0.6	20.7	208.3
8	914	0.9	20.7	248.6
5	935	60.1	17.6	238.1
4	865	81.3	15.5	231.7
13	919	82.5	13.3	237.1
9	566	0.3	20.4	268.4
3	440	56.6	17.9	275.3
7	497	59.6	17.3	292.9
6	425	75.0	16.4	274.7

the raw materials would be sampled to a varying degree. The time before sampling was also affected by the energy produced from the raw material mix which at times resulted in the temperature off-gas reaching the bag house filter being to high for the filter to be used.

On average, $0.30\ Nm^3$ off-gas was sampled per hour of silicon production. Results from 9 different experiments include a total of 27 samples where the FGR levels varied from 0 to 75.0 % for experiments at $500\ Nm^3/h$ off-gas flow rate and from 0 to 82.5 % for experiments at $1000\ Nm^3/h$. An overview of the total concentration of PAH-42, oxy- and nitro-PAH from experiments at varying FGR for 1000 and $500\ Nm^3/h$ is presented in Figure 3.3. The concentrations are a sum of 8 nitro-species, 6 oxy-species, and PAH-42, which is an extended EPA-16 list with 42 compounds that also include heterocyclic and alkylated PAHs. Overall, an increase in PAH concentration at higher FGR is observed for both the 1000 and $500\ Nm^3/h$ flowrates.

Three experiments were performed as conventional Si production cycles, without flue gas recirculation. One experiment had a gas flow rate at $500\ Nm^3/h$ and two at $1000\ Nm^3/h$. The total PAH-42 concentration for these experiments range between 14 and 22 $\mu g/Nm^3$. To compare, the PAH EPA-16 concentration range between 9 and 13 $\mu g/Nm^3$ for the same experiments, 1 and 2 $\mu g/Nm^3$ for nitro-PAHs, and 1 and 4 $\mu g/Nm^3$ for the oxy-PAHs.

During the pilot experiments several parameters changed and this is illustrated in Figure 3.4 (a) - (d), where variations in O_2, temperature, CO, and NO_x and PM are presented. Figure 3.4 (a) shows the change in O_2 as an effect of FGR, and
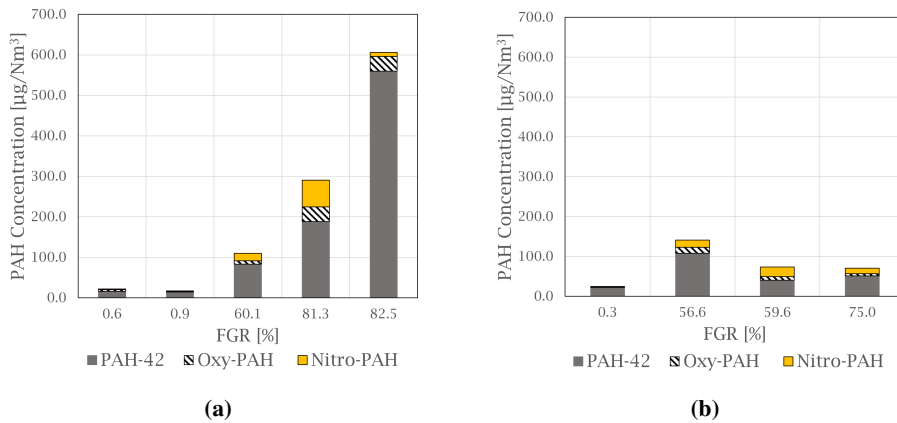
Figure 3.3: Graphs showing the measured PAH-42, oxy- and nitro-PAH concentration in the off-gas at varying FGR levels for experiments at (a) 1000 Nm^3/h and (b) 500 Nm^3/h.

similar decreasing trends are present for both 500 and 1000 Nm^3/h, with a significant drop in O_2 concentration occurring at 80 % FGR for the 1000 Nm^3/h set-point. This is also illustrated in (c), where the changes in CO levels at 1000 Nm^3/h increase from about 500 to 700 ppm when the FGR increase from 81.3 to 82.5 %, respectively, indicating variation in combustion conditions in the furnace. Andersen [95], present the O_2 and CO levels for all experiments performed in the campaign and argue the CO concentration increase more than what is expected from the recirculation effect alone for FGR rates over 70 %, indicating the additional CO is a result of incomplete combustion.

The off-gas temperature was measured before the cooler and the average temperature from each stable sampling period is presented in Figure 3.4 (b). All temperature measurements at 500 Nm^3/h were at a higher level than for 1000 Nm^3/h. The total amount of particulate matter (PM) and NO_x was measured during the experiments, and the variations are presented in Figure 3.4 (d). A correlation was found between PM and NO_x at 99 %. This correlation is also observed in experimental work performed by Kamfjord [79], where exothermic SiO combustion to particulate silica fume at the furnace charge surface create local areas with high temperature, and thermal NO_x can form.

Figure 3.5 shows how the total concentration of PAH-42 change with varying FGR ratio (a) and oxygen levels (b) for samples at 1000 and 500 Nm^3/h. At 1000 Nm^3/h, the PAH concentration increase from 16.0 to 559.7 $\mu g/Nm^3$ with decreasing O_2 levels (20.7 - 13.3 vol%) and increasing FGR (0 - 82.5 %), which are parameters that show a strong correlation in this study, at 99 % and 97 % cor-
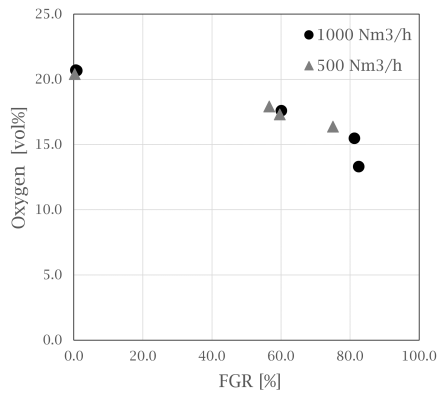
(a)
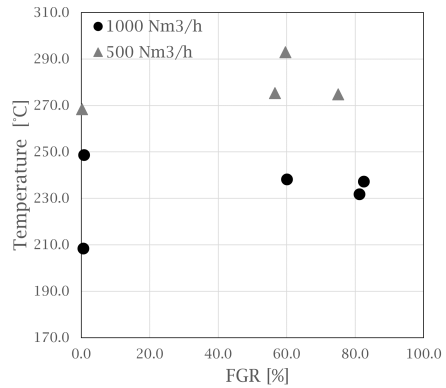
(b)
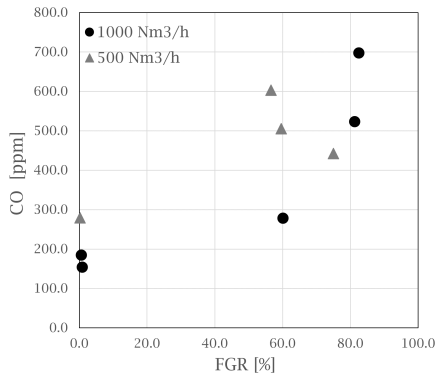
(c)
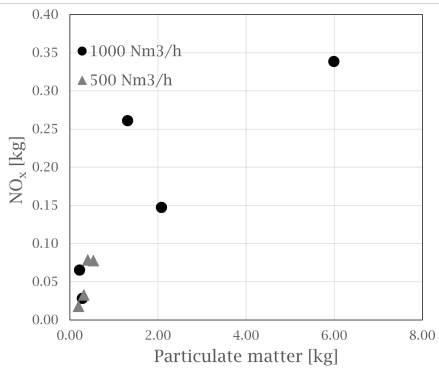
(d)

Figure 3.4: Graphs showing the changes in gas composition and temperature as an effect of FGR for the different flow rate (500 and 1000 $\mathrm{Nm^3/h}$), (a): O_2, (b): Temperature, (c): CO, (d): NO_x and PM

(a)   **(b)**
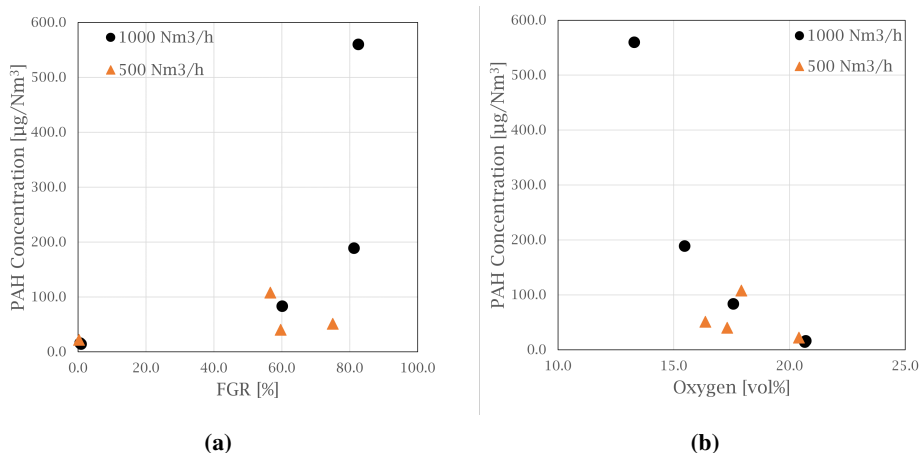
Figure 3.5: Graphs showing the total PAH-42 concentration in the off-gas at varying FGR ratios (a) and O_2 levels (b) for experiments at 1000 Nm^3/h and 500 Nm^3/h.

relation between the high molecular weight PAHs fraction and oxygen and FGR, respectively.

The increase in PAH concentration with FGR follows the trend presented in other work where the level of unburned hydrocarbons increased with increasing levels of FGR [99, 100]. This overall trend is a consequence of the lower availability of oxygen and the reduction in temperature, due to which the extent of oxidation of the PAH is reduced. Overall, the PAH concentrations are lower for the samples at 500 Nm^3/h conditions than at 1000 Nm^3/h, ranging between 22.0 and 107.8 $\mu g/Nm^3$, when comparing with similar FGR (0 - 75.0 %) and oxygen levels (20.4 - 16.4 vol%). As lower flow of flue gases is observed to increase the temperature in the furnace during experiments, this may increase the overall residence time experienced by PAH species, thus increasing the extent of oxidation of PAH species.

As shown in Figure 3.6, the generally dominating PAH fraction is of high molecular weight (HMW) with 4 - 6 rings PAHs for experiments at both 1000 and 500 Nm^3/h, with a pyrogenic ratio of LMW/HMW < 1 and does not seem to be greatly affected by the FGR rate. The HMW fraction dominate the emission profile together with production of the more thermodynamically stable species of phenanthrene and fluoranthene, suggesting the process remain at high temperature oxidative conditions even at the extreme process conditions tested in the pilot campaign. The experiment at 82.5 % FGR and 1000 Nm^3/h stand out as the 2 - 3 rings fraction dominate and is almost entirely made up of gaseous naphthalene which shift the LMW/HMW ratio from pyrogenic to petrogenic furnace condi-
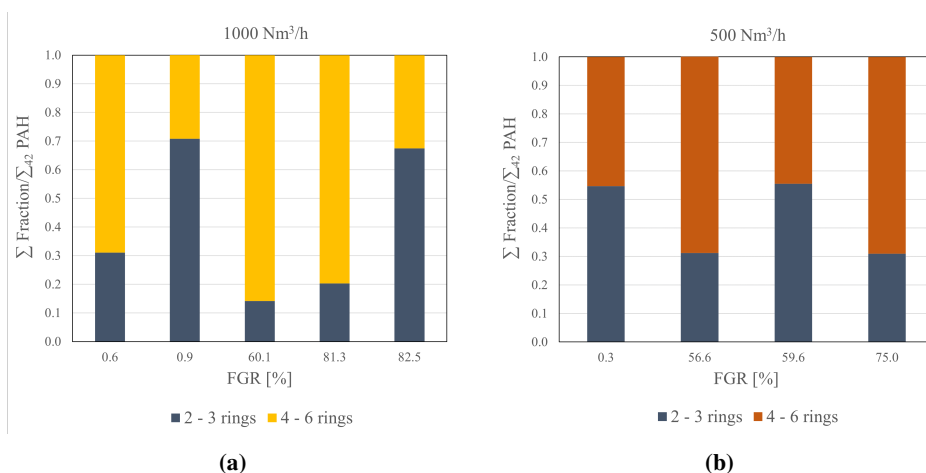
Figure 3.6: Graphs showing distribution between low molecular weight (2-3 rings) PAHs and high molecular weight (4-6 rings) PAHs in the off-gas at varying FGR. (a) experiments at $1000 \ \text{Nm}^3/\text{h}$. (b) experiments at $500 \ \text{Nm}^3/\text{h}$.

tions.

The level of nitro-PAH measured in the pilot campaign range from $1.4 \ \mu\text{g}/\text{Nm}^3$, and when combustion conditions change with higher recirculation rate and lower available oxygen, the observed level increase up to $65.9 \ \mu\text{g}/\text{Nm}^3$, but does not closely follow the increase of FGR. Similarly, the level of oxy-PAHs measured in the pilot campaign range between 1.1 and $36.6 \ \mu\text{g}/\text{Nm}^3$.

4-nitropyrene is the most abundant nitro-PAH specie in every sample, accounting for 39.5 to 91.5 % of the total measured nitro-PAH concentration. Whereas, 1,2-benzanthraquinone is the most abundant oxy-PAH specie in 7 out of 9 samples, making up between 41.2 - 69.1 % of the total concentration of the total measured oxy-PAH level, followed by 9,10-anthraquinone, accounting for up to 43.5 % of the total amount in some samples. Using 4-nitropyrene and 1,2-benzanthraquinone as examples, Figure 3.7 show the general trends, where the substituted PAHs increase in concentration from low levels of FGR and higher FGR levels, and become the abundant species, compared to their parent PAHs.

Nitrogen oxides must be present for the nitro-PAHs to form and the NO_x forming reactions are a source of radicals and atmospheric oxidative reactions. Hrdina et al. [39], describe the necessity of radicals and radical-initiated reactions, to create oxidants such as $NO_3^{\cdot}$ and $OH^{\cdot}$, which functions as an activator of a substitution reaction. Katritzky et al. [33], describe the nature of a aromatic substitution reaction where the initial reaction step produce a temporary positively charged arenium
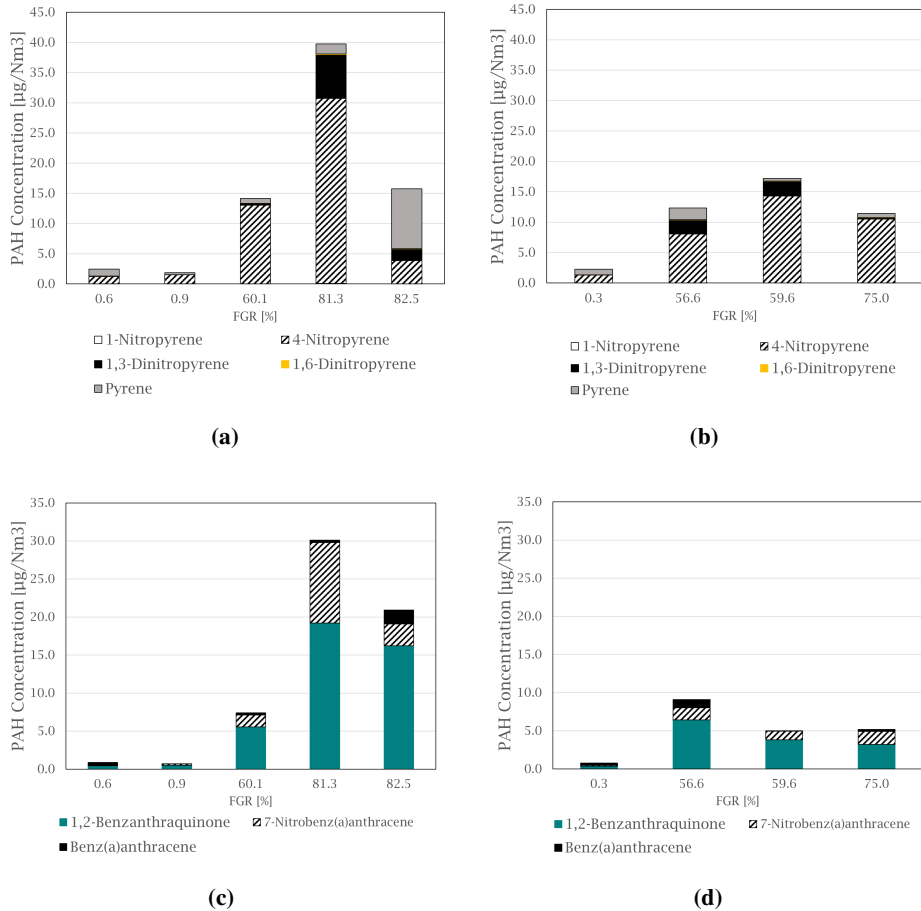
Figure 3.7: Graphs showing the distribution of nitro-PAHs and oxy-PAH with the corresponding parent PAH for experiments at 1000 $\mathrm{Nm^3/h}$ (left) and 500 $\mathrm{Nm^3/h}$ (right), (a)+(b): Pyrene species, (c)+(d): Benz(a)anthracene species.

ion. The initial reaction to form the arenium ion is typically the rate-limiting step, and will therefore react further with electron rich molecules, and in the case of this study, oxygen or NO_2 can react, and form the final oxy- or nitro-PAH molecule. Based on the preferential isomeric formation seen in results from this study, a gas phase radical substitution mechanism seem to be the formation route, based on kinetic measurements performed by Atkinson et al.[107], where nitration for pyrene was studied, and by Albinet et al.[108], where urban measurements of quinones correlated with emission from diesel engines, and was described to be a result of gas-phase formation by ozonation.

An estimation of the PAH emissions from the pilot experiments of PAH-42 and the combined oxy- and nitro-PAHs with varying FGR levels was performed. The estimation was based on the amount of PAHs in each experimental cycle which passed through the glass fibre filter used in the sampling set-up (Figure 3.2) and the amount of process gas which exited the stack. Even though process and temperature variations were not taken into account, an indication towards the PAH emissions, both PAH-42 and substituted PAHs, not being significantly increasing with added FGR was found as more of the PAHs produced would be recirculated back to the furnace. The exception was the case at 1000 Nm^3/h and 82.5 % FGR, where the filter efficiency was lower due to the furnace conditions resulted in an increase of PAHs with low molecular weight (e.g. bicyclic PAHs) which passed through the filter.

3.4.2   Simulation Results

In paper I, a Perfectly Stirred Reactor (PSR) simulation[109] was performed to study the conditions that prevent the oxidation of PAHs, in which a mixture of PAH (i.e., A1 or Benzene), O_2, CO_2 and N_2 react in a 0D reactor at constant temperature until reaching equilibrium, was used. The results from the PSR simulations suggests that at temperatures below 1000 K, with gas specie residence time smaller than a second, and low oxygen can prevent the complete oxidation of Benzene. At sufficiently high temperatures (around 1500 K) Benzene was observed to be oxidised completely but at lower temperatures it could partly be oxidised and grow into larger PAHs. If the PAH species are not oxidised, they could evolve into larger/smaller PAH molecules based on the local flow conditions as well as transported to the off gas duct of the furnace.

The maximum amount of various aromatic species as predicted by the model produced for the various flue gas recycling cases are visualised in Figure 3.8. The reduction in oxygen with increased FGR was generally observed to increase the generation of the aromatic species.
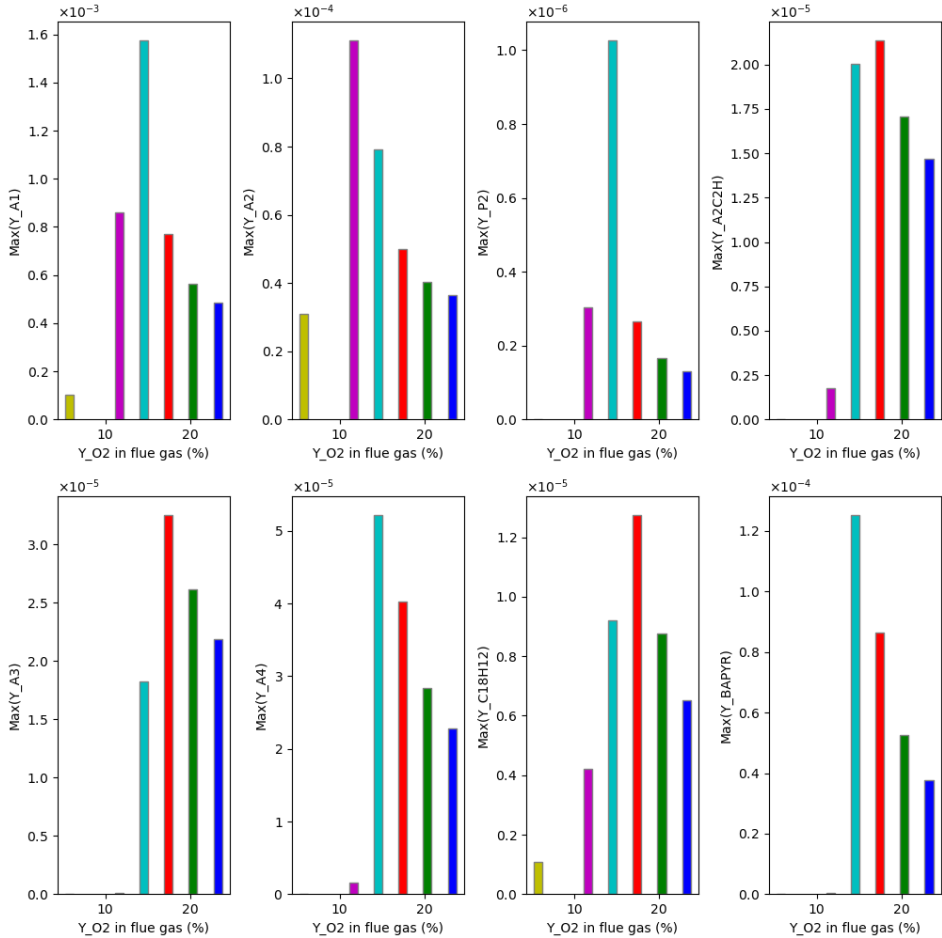
Figure 3.8: Comparison of the maximum value of mass fraction of 8 aromatic species predicted by the CFD simulations for various flue gas recycling scenarios. The x-axis of the plots represent O_2 (mass fraction based %) in the injected flue gas calculated as the mass fraction of $O_2 \times 100$. These 8 aromatic species are A1 (C_6H_6 or Benzene), A2 ($C_{10}H_8$ or Naphthalene), P2 ($C_{12}H_{10}$ or Acenaphthene), A2C2H ($C_{12}H_8$ or Acenaphthylene), A3 ($C_{14}H_{10}$ or Anthracene/Phenanthrene), A4 ($C_{16}H_{10}$ or Fluoranthene/Pyrene), C18H12 ($C_{18}H_{12}$ or Benzo(a)anthracene/Chrysene), and BAPYR ($C_{20}H_{12}$ or Benzo(a)pyrene).

The simulations predicts that although no combustion was observed in FGR with mass fraction based O_2 % of 11.6 % and 5.8 %, PAH species formed (especially A1 and A2) were approximately in the same order of magnitude as the other FGR cases. The maximum value of A2 or Naphthalene was found to increase with FGR and mass fraction based O_2 % of 11.6 %. The subsequent increase in FGR was observed to result in a reduction of A2. Comparing the maximum value of the PAH species formed, smaller PAH species like A1 and A2 tend to be formed in larger amounts when compared to the larger aromatic species (except for Benzo(a)Pyrene - which could be due to overestimation as the reaction mechanism does not consider even larger PAH species). All eight modelled aromatic species showed a steady increase in concentration, with A1 and A2 (benzene and naphthalene) being the dominating species. This was also observed in the pilot experiment with increasing concentration of naphthalene at low oxygen levels (13.3 vol%).

As lower flow of flue gases was observed to increase the temperature in the furnace during experiments, this may increase the overall residence time experienced by PAH species, thus increasing the extent of oxidation of PAH species. It should also be noted that the PSR simulations also indicate that the complete oxidation of A1 or Benzene could be prevented if residence time was lower than a second, which agrees roughly with conclusion of Panjwani et al.[94] who recommended a residence time larger than two second for complete oxidation of 1-methylnaphthalene.

3.5   Conclusions and Industrial Implications

PAH emissions from Si production with flue gas recirculation was investigated in paper I and II, through experimental testing and CFD modelling. Emission of a range of PAH species was measured from a pilot scale furnace with FGR, various levels of O_2 and flue gas flow. The PAHs measured was the list that make up "PAH-42" which are species in the range of 2 to 6 aromatic rings. This is an extension of the EPA-16 list, which also include heterocyclic and alkylated PAHs. The substituted PAHs consist of 8 nitro-species with 3 and 4 rings and 6 oxy-species with 3 to 5 rings.

A part of the challenge with decreasing PAHs emissions from Si production is understanding the connections between process conditions and furnace operations and how they affect the complex reactions of PAH formation and destruction. This work has illustrated the importance of elevated temperatures and oxygen available for PAH combustion and how changes in process conditions can affect the PAH molecular distribution which is important for efficient emission handling. In addition, to the best of the authors knowledge, the connection between elemental reactions occurring in the Si furnace and the formation of substituted nitro- and oxy-PAHs, via NO_x formation, was studied in depth for the first time.

The concentration of PAH-42 for experiments with no FGR vary between 14.1 and 22.0 $\mu g/Nm^3$. With increasing recirculation rate of furnace gas and decreasing O_2 levels the concentration of PAH increase. The PAH-42 concentration increase up to 559.7 $\mu g/Nm^3$, with 13.3 vol% O_2 at 1000 Nm^3/h. A correlation was found between the total PAH-42 concentration and the level of oxygen and FGR, at 99.0 % and 89 % confidence, respectively. Simulations show that an increased level of FGR (without any recycling of PAH) can result in larger amounts of PAH being formed. The simulations predict an increase in formation of smaller aromatic species (like Benzene and Naphthalene) when compared to the larger PAH species, which is also reflected in the experimental results. High molecular weight native PAHs dominate the PAH profile in the experimental samples, and make up on average 58 % of the total sample, but a noticeable shift is observed at low oxygen levels and high FGR, where bicyclic PAHs, such as naphthalene make up increasing levels of the total sample.

The concentration levels for oxy-PAHs were in the range of 1.1 to 4.4 $\mu g/Nm^3$, without FGR, and increased to 36.6 $\mu g/Nm^3$ at 82.5 % FGR. For the nitro-PAHs the concentration rage was between 1.4 and 1.9 $\mu g/Nm^3$, without FGR and increased to 65.9 $\mu g/Nm^3$ at 81.3 % FGR. With FGR, substituted PAH species, such as 4-nitropyrene and 1,2-benzanthraquinone, were produced in greater amounts than their parent PAH.

An increase in PAH concentration at higher FGR is observed for both the 1000 and 500 Nm^3/h flow rates. Comparing the two flue gas flows, experiments at 500 Nm^3/h produced overall lower amounts of native and substituted PAHs, as well as less SiO_2 PM and NO_x, believed to be caused by the temperature in the off-gas and increased residence time in the combustion zone which result in overall better conditions for PAH combustion.

With FGR affecting the PAH species distribution, the given system and off-gas facility should be tailored to the process as to ensure reduction of the total emission of PAH to the atmosphere.

3.6 Future Work

- In future industrial/ pilot measurement campaigns for PAH it would be important to measure the initial phase of VOCs evaporation from the raw materials, which was not performed in this study. An expanded focus on smaller organic molecules such as acetylene (ethyne) and benzene could provide more information about the presence of PAH precursors and their role in PAH formation and growth, as well as being an important addition to computational models describing and predicting PAH emission mechanisms.

- The results from this study showed increased PAH emissions, particularly of the smaller PAHs species, for the lower range of O_2 concentrations. For a similar pilot campaign with FGR, looking further into the details of these conditions with additional PAH measurements after the filter/ at the inlet gas to the furnace would provide information on the efficiency of the off-gas filter and how it is affected by the shift in the PAH emissions composition. In addition, adding PAH measurement after the filter could investigate the potential of PAH recycling and the reactions occurring over the furnace charge in more detail. Similar measurements could be performed at an industrial plant to correlate different process operations during Si production, and investigating if the variations in molecular distribution is found at an industrial scale and how this effects the filter efficiency.

- Investigating the presence of substituted PAHs in this work showed the important role of radicals as a part of the reaction mechanism, both initiating the substitution reaction and in creating the final PAH product. Looking closer into the role of water, as a potential source of oxygen and hydroxide radicals, and hydroxide substituted PAHs in the off-gas could contribute to understanding more of the complex mechanism for PAH substitution formation mechanisms.

- With the industry focus on using bio-materials in the charge mix, performing measurements on relevant raw material mixes would be of great interest to investigate if this affects the PAH emissions.

Chapter 4

Summary of Paper III - PAH Emissions from Green Anode Paste

4.1 Introduction and Motivation

According to the Norwegian Environmental Agency the yearly emission of PAHs in Norway is decreasing, but also state there is still room to improve due to the accumulative effect PAH have in the environment [7]. Data from Statistics Norway and the European Monitoring and Evaluation Program shows the emissions of POP PAHs (Benzo(a)pyrene, Benzo(b)fluoranthene, Benzo(k)fluoranthene, Indeno(1,2,3-cd)pyrene) to air are mainly dominated by the emissions from industrial processes and aluminium electrolysis is particularly mentioned as a key source due to the scale of production and the use of carbon anodes [6, 110].

The carbon anodes used for electrolysis of aluminium are a mix of petroleum coke and coal tar pitch, which contains high amounts of PAHs and act as the binder. The green anodes are baked up to 1100 °C over a 20-day period, where the volatile compounds in the anodes contribute to the baking process. Air is restricted at various steps during the baking process, i.e from use of packing coke and movable covers extracting the off-gas to the treatment centre. This can lead to conditions of incomplete combustion for PAHs and other volatile compounds. In the work of Brandvik et al.[71], the level of oxygen was measured to be 3 % at 930 °C during a baking cycle.

The study of PAH reactivity as an overall topic is widely studied at various conditions but is a great challenge due to the large variety of chemical and physical properties within the group of molecules. Generally, reactivity decrease with increased molecular size and the ability to stabilise the structure by distributing the aromaticity across a favourable molecular structure, kicked or angular, following Clar's aromatic π-sextet rule [111, 112]. The large number of PAH species result in a high degree complexity when studying chemical reactions between PAH and their surrounding conditions [113].

The anode baking process is dynamic and as a result of the changing temperatures and the evolving state of the anode, the off-gas composition will change throughout a baking cycle. This is presented by Kjos et al. [92], where VOC and PAH analysis from an anode baking facility over a 10 hour period was performed and increased VOC emissions was observed after a burner and fan was moved which cause increased heating for the next set of anodes. Sørhuus et al. [114], present technology for improved flue gas treatment from anode baking. The study shows an average of 93.1 % PAH removal efficiency and comment on the varying efficiency based on the PAH size (lower for small PAH and higher for larger PAHs). Due to the continued need to reduce PAH emissions to the environment, investigating specific conditions for anode baking and their effect on combustion mechanisms for PAHs are of interest to improve the efficiency of the flue gas treatment technologies even further.

The main objective of this study was to systematically investigate the effect of temperature and varying atmospheres on the EPA-16 PAH emissions from green anode paste (GAP) during initial heating of the anode baking process.

4.2   Experimental Method

The green anode paste (GAP) used for the experiments contained calcined petroleum coke, anode butts and coal tar pitch, which was prepared by milling (Herzog Maschinenfabrik, Osnabrück, Germany). Representative sampling was performed following sample splitting and the spoon method, as described by Petersen et al.[115].

PAH composition in the off-gas was measured by performing experiments in a laboratory alumina tube resistance furnace (Nabertherm, RHTH 120-300/16-18) (Figure 4.1). The off-gas was purged and the organic content collected in chilled 2-propanol ($\geq$ 98 % Technical, VWR Chemicals) and EPA-16 PAH content analysed using GC-MS. The choice of organic solvent was based on solubility of PAHs, solvent toxicity and volatility. 2-propanol is less toxic than i.e. benzene and less volatile than acetone, which both are better solvents for PAHs than 2-propanol, but
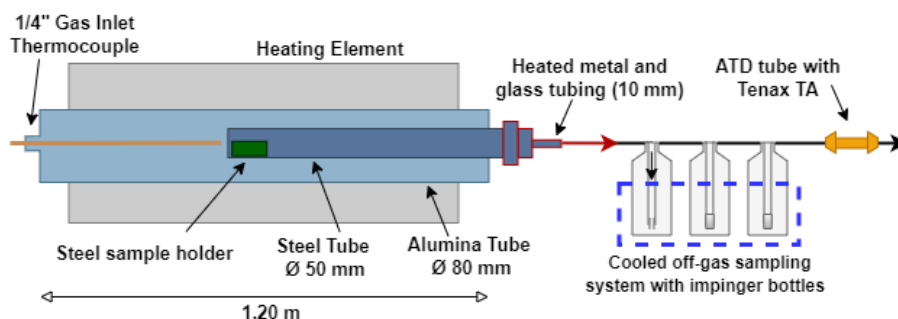
Figure 4.1: The alumina resistance furnace and off-gas sampling set-up used for experiments measuring PAH emissions from green anode paste. From Arnesen et al.[116], under the terms of the Creative Commons Attribution 4.0 International License.

Table 4.1: Atmospheres and concentrations tested for measuring PAH emissions from green anode paste.

Atmosphere	Concentration [%]
Argon	100
O_2	5
O_2	10
CO_2	5
CO_2	10

were not safe or practical to work with in the current set-up.

Using organic solvents to collect PAHs from gaseous atmosphere is an established method, but involves several challenges that must be taken into account for the set-up and method to produce reliable results. One such element was ensuring temperature control all the way from the sample to the off-gas collection system to avoid condensation of PAHs on cold-spots in the furnace and sampling equipment. To aid with this, a narrow off-gas channel with good heat transfer and short distance to the PAHs collection was beneficial. For the set-up used in this work, the material in contact with the off-gas was switched from alumina to a combination of steel and glass as we initially experienced issues with PAHs condensing on the textured alumina surface. In addition, heating bands were used on parts of the sampling line. The connecting o-ring joints in the sampling line were replaced by glass ball-joints to avoid interaction between the rubber o-rings and the organic molecules which could degrade the o-ring material resulting in leaks. The materials and parts were chosen because of heat transfer properties, being easy to replace and clean as not to cross-contaminate between experiments.
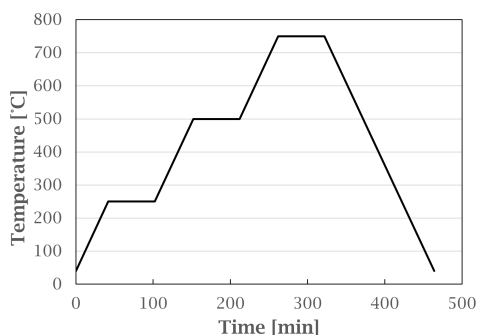
Figure 4.2: Temperature ramping program used in the baking of GAP for PAH analysis.

The atmosphere details used for the experiments are presented in Table 4.1. Argon (Instrument 5.0) was used to achieve correct concentrations of CO_2 ($\geq$ 99.7 %) and O_2 (air, Technical grade).

For each experiment the GAP (5.00 g) sample was placed in a steel holder and heated in the selected atmosphere with a set temperature ramping program (heating rate 5 °C/h), allowing off-gas sampling and exchange of bottles (Figure 4.2) through three temperature intervals, 25 – 250, 251 – 500 and 501 – 750 °C. The bottles were changed under a fume hood and the ice used to cool the 2-propanol was refilled at the end of a hold period. The sampling bottles used glass frit filters to disperse the gas bubbles and provide better contact time and area between the gas and liquid. Over time, these filters could clog from condensation and coke particles and were routinely inspected and replaced.

Due to the possibility of condensed matter on the inside of the furnace and sampling line, the equipment was cleaned thoroughly between each experiment. The furnace was then heated to 1100 °C with air to oxidise any potential contaminants. Bottles were cleaned using acetone and o-rings were cleaned and replaced when necessary.

4.3   Results and Discussion

The average mass loss (%) for the GAP samples is presented in Figure 4.3 for all atmospheres. Inert and CO_2 atmosphere show a similar mass loss of 6.5 - 7.0 %, independent of the concentration of CO_2, which could be the results from evaporation of the volatile organic components in the sample. The weight loss increased when oxygen was added, to 20.2 % and 34.2 % for 5 % and 10 % O_2, respectively, indicating additional reactions occurring compared to the inert atmosphere.
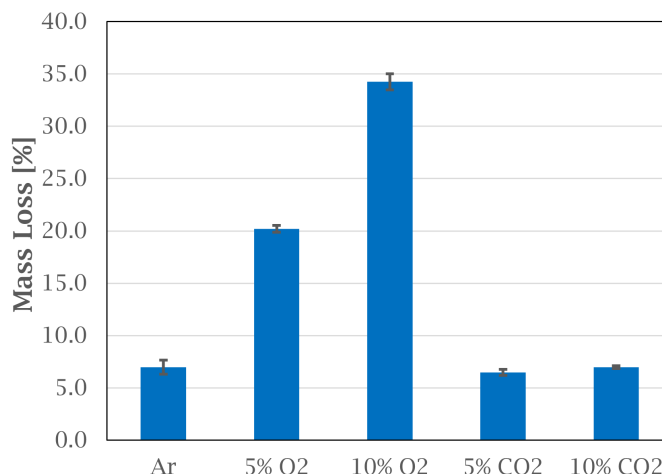
Figure 4.3: Average mass loss (%) for GAP samples at varying atmospheres. Error bars show the variation of triplicate experiments.

The PAH emissions profile for the different temperature intervals in inert atmosphere show low molecular weight (LMW) PAHs (2 and 3 rings) were the main contributors to the emission at low temperatures, from room temperature to 250 °C. Up to 500 °C, the high molecular weight (HMW) PAHs (4 - 6 rings) were emitted, at a higher concentration level. Lastly, PAH emissions decreased significantly for temperatures between 500 and 750 °C. This observation fits with the general range of boiling points for EPA-16 PAH compounds, starting at 218 °C for Naphthalene and reaching 550 °C for Benzo[g,h,i]Perylene [117]. This was also evident in Figure 4.4, where the total concentration of PAHs from each temperature interval is presented.

Figure 4.4 shows the total PAH emission levels for the temperature intervals and atmospheres tested and shows how emissions at low temperatures seem to be independent of the atmospheres tested, as the same level of emission within the standard deviation is seen. Overall, the amount of LMW PAHs present was low for all experiments compared to the HMW species. All methods of sampling, ATD tubes and pyrolysis (see paper III for details), showed similar results to the analysis of PAH content of the 2-propanol, where the smallest PAHs (especially naphthalene and acenaphthene) were not present in significant amount compared to larger PAHs (Phenanthrene and larger).

The effect of the oxygen atmosphere on the PAH emissions is shown in more detail in Figure 4.5. Compared to inert atmosphere, adding 5 % oxygen reduced the total
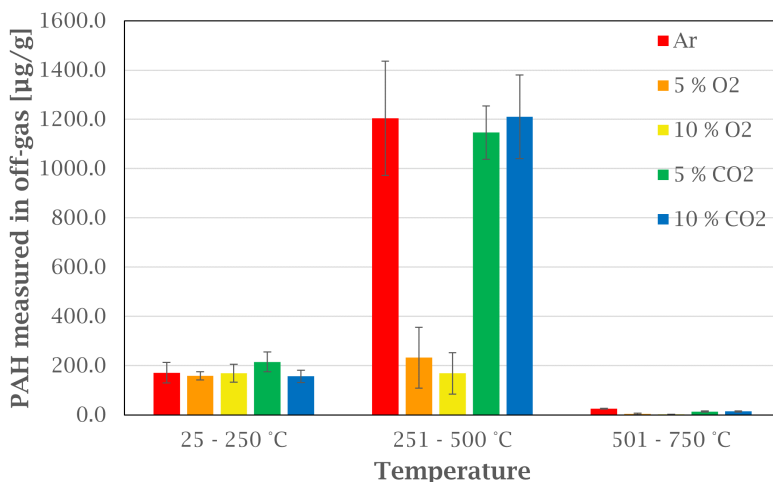
Figure 4.4: Emissions of EPA-16 PAHs at different temperature intervals from heating green anode paste in various atmospheres. Error bars show the standard deviation for the PAH concentration for each temperature interval based on three experiments.

PAH concentration by 65 %, from 1645 μg/g to 569 μg/g. At 10 % oxygen, the total PAH concentration was reduced with 75 %, to 417 μg/g (Figure 4.5). This, seen together with the increased mass loss for the GAP sample (Figure 4.3), with increasing oxygen levels, indicate increased combustion of the anode paste.

With the temperatures and residence time of the experiment, 10 % O_2 is not enough to achieve complete combustion of PAH emitted from GAP. High molecular weight PAHs seem to be more affected by the oxygen level than lower molecular weight PAHs, as the concentration level of four ring PAHs (Fluoranthene to Chrysene in Figure 4.5) do not change significantly when the oxygen level increases. As described by Sun [53] and Liu et al. [54], complete combustion of PAH depends on several factors such as temperature and oxygen levels. In this study, the seemingly stable level of four ring PAHs could be the result of combustion products from partial decomposition of other HMW PAH compounds (i.e partial combustion of benz(a)pyrene could produce pyrene), where the insufficient temperature levels and available oxygen could lead to stabilisation of PAH radical combustion products. The majority of the emissions from the experiments occur at temperatures of 500 °C or lower, where the HMW PAHs would be in a condensed state. In this state, the molecules could be susceptible to catalytic degradation in a gassolid phase initiated by the trace elements nickel, vanadium and iron in the GAP mixture, as described by Pujro et al.[58].
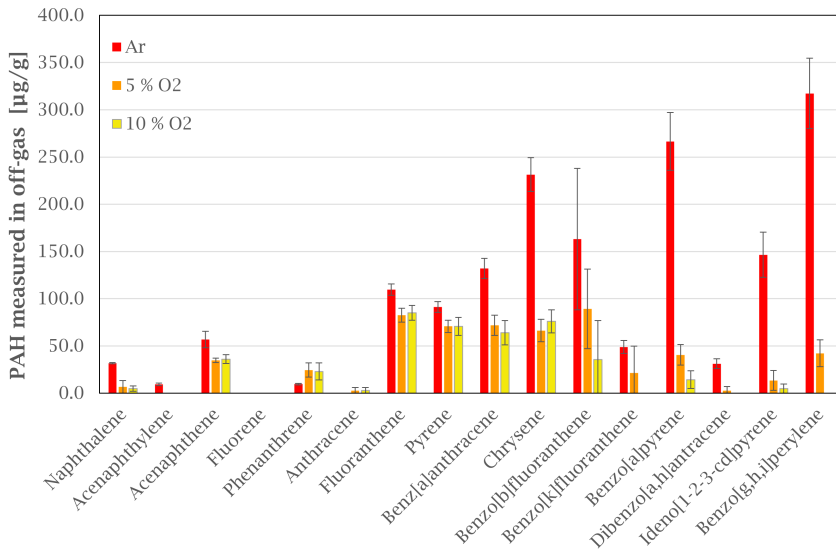
Figure 4.5: Comparing EPA-16 PAH emissions in off-gas from green anode paste heated in argon and oxygen (5 and 10 %) atmospheres. Error bars show the standard deviation for each compound based on three experiments.

Adding CO_2 to the atmosphere did not affect the total PAH concentration or species distribution significantly compared to the argon atmosphere. The total PAH concentration for atmospheres with 5 and 10 % CO_2 were 1547 and 1666 μg/g, respectively. The weight loss of GAP samples in CO_2 was similar to that in argon, indicating that no significant oxidation of the material occurred for this temperature range and CO_2 levels. Guizani (2014) [118], state the use of CO_2 in pyrolysis of biomass mainly contribute to the production of CO and synthesis gas. According to the thermodynamics of the Boudouard reaction, CO formation is favoured at temperatures above 700 °C [119]. This provides an plausible explanation to the observations made in this work.

4.4 Conclusions and Industrial Implications

The effects of temperature and atmosphere on EPA-16 PAH emissions from green anode paste used in pre-baked anodes for aluminium production were investigated in a laboratory alumina tube furnace setup with off-line PAH analysis. The atmospheres and gas levels used for testing reflect conditions relevant for the baking process and were CO_2 and O_2, compared to an argon baseline, with the temperature intervals ranging from room temperature to 750 °C.

Results show PAH emissions at the level of 1645 μg/g and, 1547 and 1666 μg/g, from inert and CO_2 atmospheres (5 % and 10 %). With added oxygen, concentrations decreased to 569 μg/g and 417 μg/g for 5 % and 10 % O_2, respectively, corresponding to 65 % and 75 % emission reduction. For the current setup with the given temperatures, available oxygen and residence time, complete combustion of PAHs was not achieved. At these conditions, differences in reactivity was observed as the level of four-ring PAHs was stable for both concentrations of O_2 tested. This shows the importance of appropriate conditions to archive complete combustion and reduced emissions.

Performing experimental work to learn more about PAH reactivity during controlled conditions was challenging work resulting in leaning outcomes related to the practical work. Experiences have been described in the method section, but the main take-away is the importance of temperature control in the set-up. Both for the high temperature section where the sample is heated and the reactions occur, to avoid condensation of the reactants underway in the sampling systems, and at the sampling section where a rapid, efficient cooling is needed to avoid analytes passing though the absorbent.

In light of this together with other studies, continued focus on optimal and tailored combustion and post combustion of PAHs during the process and flue gas treatment for the industry is recommended.

4.5 Future Work

These experiments are time and resource demanding where much work have been done to ensure reproducible results and producing a reliable method, from handling industrial materials to the final analysis of PAHs. Ideally a broader range of PAHs analysis would be of interest to understand more of that mechanism behind PAHs evaporation, thermal impact and oxidation reactions. This would increase the cost of analysis significantly and it would therefore be recommended to have a well thought out experimental matrix and perhaps consider starting out with a broad scope of analysis, followed by a selection to study in detail together with gas analysis of decomposition product such as H_2O, H_2 CO/CO_2 to have a better overall view of the combustion reactions. A suggestion for a new experimental set-up is presented as a draft in Figure 4.6, where the design is thought to reduce challenges met in this work. Suggestions are summarised below.

- A suggestion for future work is expanding the analysis techniques for the off-gas to include gas components such as CO/CO_2 and H_2 and other VOCs to investigate the formation and destruction mechanisms of PAHs in more detail, as well as establishing a mass balance to evaluate the combustion

efficiency.

- The test conditions could be expanded to include a broader temperature range, as the anode baking process reach about 1100 °C, to include the range where different mechanisms for the PAH formation and destruction can dominate.

- The experimental set-up could be used to compare different carbon materials at similar conditions, for example if the composition of the green anode mixture change.

- Evaluating a new experimental design could provide increased experimental control and flexibility to include new absorbents and measurement techniques, i.e in-line (direct analysis during experiments) and online (sampling and analysis through bypass line) measurements.
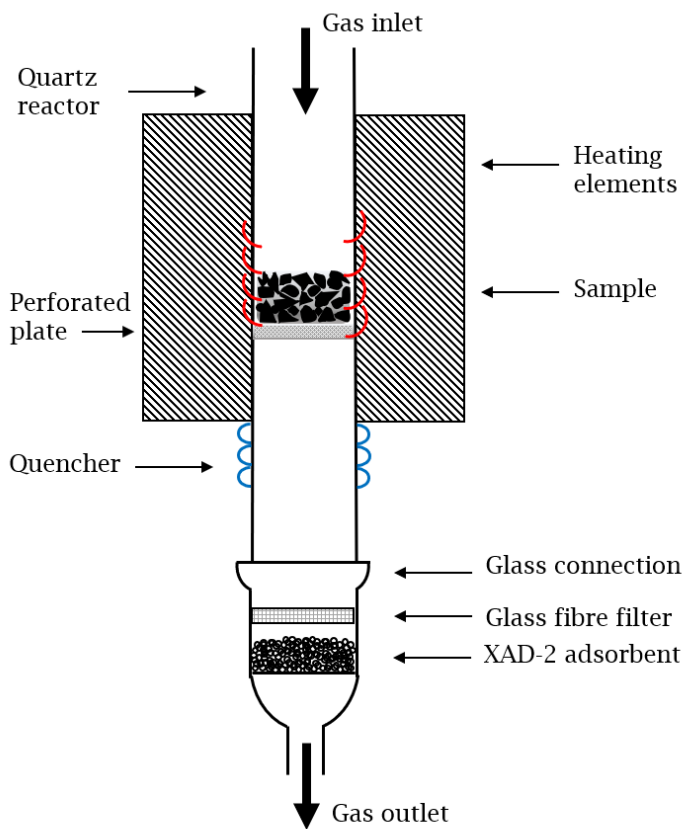
Figure 4.6: Schematic of a quartz furnace for sampling PAH emissions on glass fibre filter and XAD-2 from solid samples.

Chapter 5

Summary of Paper IV - Sulfonated PAHs

5.1 Introduction and Motivation

In Paper IV, condensed hydrocarbon residue samples from an off-gas treatment facility were characterised to investigate the presence of PAHs and other aromatic species. In particular, the presence of aromatic species containing sulfur was in focus in this study. Aluminium produced by electrolysis use carbon anodes as reductants, which in addition to petroleum coke and coal tar pitch, naturally contain aromatic compounds and sulfur (1.5 - 3.5 wt%). The sulfur can exist as elemental sulfur, or as a part of an organic structure such as thiophene. Some sulfur in the anodes is preferred because it improves the CO_2 reactivity of the anode and according to an overview by Aarhaug and Ratvik [74], the sulfur content in an anode of 1.5 - 2 wt% results in 12 - 16 kg SO_2 produced per tonne of produced Aluminium. Sulfur in the off-gas from electrolysis is mainly produced as carbonyl sulfide (COS) which will form SO_2 in air. Through oxidation, SO_3 can be formed and can react further to sulfuric acid in contact with humidity [74]. The conditions causing incomplete combustion of organic compounds during anode baking could simultaneously lead to reactions with aromatic hydrocarbons and create substituted species. Such reactions would create polycyclic aromatic compounds not covered by the EPA-16 PAH list. Substituted PAH have different properties then native PAHs and due to increased polarity have increased solubility in water, which would shift the distribution of PAHs throughout the off-gas cleaning facility. A plausible substitution of naphthalene reacting with sulfuric acid to form naphthalene sulfuric acid is shown in Figure 5.1.
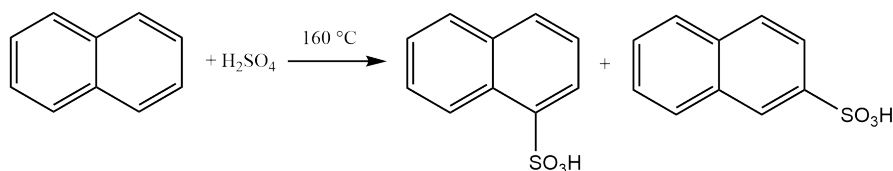
Figure 5.1: Sulfonation reaction of naphthalene by sulfuric acid in a elecrophilic substitution reaction. Recreated from Zhang et al.[120], under the terms of the Creative Commons Attribution 3.0 License

Organic compounds such as sulfonated aromatic species are not well investigated as products of industrial processes, but are frequently used as reactants in the chemical industry and share properties such as polarity and acidity with other substituted PAC spices such as nitro- and oxy-PAHs. Andersson and Achten [9], argue that substituted PACs have been neglected as a monitored environmental pollutant as they have common emissions sources as the EPA-16 PAHs and with continued documentation toxicity equivalence factors (TEF) of substituted species are found to match that of the traditional PAHs and should be investigated further (e.g. TEF of 1,6-dinitropyrene equals 10 compared to toxicity of Benzo[a]Pyrene).

Due to the nature of the raw materials and the conditions in the anode baking plant, the possible interaction between SO_x and aromatic carbon structures in the residue samples were investigated using an experimental approach and non-standard characterisation methods and analysis to investigate the content of the residue.

5.2   Experimental Method

One goal for the experimental work was to examine reliable analyses methods for characterising the unknown sample for polycyclic aromatic compounds as this is not established. As outlined above, the sample of condensed hydrocarbon residue was collected from an off-gas cleaning facility for an anode baking furnace. The sampling location was after a regenerative thermal oxidiser (RTO) and a wet scrubber. The residue was semi-hard and tar like with small amounts of enclosed droplet of clear liquid and is shown in Figure 5.2. An aqueous sample was also collected from the wet scrubber.

To investigate the carbon structure and functional groups present in the hydrocarbon residue, nuclear magnetic resonance analysis was performed and the sulfur content was quantified using ICP-MS. Further details on these methods can be found in the Appendix, Paper IV.

Figure 5.2: Picture of the condensed hydrocarbon residue from an anode baking furnace off-gas cleaning facility. From Arnesen et al.[70], with permission from Springer Nature.

Fluorescence Spectroscopy

Fluorescence spectroscopy was used for detection and quantification of PACs due to the rigid molecular structure and delocalised electrons of aromatic hydrocarbons. The instrument was used to investigate the solubility of the hydrocarbon condensate and phase affinity of the PACs in different solvents (organic solvents and aqueous solutions). Non-aromatic solvents with low solubility in water was selected and combinations of n-hexane, cyclohexane, and dichloromethane (HPLC, Sigma-Aldrich, Germany) and distilled water, with or without sodium hydroxide (Reag.Ph.Eur. VWR Chemicals) at various concentrations (1.0 M, 2.0 M, 3.0 M, 5.0 M) was tested (Figure 5.3). After a set mixing time the phases were separated using a separation funnel and fluorescence was measured.

Figure 5.3: A series with sample dissolved in n-Hexane and increasing concentration of NaOH (l - r: Water, 1.0 M, 2.0 M, 3.0 M, 5.0 M). Organic phase is on the top and aqueous on the bottom of the flask.

UHPLC-Fluorescence/UV and UHPLC-HRMS

The presence of 22 PAHs (including 15 of the EPA-16 and 4 methylated species) in the condensate and aqueous sample, with coal tar pitch as a reference, was analysed using ultra-high-performance liquid chromatography (UHPLC)-Fluorescence. These analyses were performed by the French National Institute for Industrial Environment and Risks (INERIS). Analysis for the presence of potential sulfate- or sulfonate-PAHs (SO_3-PAHs) is not a standard analysis method and was therefore evaluated using a non-targeted screening (NTS) which was based on UHPLC-high resolution mass spectrometry (HRMS) analysis. The presence of potential SO_3-PAHs was based on specific fragmentation pattern and characteristic fragments, SO_3- (m/z 79.9559) and HSO_4- (m/z 96.9607) fragments. Ten commercially available sulfate and sulfonate organic analytical standards were analysed to study their fragmentation patterns, which is shown in Table 5.1. Additional suspect screening analyses was also performed targeting these compounds as well as based on theoretical m/z of sulfates and sulfonates corresponding to the quantified PAHs in the samples.

Table 5.1: Sulfate standards, with CAS numbers, used in non-targeted screening with UHPLC-HRMS analysis.

Name	CAS number
Octylsulfate	142-31-4
2-Formylbenzenesulfonic acid	1008-72-6
4-Hydroxybenzenesulfonic acid	98-67-9
4-Sulfobenzioc acid	5399-63-3
1-Naphthalene sulfonate	130-14-3
2-Naphthalene sulfonate	532-02-5
1-Anthracene sulfonic acid	15100-52-4
3-Phenanthrene sulfonic acid	2039-95-4
3-Fluoranthene sulfonate	1007498-03-4
1-Pyrene sulfonate	59323-54-5

5.3   Results and Discussion

The results from ^{13}C-NMR analysis showed the presence of aromatic carbon in the sample. With acetone used as solvent an aliphatic carbon signal was found in addition to the aromatic signal. This was not seen for methanol and was thought to be caused by the increased polarity of methanol compared to acetone, causing a decrease in solubility of the aliphatic species.

ICP-MS analysis found the average concentration of sulfur in the residue sample to be 9.49 mg/g, which was more than that found in the coal tar pitch raw material used in the anode (4.68 mg/g).

Fluorescence Spectroscopy

Fluorescence was measured to compare solubility of the residue sample and the interactions of the dissolved PACs with the organic and aqueous solvents. Figure 5.4 shows the normalised fluorescence signal from the aqueous phase with varying concentrations of NaOH, for samples with 10 min and 60 min mixing times.
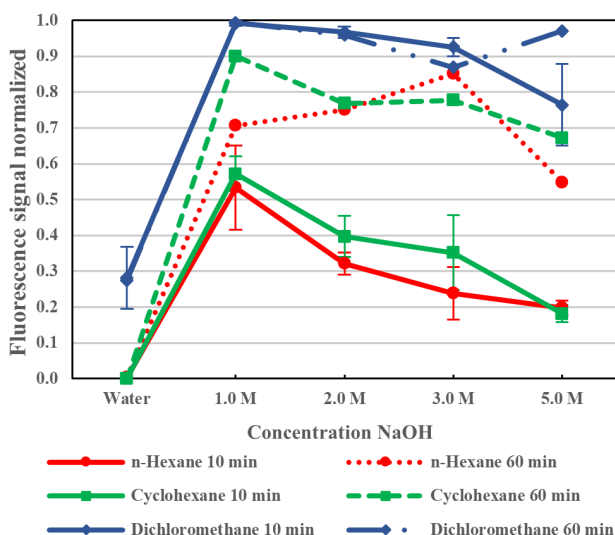
Figure 5.4: Normalised fluorescence signal from the aqueous phase after 10 and 60 minutes sample dissolution time. Excitation wavelength at 405 nm and emission wavelengths between 400 – 1100 nm. Measurements after 10 minutes are an average of triplicate tests.

The fluorescence signal varied with mixing time, organic solvent interaction and the NaOH concentration. An overall trend was an increased fluorescence signal when the sample was dissolved in an aqueous solution containing NaOH. The
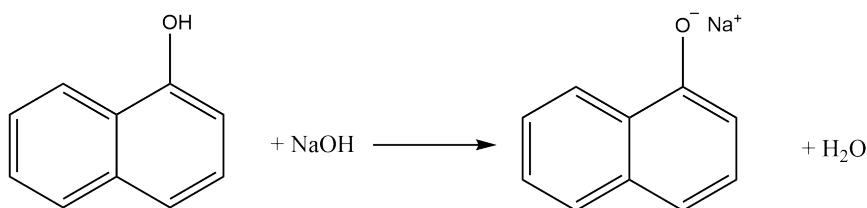
Figure 5.5: Acid base reaction between naphthol and sodium hydroxide creating a naphthol salt and water.

added hydroxyl ions could react with dissolved aromatic hydrocarbons, creating aromatic hydrocarbon salts by an acid-base reaction (example is shown in Figure 5.5. This reaction would increase the water solubility of the aromatic compounds and explain the increased fluorescence compared to the signal produced in pure water.

Similar analysis for the organic phase was performed and showed dichloromethane being a more efficient solvent for the condensed residue with a stronger fluorescence signal from the aromatic components compared to n-hexane and cyclohexane.

UHPLC-Fluorescence/UV and UHPLC-HRMS

The total PAH concentrations (Σ_{22} PAHs) found in the residue samples were similar (about 160 μg/g) and about 1.6 times higher than in the coal tar pitch raw material (about 95 μg/g). The aqueous sample showed concentrations of about 210 ng/ml. The PAH profile of coal tar pitch showed larger amounts of PAHs with 5 rings or more than found in the residue sample. The opposite was found in the water sample, where smaller PAH dominated (4 rings or less), which was expected as water solubility for PAHs decrease with increasing molecular weight.

The non targeted screening analyses showed characteristic SO_3^-- and/or HSO_4^--fragments in all the samples, which could indicate the presence of organic sulfate and sulfonate species. The same potential organic sulfate was detected in all the solid samples. For the aqueous sample, two organic sulfonates and one organic sulfate were detected. None of the standard sulfate or sulfonates organic compounds available were detected in any of the samples, but screening based on theoretical m/z of SO_3-PAHs highlighted the presence of methylnaphthalene sulfate in the aqueous sample (Figure 5.6).
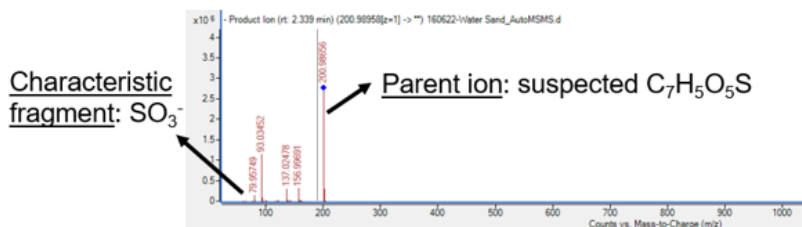
Figure 5.6: Example of aromatic sulfonate (probable SO3-PAH) detected in the aqueous sample.

5.4 Conclusions and Industrial Implications

Paper IV present the work of a multi-method study of condensed hydrocarbon residues from an aluminium anode baking off-gas cleaning facility with the intent to expand the knowledge of the mechanisms affecting PAH emissions at industrial conditions. Investigating the presence of polar and/or sulfur-substituted PACs outside the conventional EPA-16 PAH range was of particular interest as this has not been given much attention in the past and has implications of the potential PAH emissions to water.

The methods used to characterise the industrial residue samples each give different insights into the properties of the condensed off-gas treatment residue. ^{13}C-NMR and fluorescence spectroscopy analyses of the industrial residue confirmed the presence of both polar aromatic and aliphatic compounds in the sample. ICP-MS confirmed the presence of sulfur, and together with UHPLC-HRMS analysis highlighted the presence of sulfate and/or sulfonated aromatic species.

The analytical evidence seen together, suggest that the presence of polar aromatic hydrocarbons in the condensed residues, with properties unlike traditional PAH, was due to alkylation and/or substitution reactions which occurred during the creation of the raw materials, during the anode production or in the off-gas cleaning facility.

This study confirms the complexity of PAH chemistry in an industrial setting and suggests expanding the focus from the EPA-16 PAH to include a broader range of PAHs to aid with reducing the total PAH emissions to the air and water, which are receiving increasing focus for the future.

5.5   Future Work

- A natural continuation of this work would be to perform laboratory scale experiments to investigate the sulfonation reaction in detail using the raw materials for anode production at relevant conditions. A suggestion is to vary the oxygen levels to reflect the changes during a baking cycle and study the affect of the available oxygen on the reaction pathway. This would be of great value to expand the understanding of the mechanisms involving PAH transformation and/ or destruction.

- The analyses scope could be expanded to include oxygenated and hydroxide PAHs as these are potential substitution species and PAH degradation products. By including other decomposition products such as CO, CO_2 and H_2 more information could be used to evaluate the reaction mechanisms in greater detail.

- Continued method development of the analytical techniques sould be performed to better identify sulfate and sulfonate PAC species. This could be of great value with the future trends of increased sulfur in the raw materials and focus of reduced emissions in mind. In the review of Pulleyblank et al. [121], a historical view of progress and challenges are summarised for the detection of oxygenated PAHs. Here, key starting points for development are mentioned as collecting information on toxicology etc., occurrence in the environment and development of analytical methods. In the case of sulfonated PAH species, this work should be performed as it will be time and resource consuming and require further development in several areas of research such as source identification, sampling, handling and processing, synthesis of standards and analyses.

Chapter 6

Final Conclusions and Industrial Implications

The main objectives of this thesis work have been to investigate the emissions of polycyclic aromatic hydrocarbons from metal production processes through experimental work in laboratory and pilot-scale using industrially relevant materials and analysis of industrial samples. Special emphasis was put on extending the current knowledge related to a wider range of PAH spices, including substituted PAH, in connection to industrial process parameters.

From the pilot-scale silicon alloy production with flue gas recirculation conclusions were drawn on the effect of varying process conditions on evolution of PAHs, nitro- and oxy-PAHs:

- PAH emissions of native and substituted PAHs, 56 species in total, was influenced by the changing process conditions caused by flue gas recirculation. Both the level of flue gas recirculation and oxygen correlated with the PAH emissions and the emission levels rose with increasing flue gas recirculation and decreasing concentrations of oxygen. The poorer combustion conditions also influenced the amount of substituted PAHs produced and both oxy- and nitro-PAHs were produced in greater amounts than their parent PAHs at elevated flue gas recirculation levels.

- The molecular distribution of the PAH emissions was found to be influenced by temperature, component residence time, oxygen concentration, and the local reactions in the Si furnace, such as NO_x production. The changing process conditions caused by flue gas recirculation resulted in elevated

PAH emissions of lower molecular weight (bicyclic species) and species of greater thermal stability.

- With flue gas recirculation affecting the PAH species distribution, the given system and off-gas facility should be tailored to the process as to ensure reduction of the total emission of PAH to the atmosphere.

Laboratory scale experiments were performed to investigate the effect of temperature and atmosphere on EPA-16 PAH emissions from green anode paste used in pre-baked anodes production for aluminium electrolysis. These experiments led to the following conclusions:

- The profile of EPA-16 PAH emissions from the green anode paste in inert and CO_2 atmospheres followed the same trends, independent of CO_2 concentration. Emission levels peaked at temperatures close to 500 °C and was dominated by PAHs species of four- and five-rings.

- The emissions of EPA-16 PAH in atmospheres containing 5 and 10 % oxygen compared to inert and CO_2-containing atmospheres were reduced significantly, but with the current temperatures of maximum 750 °C, oxygen levels and residence time, complete combustion of PAHs was not achieved.

- In spite the level of total emissions being influenced by atmosphere, the level of four-ring PAHs was stable for all atmospheres as a result of varying molecular reactivity.

- In light of this work, continued focus on optimal and tailored combustion and post combustion of PAHs during the process and flue gas treatment for the industry is recommended.

Lastly, the characterisation of solid and liquid samples collected from an anode baking off-gas treatment facility, with specific focus on sulfur containing species, resulted in the following conclusions:

- ^{13}C-NMR and fluorescence spectroscopy analysis of the industrial residue sample confirmed the presence of both polar aromatic and aliphatic compounds in the sample.

- LC-HRMS analysis confirmed the presence of native PAHs and found differences in species distribution between the residue, coal tar pitch and aqueous samples. The residue and coal tar pitch were dominated by heavier species, and the aqueous sample was dominated by lighter species.

- ICP-MS and UHPLC-HRMS analyses showed the presence of sulfur and highlighted the presence of sulfate and/or sulfonated aromatic species in the samples.

- This study confirms the complexity of PAH chemistry in an industrial setting and suggests expanding the focus from the EPA-16 PAH to include a broader range of PAHs to aid with reducing the total PAH emissions to the air and water, which are receiving increasing focus for the future.

Chapter 7

Future Work

Detailed understanding of mechanisms for PAH formation and destruction for specific industrial processes within the metallurgical field is still lacking. The connection between PAH emissions and process conditions will have to be studied in a greater extent to broaden the general scope and include an increasing number of processes, conditions and carbon materials to eventually reduce atmospheric and aqueous emissions and human exposure. Recommendations for future work are presented based on knowledge and experiences gained from this current project.

- Continued small scale experiments are recommend as they provide detailed understanding and insight into the mechanisms of PAH reactivity and the following change caused by the surrounding conditions. A broad range of PAHs analysis and other combustion products, such as H_2O, H_2, CO and CO_2, are of interest to understand more of the mechanisms behind PAHs reactivity, thermal impact, oxidation reactions and variations between different carbon materials, together with a component mass balance. This would increase the cost of analysis significantly and it would therefor be recommended to have a well thought out experimental matrix and perhaps consider starting out with a broad scope of analysis, followed by a selection to study in detail together with gas analysis, and possible in-house analysis could decrease cost and provide continuous optimisation and follow-up.

- In future industrial/ pilot measurement campaigns for PAH it would be important to measure the initial phase of VOCs evaporation from the raw materials, which was not performed in this study. An expanded focus on smaller organic molecules such as acetylene (ethyne) and benzene could provide more information about the presence of PAH precursors and their role in

PAH formation and growth, as well as being an important addition to computational models describing and predicting PAH emission mechanisms.

- A learning outcome for the Si pilot-scale campaign was the connection between oxygen level and the distribution of PAH species in the off-gas. At a future pilot campaign with FGR, looking further into the details of this observation with additional PAH measurements could provide information on the efficiency of the off-gas cleaning/ filtering and how it is affected by the shift in the PAH emissions composition. In addition, PAH measurements after the filtering system could provide insight into the reactions occurring in the furnace and/or cell in more detail. Similar measurements could be performed at an industrial plant to correlate different process operations during production, and investigate the variations in molecular distribution at industrial scale and how this effects the off-gas cleaning efficiency.

- Investigating the presence of substituted PAHs in this work showed the importance of an extended PAH analysis to get a better understanding of the complexity of reactions involving PAHs. Much work have already been done to investigate oxygenated and nitrated PAH species, and with the extended knowledge, an increasing number of species are being studied and emissions are reported. This methodical work should also be performed for sulfonated PAH, starting with toxicology studies, continued analytical method development, production of analytical standards and measuring environment presence.

- Laboratory scale experiments should be done to investigate the sulfonation reaction using the raw materials for anode production at relevant conditions, i.e. various oxygen levels to reflect the changes during a baking cycle. This would be of great value to expand the understanding of the substitution reaction at industrial conditions. Expanding the analysis scope to include oxygenated and hydroxide PAHs, as these are other potential substitution species and degradation products of PAH, could contribute to understanding more of the complex mechanism for PAH substitution formation mechanisms and in addition, the role of water in the reactions as a source of oxygen and hydroxide radicals.

Bibliography

[1]   Hussein I. Abdel-Shafy and Mona S. M. Mansour. "A review on poly-cyclic aromatic hydrocarbons: Source, environmental impact, effect on human health and remediation". In: *Egyptian Journal of Petroleum* 25.1 (Mar. 2016), pp. 107–123. DOI: 10.1016/j.ejpe.2015.03.011. URL: http://www.sciencedirect.com/science/article/pii/S1110062114200237 (visited on 27/11/2018).

[2]   Miljøverndepartementet. *St.meld. nr. 21 (2004-2005)*. no. Stortingsmeld-ing. Mar. 2005. URL: https://www.regjeringen.no/no/dokumenter/stmeld-nr-21-2004-2005-/id406982/ (visited on 03/09/2018).

[3]   European Union. *Decision No 1386/2013/EU of the European Parliament and of the Council of 20 November 2013 on a General Union Environment Action Program to 2020 'Living well, within the limits of our planet' Text with EEA relevance*. en. Dec. 2013. URL: http://data.europa.eu/eli/dec/2013/1386/oj/eng (visited on 13/12/2018).

[4]   Huizhong Shen et al. "Global Atmospheric Emissions of Polycyclic Aro-matic Hydrocarbons from 1960 to 2008 and Future Predictions". In: *Envir-onmental Science & Technology* 47.12 (June 2013). Publisher: American Chemical Society, pp. 6415–6424. DOI: 10.1021/es400857z. URL: https://doi.org/10.1021/es400857z (visited on 23/09/2021).

[5]   Mike Howsam and Kevin C. Jones. "Sources of PAHs in the Environ-ment". en. In: *PAHs and Related Compounds: Chemistry*. Ed. by Alasdair H. Neilson. The Handbook of Environmental Chemistry. Berlin, Heidel-berg: Springer Berlin Heidelberg, 1998, pp. 137–174. ISBN: 978-3-540-49697-7. DOI: 10.1007/978-3-540-49697-7_4. URL: https://doi.org/10.1007/978-3-540-49697-7%5C_4 (visited on 18/06/2019).

[6]   *EMEP Centre on Emission Inventories and Projections*. en-US. 2023. URL: https://www.ceip.at/ (visited on 06/05/2023).

[7]   Norwegian Environmental Agency. *Polysykliske aromatiske hydrokarboner (PAH)*. nb. URL: https://miljostatus.miljodirektoratet.no/tema/miljogifter/prioriterte-miljogifter/polysykliske-aromatiske-hydrokarboner-pah/ (visited on 01/10/2021).

[8]   Arctic Monitoring and Assessment Programme (AMAP). *AMAP Assessment 2016: Chemicals of Emerging Arctic Concern*. en. Technical Report. Accepted: 2018-01-29T12:53:58Z ISBN: 9788279711049. Arctic Monitoring and Assessment Programme (AMAP), Dec. 2017. URL: https://oaarchive.arctic-council.org/handle/11374/2115 (visited on 23/09/2021).

[9]   Jan T. Andersson and Christine Achten. "Time to Say Goodbye to the 16 EPA PAHs? Toward an Up-to-Date Use of PACs for Environmental Purposes". In: *Polycyclic Aromatic Compounds* 35.2-4 (Mar. 2015), pp. 330–354. ISSN: 1040-6638. DOI: 10.1080/10406638.2014.991042. URL: https://doi.org/10.1080/10406638.2014.991042 (visited on 13/05/2019).

[10] *Norwegian Environmental Agency, Norske utslipp - Utslipp til luft og vann og generert avfall, PAH-16-USEPA*. URL: https://www.norskeutslipp.no/no/Komponenter/Utslipp/PAH-16-USEPA/?ComponentType=utslipp%5C&ComponentPageID=1155 (visited on 01/10/2021).

[11] Ida Teresia Kero, Per Anders Eidem, Yan Ma, Hege Indresand, Thor Anders Aarhaug and Svend Grådahl. "Airborne Emissions from Mn Ferroalloy Production". en. In: *JOM* (Oct. 2018). ISSN: 1543-1851. DOI: 10.1007/s11837-018-3165-9. URL: https://doi.org/10.1007/s11837-018-3165-9 (visited on 10/10/2018).

[12] Ronald G. Harvey. "Environmental Chemistry of PAHs". en. In: *PAHs and Related Compounds: Chemistry*. Ed. by Alasdair H. Neilson. The Handbook of Environmental Chemistry. Berlin, Heidelberg: Springer Berlin Heidelberg, 1998, pp. 1–54. ISBN: 978-3-540-49697-7. DOI: 10.1007/978-3-540-49697-7_1. URL: https://doi.org/10.1007/978-3-540-49697-7%5C_1 (visited on 18/06/2019).

[13] Christine Achten and Jan Andersson. "Overview of Polycyclic Aromatic Compounds (PAC)". In: *Polycyclic Aromatic Compounds* 35 (Mar. 2015). DOI: 10.1080/10406638.2014.994071.

[14] Terry F. Bidleman, W. Neil. Billings and William T. Foreman. "Vapor-particle partitioning of semivolatile organic compounds: estimates from field collections". In: *Environmental Science & Technology* 20.10 (1986),

pp. 1038–1043. DOI: 10.1021/es00152a013. URL: https://pubs.acs.org/doi/abs/10.1021/es00152a013 (visited on 23/08/2021).

[15]   Fatma Esen, S. Siddik Cindoruk and Yücel Tasdemir. "Ambient Concentrations and Gas/Particle Partitioning of Polycyclic Aromatic Hydrocarbons in an Urban Site in Turkey". In: *Environmental Forensics* 7.4 (Dec. 2006), pp. 303–312. ISSN: 1527-5922. DOI: 10.1080/15275920600996099. URL: https://doi.org/10.1080/15275920600996099 (visited on 23/08/2021).

[16]   Paula Yurkanis Bruice. *Essential organic chemistry*. eng. 2nd ed., Pearson new international ed. Essex: Pearson, 2014. ISBN: 978-1-292-02081-5.

[17]   Stanley E. Manahan. *Environmental chemistry*. eng. 9th ed. Boca Raton, Fla: CRC Press, 2010. ISBN: 978-1-4200-5920-5.

[18]   Susan C. Wilson and Kevin C. Jones. "Bioremediation of soil contaminated with polynuclear aromatic hydrocarbons (PAHs): A review". en. In: *Environmental Pollution* 81.3 (Jan. 1993), pp. 229–249. ISSN: 0269-7491. DOI: 10.1016/0269-7491(93)90206-4. URL: https://www.sciencedirect.com/science/article/pii/0269749193902064 (visited on 12/01/2023).

[19]   Jordi Poater, Miquel Duran and Miquel Solà. "Aromaticity Determines the Relative Stability of Kinked vs. Straight Topologies in Polycyclic Aromatic Hydrocarbons". In: *Frontiers in Chemistry* 6 (2018). ISSN: 2296-2646. DOI: 10.3389/fchem.2018.00561. URL: https://www.frontiersin.org/articles/10.3389/fchem.2018.00561 (visited on 16/11/2022).

[20]   Gabriela L. Borosky. "Theoretical Study Related to the Carcinogenic Activity of Polycyclic Aromatic Hydrocarbon Derivatives". In: *The Journal of Organic Chemistry* 64.21 (Oct. 1999). Publisher: American Chemical Society, pp. 7738–7744. ISSN: 0022-3263. DOI: 10.1021/jo990545f. URL: https://doi.org/10.1021/jo990545f (visited on 06/01/2023).

[21]   Luke Ukiwe, Ubaezue Egereonu, Pascal Njoku, Christopher Nwoko and Jude Allinor. "Polycyclic Aromatic Hydrocarbons Degradation Techniques: A Review". en. In: *International Journal of Chemistry* 5.4 (Sept. 2013). Number: 4, p43. ISSN: 1916-9698. DOI: 10.5539/ijc.v5n4p43. URL: https://ccsenet.org/journal/index.php/ijc/article/view/30512 (visited on 16/11/2022).

[22]   *World Health Organization, Agents Classified by the IARC Monographs, Volumes 1–132 – IARC Monographs on the Identification of Carcinogenic Hazards to Humans*. 2022. URL: https://monographs.iarc.who.int/agents-classified-by-the-iarc/ (visited on 12/01/2023).

[23] Thamaraiselvan Rengarajan, Peramaiyan Rajendran, Natarajan Nandaku-
      mar, Boopathy Lokeshkumar, Palaniswami Rajendran and Ikuo Nishigaki.
      "Exposure to polycyclic aromatic hydrocarbons with special focus on can-
      cer". In: *Asian Pacific Journal of Tropical Biomedicine* 5.3 (2015), pp. 182–
      189. DOI: 10.1016/S2221-1691(15)30003-4. URL: http://www.sciencedirect.
      com/science/article/pii/S2221169115300034 (visited on 30/10/2018).

[24] Laurence A. Moran, David Rawn, Gary Scrimgeour, Marc Horton Perry,
      Robert A. Horton and Moran Horton. *Principles of biochemistry*. eng. 5th
      ed. Boston: Pearson, 2012. ISBN: 978-0-321-79579-3.

[25] H Richter and J. B Howard. "Formation of polycyclic aromatic hydrocar-
      bons and their growth to soot—a review of chemical reaction pathways".
      In: *Progress in Energy and Combustion Science* 26.4 (2000), pp. 565–608.
      DOI: 10.1016/S0360-1285(00)00009-5. URL: http://www.sciencedirect.
      com/science/article/pii/S0360128500000095 (visited on 29/11/2018).

[26] Edina Reizer, Béla Viskolcz and Béla Fiser. "Formation and growth mech-
      anisms of polycyclic aromatic hydrocarbons: A mini-review". In: *Chemo-
      sphere* 291 (Mar. 2022), p. 132793. DOI: 10.1016/j.chemosphere.2021.
      132793. (Visited on 21/12/2022).

[27] Md Obaidullah, Svend Bram and Jacques De Ruyck. "Characteristics of
      Particle Mass Concentrations from Small Scale Biomass Combustion: A
      Review". In: Cuba, Feb. 2012. ISBN: 978-959-250-693-0.

[28] Michael Frenklach, David W. Clary, William C. Gardiner and Stephen E.
      Stein. "Detailed kinetic modeling of soot formation in shock-tube pyro-
      lysis of acetylene". In: *Symposium (International) on Combustion*. Twen-
      tieth Symposium (International) on Combustion 20.1 (1985), pp. 887–901.
      ISSN: 0082-0784. DOI: 10.1016/S0082-0784(85)80578-6. URL: https:
      //www.sciencedirect.com/science/article/pii/S0082078485805786 (visited
      on 09/03/2023).

[29] Long Zhao, Ralf I. Kaiser, Bo Xu, Utuq Ablikim, Musahid Ahmed, Marsel
      V. Zagidullin, Valeriy N. Azyazov, A. Hasan Howlader, Stanislaw F. Wnuk
      and Alexander M. Mebel. "VUV Photoionization Study of the Formation
      of the Simplest Polycyclic Aromatic Hydrocarbon: Naphthalene (C10H8)".
      In: *The Journal of Physical Chemistry Letters* 9.10 (May 2018). Publisher:
      American Chemical Society, pp. 2620–2626. DOI: 10.1021/acs.jpclett.
      8b01020. URL: https://doi.org/10.1021/acs.jpclett.8b01020 (visited on
      09/03/2023).

[30] Long Zhao, Ralf I. Kaiser, Bo Xu, Utuq Ablikim, Musahid Ahmed, Mikhail M. Evseev, Eugene K. Bashkirov, Valeriy N. Azyazov and Alexander M. Mebel. "Low-temperature formation of polycyclic aromatic hydrocarbons in Titan's atmosphere". en. In: *Nature Astronomy* 2.12 (Dec. 2018). Number: 12 Publisher: Nature Publishing Group, pp. 973–979. ISSN: 2397-3366. DOI: 10.1038/s41550-018-0585-y. URL: https://www.nature.com/articles/s41550-018-0585-y (visited on 09/03/2023).

[31] Maia Weissman and Sydney W. Benson. "Pyrolysis of methyl chloride, a pathway in the chlorine-catalyzed polymerization of methane". en. In: *International Journal of Chemical Kinetics* 16.4 (1984), pp. 307–333. ISSN: 1097-4601. DOI: 10.1002/kin.550160403. URL: https://onlinelibrary.wiley.com/doi/abs/10.1002/kin.550160403 (visited on 10/03/2023).

[32] Bikau Shukla, Akira Miyoshi and Mitsuo Koshi. "Role of Methyl Radicals in the Growth of PAHs". en. In: *Journal of the American Society for Mass Spectrometry* 21.4 (Apr. 2010), pp. 534–544. ISSN: 1044-0305. DOI: 10.1016/j.jasms.2009.12.019. URL: https://www.sciencedirect.com/science/article/pii/S1044030510000036 (visited on 10/03/2023).

[33] Alan R. Katritzky, Myong Sang Kim, Dmytro Fedoseyenko, Khalid Widyan, Mike Siskin and Manuel Francisco. "The sulfonation of aromatic and heteroaromatic polycyclic compounds". In: *Tetrahedron* 65.6 (Feb. 2009). ISSN: 0040-4020. DOI: 10.1016/j.tet.2008.11.023. URL: http://www.sciencedirect.com/science/article/pii/S0040402008019613 (visited on 07/05/2019).

[34] Layne Morsch and Steven Farmer. *16.2: Other Aromatic Substitutions*. 2015. URL: https://chem.libretexts.org/Bookshelves/Organic_Chemistry/Organic_Chemistry_(LibreTexts)/16%3A_Chemistry_of_Benzene_-_Electrophilic_Aromatic_Substitution/16.02%3A_Other_Aromatic_Substitutions (visited on 19/01/2023).

[35] Benjamin A. Musa Bandowe and Hannah Meusel. "Nitrated polycyclic aromatic hydrocarbons (nitro-PAHs) in the environment – A review". en. In: *Science of The Total Environment* 581-582 (Mar. 2017), pp. 237–257. ISSN: 0048-9697. DOI: 10.1016/j.scitotenv.2016.12.115. URL: https://www.sciencedirect.com/science/article/pii/S0048969716328030 (visited on 16/12/2021).

[36] Alexandre Albinet, Eva Leoz-Garziandia, Helene Budzinski, Eric Villenave and Jean-Luc Jaffrezo. "Nitrated and oxygenated derivatives of polycyclic aromatic hydrocarbons in the ambient air of two French alpine valleys: Part 1: Concentrations, sources and gas/particle partitioning". In: *Atmospheric*

Environment 42.1 (2008), pp. 43–54. ISSN: 1352-2310. DOI: 10.1016/j. atmosenv.2007.10.009. URL: https://www.sciencedirect.com/science/article/pii/S1352231007008965 (visited on 30/01/2023).

[37] Matteo Carrara, Jan-Christoph Wolf and Reinhard Niessner. "Nitro-PAH formation studied by interacting artificially PAH-coated soot aerosol with NO2 in the temperature range of 295–523K". en. In: *Atmospheric Environment* 44.32 (Oct. 2010), pp. 3878–3885. ISSN: 1352-2310. DOI: 10.1016/j.atmosenv.2010.07.032. URL: https://www.sciencedirect.com/science/article/pii/S1352231010006011 (visited on 30/01/2023).

[38] Martin Nottebohm and Tobias Licha. "Detection of Naphthalene Sulfonates from Highly Saline Brines with High-Performance Liquid Chromatography in Conjunction with Fluorescence Detection and Solid-Phase Extraction". In: *Journal of Chromatographic Science* 50.6 (July 2012), pp. 477–481. DOI: 10.1093/chromsci/bms029. URL: https://academic.oup.com/chromsci/article/50/6/477/326148 (visited on 07/02/2019).

[39] Amy I. H. Hrdina, Ishwar N. Kohale, Simran Kaushal, Jamie Kelly, Noelle E. Selin, Bevin P. Engelward and Jesse H. Kroll. "The Parallel Transformations of Polycyclic Aromatic Hydrocarbons in the Body and in the Atmosphere". In: *Environmental Health Perspectives* 130.2 (2022). DOI: 10.1289/EHP9984. URL: https://ehp.niehs.nih.gov/doi/full/10.1289/EHP9984 (visited on 01/02/2023).

[40] Janet Arey, Barbara Zielinska, Roger Atkinson, Arthur M. Winer, Thomas Ramdahl and James N. Pitts. "The formation of nitro-PAH from the gas-phase reactions of fluoranthene and pyrene with the OH radical in the presence of NOx". en. In: *Atmospheric Environment (1967)* 20.12 (Jan. 1986), pp. 2339–2345. ISSN: 0004-6981. DOI: 10.1016/0004-6981(86)90064-8. URL: https://www.sciencedirect.com/science/article/pii/0004698186900648 (visited on 30/01/2023).

[41] R. Ana Gimeno, A. F. Maarten Altelaar, Rosa M. Marcé and Francesc Borrull. "Determination of polycyclic aromatic hydrocarbons and polycylic aromatic sulfur heterocycles by high-performance liquid chromatography with fluorescence and atmospheric pressure chemical ionization mass spectrometry detection in seawater and sediment samples". In: *Journal of Chromatography A* 958.1 (2002), pp. 141–148. ISSN: 0021-9673. DOI: 10.1016/S0021-9673(02)00386-2. URL: http://www.sciencedirect.com/science/article/pii/S0021967302003862 (visited on 10/05/2019).

[42] Amy E. Witter and Minh H. Nguyen. "Determination of oxygen, nitrogen, and sulfur-containing polycyclic aromatic hydrocarbons (PAHs) in urban

stream sediments". In: *Environmental Pollution* 209 (Feb. 2016), pp. 186–196. ISSN: 0269-7491. DOI: 10.1016/j.envpol.2015.10.037. URL: http://www.sciencedirect.com/science/article/pii/S026974911530138X (visited on 21/06/2019).

[43] Christophe Walgraeve, Kristof Demeestere, Jo Dewulf, Ralf Zimmermann and Herman Van Langenhove. "Oxygenated polycyclic aromatic hydrocarbons in atmospheric particulate matter: Molecular characterization and occurrence". en. In: *Atmospheric Environment* 44.15 (May 2010), pp. 1831–1846. ISSN: 1352-2310. DOI: 10.1016/j.atmosenv.2009.12.004. URL: https://www.sciencedirect.com/science/article/pii/S1352231009010140 (visited on 07/02/2023).

[44] Norbert V. Heeb et al. "Secondary Effects of Catalytic Diesel Particulate Filters: Conversion of PAHs versus Formation of Nitro-PAHs". In: *Environmental Science & Technology* 42.10 (May 2008), pp. 3773–3779. ISSN: 0013-936X. DOI: 10.1021/es7026949. URL: https://doi.org/10.1021/es7026949 (visited on 02/02/2023).

[45] Kazuichi Hayakawa. "Environmental Behaviors and Toxicities of Polycyclic Aromatic Hydrocarbons and Nitropolycyclic Aromatic Hydrocarbons". In: *Chemical and Pharmaceutical Bulletin* 64.2 (2016), pp. 83–94. DOI: 10.1248/cpb.c15-00801.

[46] Tatiana Drotikova, Aasim M. Ali, Anne Karine Halse, Helena C. Reinardy and Roland Kallenborn. "Polycyclic aromatic hydrocarbons (PAHs) and oxy- and nitro-PAHs in ambient air of the Arctic town Longyearbyen, Svalbard". English. In: *Atmospheric Chemistry and Physics* 20.16 (Aug. 2020), pp. 9997–10014. ISSN: 1680-7316. DOI: 10.5194/acp-20-9997-2020. URL: https://acp.copernicus.org/articles/20/9997/2020/ (visited on 06/02/2023).

[47] Inaki Adánez-Rubio, Fausto Viteri, Ángela Millera, Rafael Bilbao and Maria U. Alzueta. "S-PAH, oxy-PAH and EPA-PAH formation during ethylene-SO2 pyrolysis". In: *Fuel Processing Technology* 182 (2018), pp. 68–76. ISSN: 0378-3820. DOI: 10.1016/j.fuproc.2018.10.018. URL: http://www.sciencedirect.com/science/article/pii/S0378382018316606 (visited on 20/11/2018).

[48] Thorsten Streibel, Fabian Mühlberger, Robert Geißler, Mohammad Saraji-Bozorgzad, Thomas Adam and Ralf Zimmermann. "Influence of sulphur addition on emissions of polycyclic aromatic hydrocarbons during biomass combustion". In: *Proceedings of the Combustion Institute* 35.2 (2015). ISSN: 1540-7489. DOI: 10.1016/j.proci.2014.07.046. URL: http://www.

sciencedirect . com / science / article / pii / S1540748914003563 (visited on 10/05/2019).

[49]   Tayssir Kadri, Tarek Rouissi, Satinder Kaur Brar, Maximiliano Cledon, Saurabhjyoti Sarma and Mausam Verma. "Biodegradation of polycyclic aromatic hydrocarbons (PAHs) by fungal enzymes: A review". In: *Journal of Environmental Sciences* 51 (Jan. 2017), pp. 52–74. ISSN: 1001-0742. DOI: 10.1016/j.jes.2016.08.023. URL: http://www.sciencedirect.com/ science/article/pii/S1001074216306167 (visited on 03/12/2018).

[50]   James G. Speight. "Chapter 10 - Combustion of Hydrocarbons". en. In: *Handbook of Industrial Hydrocarbon Processes*. Ed. by James G. Speight. Boston: Gulf Professional Publishing, Jan. 2011, pp. 355–393. ISBN: 978-0-7506-8632-7. DOI: 10.1016/B978-0-7506-8632-7.10010-6. URL: https: //www.sciencedirect.com/science/article/pii/B9780750686327100106 (visited on 10/03/2023).

[51]   Shiju Thomas and Mary J. Wornat. "The effects of oxygen on the yields of polycyclic aromatic hydrocarbons formed during the pyrolysis and fuel-rich oxidation of catechol". en. In: *Fuel* 87.6 (May 2008), pp. 768–781. ISSN: 0016-2361. DOI: 10.1016/j.fuel.2007.07.016. URL: https://www. sciencedirect . com / science / article / pii / S0016236107003353 (visited on 02/02/2023).

[52]   Chao Gai, Yuping Dong, Shuai Yang, Zhaoling Zhang, Jingcui Liang and Jingdong Li. "Thermal decomposition kinetics of light polycyclic aromatic hydrocarbons as surrogate biomass tar". en. In: *RSC Advances* 6.86 (Aug. 2016), pp. 83154–83162. ISSN: 2046-2069. DOI: 10.1039/C6RA15513H. URL: https://pubs.rsc.org/en/content/articlelanding/2016/ra/c6ra15513h (visited on 03/12/2018).

[53]   Ping Sun. "Investigation of polycyclic aromatic hydrocarbons (PAHs) on dry flue gas desulfurization (FGD) by-products". PhD thesis. The Ohio State University, 2004. URL: https://etd.ohiolink.edu (visited on 18/01/2023).

[54]   Kunlei Liu, Wenjun Han, Wei-Ping Pan and John T Riley. "Polycyclic aromatic hydrocarbon (PAH) emissions from a coal-fired pilot FBC system". en. In: *Journal of Hazardous Materials* 84.2 (June 2001), pp. 175–188. ISSN: 0304-3894. DOI: 10.1016/S0304-3894(01)00196-0. (Visited on 06/01/2023).

[55]   Joanna Łojewska and Andrzej Kołodziej. "Chapter 16 - Advances in Catalyst and Process Design for Air Pollutants Abatement". en. In: *New and Future Developments in Catalysis*. Ed. by Steven L. Suib. Amsterdam: Elsevier, Jan. 2013, pp. 461–486. ISBN: 978-0-444-53870-3. DOI: 10.1016/

B978- 0- 444- 53870- 3.00018- 6. URL: https://www.sciencedirect.com/
science/article/pii/B9780444538703000186 (visited on 20/04/2023).

[56]   Z. Gerald Liu, John C. Wall, Nathan A. Ottinger and Dana McGuffin.
        "Mitigation of PAH and Nitro-PAH Emissions from Nonroad Diesel En-
        gines". In: *Environmental Science & Technology* 49.6 (Mar. 2015). Pub-
        lisher: American Chemical Society, pp. 3662–3671. ISSN: 0013-936X. DOI:
        10.1021/es505434r. URL: https://doi.org/10.1021/es505434r (visited on
        08/02/2023).

[57]   Iori Shimada, Chiaki Uno, Yuta Watanabe and Toru Takatsuka. "Catalytic
        cracking of three-ring polycyclic aromatic hydrocarbons in the presence
        of hydrogen donors". en. In: *Fuel Processing Technology* 232 (July 2022),
        p. 107267. ISSN: 0378-3820. DOI: 10.1016/j.fuproc.2022.107267. URL:
        https://www.sciencedirect.com/science/article/pii/S0378382022001072
        (visited on 20/04/2023).

[58]   Richard Pujro, Marisa Falco and Ulises Sedran. "Catalytic Cracking of
        Heavy Aromatics and Polycyclic Aromatic Hydrocarbons over Fluidized
        Catalytic Cracking Catalysts". In: *Energy & Fuels* 29.3 (Mar. 2015), pp. 1543–
        1549. ISSN: 0887-0624. DOI: 10.1021/ef502707w. (Visited on 01/04/2023).

[59]   Gajendra Kumar Gaurav, Tariq Mehmood, Manoj Kumar, Liu Cheng, Kup-
        pusamy Sathishkumar, Amit Kumar and Deepak Yadav. "Review on poly-
        cyclic aromatic hydrocarbons (PAHs) migration from wastewater". en. In:
        Journal of Contaminant Hydrology 236 (Jan. 2021), p. 103715. ISSN: 0169-
        7722. DOI: 10.1016/j.jconhyd.2020.103715. URL: https://www.sciencedirect.
        com/science/article/pii/S0169772220303041 (visited on 10/03/2023).

[60]   James G. Speight. "Chapter 2 - Organic Chemistry". In: *Environmental
        Organic Chemistry for Engineers*. Ed. by James G. Speight. Butterworth-
        Heinemann, Jan. 2017, pp. 43–86. ISBN: 978-0-12-804492-6. DOI: 10 .
        1016/B978- 0- 12- 804492- 6.00002- 2. URL: http://www.sciencedirect.
        com/science/article/pii/B9780128044926000022 (visited on 20/11/2018).

[61]   Brendan J. McConkey, L. Mark Hewitt, David G. Dixon and Benjamin
        M. Greenberg. "Natural Sunlight Induced Photooxidation of Naphthalene
        in Aqueous Solution". en. In: *Water, Air, and Soil Pollution* 136.1 (May
        2002), pp. 347–359. ISSN: 1573-2932. DOI: 10.1023/A:1015223806182.
        URL: https://doi.org/10.1023/A:1015223806182 (visited on 16/04/2023).

[62]   Anil. K. Haritash and Chetan P. Kaushik. "Biodegradation aspects of Poly-
        cyclic Aromatic Hydrocarbons (PAHs): A review". In: *Journal of Haz-
        ardous Materials* 169.1 (Sept. 2009), pp. 1–15. ISSN: 0304-3894. DOI:

10.1016/j.jhazmat.2009.03.137. URL: http://www.sciencedirect.com/science/article/pii/S0304389409005494 (visited on 03/12/2018).

[63]   Ellen H. M. Moors. "Technology strategies for sustainable metals production systems: a case study of primary aluminium production in The Netherlands and Norway". en. In: *Journal of Cleaner Production*. Improving Environmental, Economic and Ethical Performance in the Mining Industry. Part 2. Life cycle and process analysis and technical issues (Jan. 2006). ISSN: 0959-6526. DOI: 10.1016/j.jclepro.2004.08.005. URL: https://www.sciencedirect.com/science/article/pii/S0959652605000594 (visited on 08/09/2022).

[64]   Trond Brandvik, Zhaohui Wang, Arne Petter Ratvik and Tor Grande. "Autopsy of refractory lining in anode kilns with open and closed design". In: *International Journal of Applied Ceramic Technology* (2019). ISSN: 1744-7402. DOI: 10.1111/ijac.13108. (Visited on 08/09/2022).

[65]   Abdul Raouf Tajik, Tariq Shamim, Rashid K Abu Al-Rub and Mouna Zaidani. "Performance Analysis of a Horizontal Anode Baking Furnace for Aluminum Production". en. In: Muscat, Oman, 2017.

[66]   Les Edwards. "The History and Future Challenges of Calcined Petroleum Coke Production and Use in Aluminum Smelting". en. In: *JOM* (Feb. 2015). ISSN: 1543-1851. DOI: 10.1007/s11837-014-1248-9. URL: https://doi.org/10.1007/s11837-014-1248-9 (visited on 08/09/2022).

[67]   Mira Legin-Kolar and Dubravka Ugarković. "Petroleum coke structure: Influence of feedstock composition". en. In: *Carbon* (Jan. 1993). ISSN: 0008-6223. DOI: 10.1016/0008-6223(93)90043-A. URL: https://www.sciencedirect.com/science/article/pii/000862239390043A (visited on 08/09/2022).

[68]   Jin Xiao, Qifan Zhong, Fachuang Li, Jindi Huang, Yanbin Zhang and Bingjie Wang. "Modeling the Change of Green Coke to Calcined Coke Using Qingdao High-Sulfur Petroleum Coke". In: *Energy & Fuels* (May 2015). Publisher: American Chemical Society. ISSN: 0887-0624. DOI: 10.1021/acs.energyfuels.5b00021. URL: https://doi.org/10.1021/acs.energyfuels.5b00021 (visited on 08/09/2022).

[69]   Gøril Jahrsengene. "Coke impurity characterisation and electrochemical performance of carbon anodes for aluminium production". PhD thesis. Trondheim: Norwegian University of Science and Technology, 2019.

[70]   Kamilla Arnesen, Alexandre Albinet, Claudine Chatellier, Nina Huynh, Thor Anders Aarhaug, Kristian Etienne Einarsrud and Gabriella Tranell. "Characterization of Industrial Hydrocarbon Samples from Anode Baking Furnace Off-Gas Treatment Facility". en. In: *Light Metals 2023*. Ed. by Stephan Broek. The Minerals, Metals & Materials Series. Cham: Springer Nature Switzerland, 2023, pp. 680–687. ISBN: 978-3-031-22532-1. DOI: 10.1007/978-3-031-22532-1_91.

[71]   Trond Brandvik, Heiko Gaertner, Arne P. Ratvik, Tor Grande and Thor A. Aarhaug. "In Situ Monitoring of Pit Gas Composition During Baking of Anodes for Aluminum Electrolysis". In: *Metallurgical and Materials Transactions B* (Jan. 2019). ISSN: 1543-1916. DOI: 10.1007/s11663-018-1500-8. (Visited on 15/02/2019).

[72]   Qifan Zhong, Jin Xiao, Haojin Du and Zhen Yao. "Thiophenic Sulfur Transformation in a Carbon Anode during the Aluminum Electrolysis Process". In: *Energy & Fuels* (Apr. 2017). Publisher: American Chemical Society. ISSN: 0887-0624. DOI: 10.1021/acs.energyfuels.6b03018. URL: https://doi.org/10.1021/acs.energyfuels.6b03018 (visited on 08/09/2022).

[73]   Carl Behrens, Oscar Espeland and Bjarne Nenseter. "Emissions of dioxins and VOC's from the Årdal carbon plant". en. In: *Light Metals*. The Minerals, Metals & Materials Series. Springer International Publishing, 2007.

[74]   Thor Anders Aarhaug and Arne Petter Ratvik. "Aluminium Primary Production Off-Gas Composition and Emissions: An Overview". en. In: *JOM* 71.9 (Sept. 2019), pp. 2966–2977. ISSN: 1543-1851. DOI: 10.1007/s11837-019-03370-6. URL: https://doi.org/10.1007/s11837-019-03370-6 (visited on 11/04/2023).

[75]   Norwegian Environmental Agency. *Norske utslipp - Utslipp til luft og vann og generert avfall, PAH-16-USEPA*. Publication Title: Norske Utslipp. URL: https://www.norskeutslipp.no/no/Komponenter/Utslipp/PAH-16-USEPA/?ComponentType=utslipp&ComponentPageID=1155 (visited on 01/10/2021).

[76]   Viktor Myrvågnes. *Analyses and Characterization of Fossil Carbonaceous Materials for Silicon Production*. eng. Fakultet for naturvitenskap og teknologi, 2008. ISBN: 978-82-471-6485-3. URL: https://ntnuopen.ntnu.no/ntnu-xmlui/handle/11250/248717 (visited on 03/04/2019).

[77]   Anders Schei, Johan Tuset and Halvard Tveit. *Production of high silicon alloys*. eng. Trondheim: Tapir, 1998. ISBN: 978-82-519-1317-1.

[78] Ida Kero, Svend Grådahl and Gabriella Tranell. "Airborne Emissions from Si/FeSi Production". en. In: *JOM* 69.2 (Feb. 2017), pp. 365–380. ISSN: 1543-1851. DOI: 10.1007/s11837-016-2149-x. URL: https://doi.org/10.1007/s11837-016-2149-x (visited on 06/09/2018).

[79] Nils Eivind Kamfjord. "Mass and energy balances of the silicon process : improved emission standards". eng. PhD thesis. Trondheim: Norwegian University of Science and Technology, 2012.

[80] Trygve Eidet and Øyvind Mikkelsen. "PAH-free binders in metallurgical carbon pastes". In: *The 15th International Ferroalloys Congress INFACON XV, Cape Town, South Africa*. Ed. by R.T. Jones, P. den Hoed and M W Erwee. Cape Town: Southern African Institute of Mining and Metallurgy, 2018.

[81] Heiko Gaertner, T. A. Aarhaug, B. Wittgens, Leif Hunsbedt, Mildrid Legård and Gabriella Tranell. "Measurements of PAH emissions in the ferro-alloy industry". In: *The 15th International Ferroalloys Congress INFACON XV*. Cape Town: Southern African Institute of Mining and Metallurgy, 2018.

[82] Ray Sinnott and Gavin Towler. *Chemical Engineering Design: SI edition*. Oxford, United kingdom: Elsevier Science & Technology, 2009. ISBN: 978-0-08-094249-0. URL: http://ebookcentral.proquest.com/lib/ntnu/detail.action?docID=802531 (visited on 08/03/2023).

[83] Peter Quicker. "Waste, 7. Thermal Treatment". en. In: *Ullmann's Encyclopedia of Industrial Chemistry*. John Wiley & Sons, Ltd, 2020, pp. 1–54. ISBN: 978-3-527-30673-2. URL: https://onlinelibrary.wiley.com/doi/abs/10.1002/14356007.w28_w02 (visited on 19/04/2023).

[84] Frederik Neuwahl, Gianluca Cusano, BENAVIDES Jorge Gómez, Simon Holbrook and Serge Roudier. *Best Available Techniques (BAT) Reference Document for Waste Incineration: Industrial Emissions Directive 2010/75/EU (Integrated Pollution Prevention and Control)*. en. ISBN: 9789276129936 ISSN: 1831-9424. Jan. 2020. DOI: 10.2760/761437. URL: https://publications.jrc.ec.europa.eu/repository/handle/JRC118637 (visited on 01/04/2023).

[85] Changming Li, Lin Huangfu, Jianling Li, Shiqiu Gao, Guangwen Xu and Jian Yu. "Recent advances in catalytic filters for integrated removal of dust and NOx from flue gas: fundamentals and applications". en. In: *Resources Chemicals and Materials* 1.3 (Sept. 2022), pp. 275–289. ISSN: 2772-4433. DOI: 10.1016/j.recm.2022.06.002. URL: https://www.sciencedirect.com/science/article/pii/S2772443322000228 (visited on 19/04/2023).

[86] *Catalytic Products International - What is a regenerative thermal oxidizer?* URL: https://www.cpilink.com/ (visited on 10/05/2023).

[87] Hege Indresand and Ida T. Kero. *Polycyclic aromatic hydrocarbons (PAH) in industrial emissions - Challenges and strategies to measure, monitor, control and reduce PAH emissions*. eng. Accepted: 2023-01-13T13:35:58Z Journal Abbreviation: Polycyclic aromatic hydrocarbons (PAH) in industrial emissions - Challenges and strategies to measure, monitor, control and reduce PAH emissions Publication Title: 23. SINTEF AS, 2022. ISBN: 978-82-14-07577-9. URL: https://sintef.brage.unit.no/sintef-xmlui/handle/11250/3043416 (visited on 13/01/2023).

[88] International Organization for Standardization. *ISO 11338-1:2003 Stationary source emissions — Determination of gas and particle-phase polycyclic aromatic hydrocarbons — Part 1: Sampling*. en. URL: https://www.iso.org/standard/32903.html (visited on 31/01/2023).

[89] Kamilla Arnesen, Kurian J. Vachaparambil, Vegar Andersen, Balram Panjwani, Katarina Jakovljevic, Ellen Katrin Enge, Heiko Gaertner, Thor Anders Aarhaug, Kristian Etienne Einarsrud and Gabriella Tranell. "Analysis of Polycyclic Aromatic Hydrocarbon Emissions from a Pilot Scale Silicon Process with Flue Gas Recirculation". In: *Industrial & Engineering Chemistry Research* 62.19 (May 2023). Publisher: American Chemical Society, pp. 7525–7538. ISSN: 0888-5885. DOI: 10.1021/acs.iecr.2c04578. URL: https://doi.org/10.1021/acs.iecr.2c04578 (visited on 20/06/2023).

[90] Alf Bjørseth. *Handbook of polycyclic aromatic hydrocarbons*. eng. United States: Marcel Dekker,New York, NY, 1983.

[91] Ole S. Kjos, Thor Anders Aarhaug, Bernd Wittgens and Anders Brunsvik. "At-Line Analysis of Polycyclic Aromatic Hydrocarbons in Aluminium Primary Production". In: *Light Metals 2014*. Wiley Blackwell, 2014, pp. 541–546. ISBN: 978-1-118-88843-8.

[92] Ole S. Kjos, Thor Aarhaug, Heiko Gaertner and Anders Brunsvik. "Dynamics of Anode Baking Furnace VOC Emissions Through a Firing Cycle". en. In: *Light Metals 2022*. Ed. by Dmitry Eskin. The Minerals, Metals & Materials Series. Cham: Springer International Publishing, 2022, pp. 861–868. ISBN: 978-3-030-92529-1. DOI: 10.1007/978-3-030-92529-1_113.

[93] Thor Anders Aarhaug. *SINTSENSE: VOC Sensor System for Air Quality Monitoring*. en-GB. June 2020. URL: https://blog.sintef.com/industry-en/sintsense-voc-sensor-system-for-air-quality-monitoring/ (visited on 31/01/2023).

[94] Balram Panjwani, Stefan Andersson, Bernd Wittgens and Jan Erik Olsen. *Cleaning of polycyclic aromatic hydrocarbons (PAH) obtained from ferroalloys plant*. eng. SINTEF Academic Press, 2017. ISBN: 978-82-536-

1544-8. URL: https://brage.bibsys.no/xmlui/handle/11250/2480080 (visited on 05/10/2018).

[95]   Vegar Andersen. "Flue Gas Recirculation for the Silicon Process". PhD thesis. Trondheim: Norwegian University of Science and Technology, 2023.

[96]   Fredrik Normann, Ragnhild Skafestad, Maximillian Bierman, Jens Wolf and Anette Mathisen. *Reducing the Cost of Carbon Capture in Process Industry*. English. 2019. URL: https://www.sintef.no (visited on 20/05/2022).

[97]   Anette Mathisen, Fredrik Normann, Maximilian Biermann, Ragnhild Skagestad and Alf Tore Haug. *CO2 Capture Opportunities in the Norwegian Silicon Industry*. eng. SINTEF Academic Press, 2019. ISBN: 978-82-536-1646-9. URL: https://sintef.brage.unit.no/sintef-xmlui/handle/11250/2637936 (visited on 04/11/2022).

[98]   Eran Sher. "Chapter 2 - Environmental Aspects of Air Pollution". In: *Handbook of Air Pollution From Internal Combustion Engines*. Ed. by Eran Sher. San Diego: Academic Press, 1998, pp. 27–41. ISBN: 978-0-12-639855-7. DOI: https://doi.org/10.1016/B978-012639855-7/50041-7. URL: https://www.sciencedirect.com/science/article/pii/B9780126398557500417.

[99]   Shida Chen, Kangping Cui, Jinning Zhu, Yixiu Zhao, Lin-Chi Wang and Justus Kavita Mutuku. "Effect of Exhaust Gas Recirculation Rate on the Emissions of Persistent Organic Pollutants from a Diesel Engine". en. In: *Aerosol and Air Quality Research* 19.4 (2019), pp. 812–819. ISSN: 2071-1409. DOI: 10.4209/aaqr.2019.01.0047. URL: https://aaqr.org/articles/aaqr-19-01-oa-0047 (visited on 28/10/2022).

[100]   Mohsen Abdelaal, Medhat El-Riedy and Ahmed El-Nahas. "Effect of flue gas recirculation on burner performance and emissions". en. In: *Journal of Al-Azhar University Engineering Sector* 11.41 (Oct. 2016), pp. 1275–1284. ISSN: 1687-8418. DOI: 10.21608/auej.2016.19347. URL: https://jaes.journals.ekb.eg/article_19347.html (visited on 20/08/2021).

[101]   Peng Liu, Yiran Zhang, Lijun Wang, Bo Tian, Bin Guan, Dong Han, Zhen Huang and He Lin. "Chemical Mechanism of Exhaust Gas Recirculation on Polycyclic Aromatic Hydrocarbons Formation Based on Laser-Induced Fluorescence Measurement". In: *Energy & Fuels* 32.6 (June 2018), pp. 7112–7124. ISSN: 0887-0624. DOI: 10.1021/acs.energyfuels.8b00422. URL: https://doi.org/10.1021/acs.energyfuels.8b00422 (visited on 28/10/2022).

[102]   Vegar Andersen, Ingeborg Solheim, Heiko Gaertner, Bendik Sægrov-Sorte, Kristian Etienne Einarsrud and Gabriella Tranell. "Pilot Scale Test of Flue Gas Recirculation for the Silicon Process". en. In: *REWAS 2022: Developing Tomorrow's Technical Cycles (Volume I)*. Ed. by Adamantia Lazou,

Katrin Daehn, Camille Fleuriault, Mertol Gökelma, Elsa Olivetti and Christina Meskers. Cham: Springer International Publishing, 2022, pp. 555–564. ISBN: 978-3-030-92562-8 978-3-030-92563-5. URL: https://link.springer.com/10.1007/978-3-030-92563-5_58 (visited on 24/02/2022).

[103]   Vegar Andersen, Ingeborg Solheim, Heiko Gaertner, Bendik Sægrov-Sorte, Kristian Etienne Einarsrud and Gabriella Tranell. "Pilot-Scale Test of Flue Gas Recirculation for The Silicon Process". en. In: *Journal of Sustainable Metallurgy* (Dec. 2022). ISSN: 2199-3831. DOI: 10.1007/s40831-022-00639-0. URL: https://doi.org/10.1007/s40831-022-00639-0 (visited on 20/12/2022).

[104]   *National Institute of Health, PubChem (2022)*. en. URL: https://pubchem.ncbi.nlm.nih.gov/%20(2022-03-14) (visited on 14/03/2022).

[105]   Nadezda Slavinskaya, Aziza Mirzayeva, Ryan Whitside, JanHendrik Starke, Mhedi Abbasi, Moldir Auyelkhankyzy and Victor Chernov. "A modelling study of acetylene oxidation and pyrolysis". en. In: *Combustion and Flame* 210 (Dec. 2019), pp. 25–42. ISSN: 0010-2180. DOI: 10.1016/j.combustflame.2019.08.024. URL: https://www.sciencedirect.com/science/article/pii/S0010218019303876 (visited on 21/12/2022).

[106]   Christopher Greenshields. *OpenFOAM v8 User Guide*. London, UK: The OpenFOAM Foundation, 2020. URL: https://doc.cfd.direct/openfoam/user-guide-v8.

[107]   Roger Atkinson, Ernesto C. Tuazon and Janet Arey. "Reactions of naphthalene in N2O5-NO3-NO2- air mixtures". en. In: *International Journal of Chemical Kinetics* 22.10 (1990), pp. 1071–1082. ISSN: 1097-4601. DOI: 10.1002/kin.550221006. URL: https://onlinelibrary.wiley.com/doi/abs/10.1002/kin.550221006 (visited on 07/02/2023).

[108]   Alexandre Albinet, Eva Leoz-Garziandia, Hélène Budzinski and Eric ViIlenave. "Polycyclic aromatic hydrocarbons (PAHs), nitrated PAHs and oxygenated PAHs in ambient air of the Marseilles area (South of France): Concentrations and sources". en. In: *Science of The Total Environment* 384.1 (Oct. 2007), pp. 280–292. ISSN: 0048-9697. DOI: 10.1016/j.scitotenv.2007.04.028. URL: https://www.sciencedirect.com/science/article/pii/S0048969707004949 (visited on 19/01/2023).

[109]   Ellen Meeks, Joseph F. Grcar, Robert J. Kee and Harry K. Moffat. *AURORA: A FORTRAN program for modeling well stirred plasma and thermal reactors with gas and surface reactions*. English. Tech. rep. SAND-96-8218. Sandia National Lab. (SNL-CA), Livermore, CA (United States),

Feb. 1996. DOI: 10.2172/206570. URL: https://www.osti.gov/biblio/206570 (visited on 08/12/2022).

[110]   Statistics Norway. *Reduced emissions of hazardous substances*. en. 2007. URL: https://www.ssb.no/en/natur-og-miljo/statistikker/milgiftn/arkiv/2007-02-12 (visited on 23/09/2021).

[111]   Biswa Mohan Sahoo, Bera Venkata Varaha Ravi Kumar, Bimal Krishna Banik and Preetismita Borah. "Polyaromatic Hydrocarbons (PAHs): Structures, Synthesis and their Biological Profile". In: *Current Organic Synthesis* 17.8 (), pp. 625–640. (Visited on 01/06/2023).

[112]   Miquel Solà. "Forty years of Clar's aromatic pi-sextet rule". In: *Frontiers in Chemistry* 1 (2013). ISSN: 2296-2646. DOI: 10.3389/fchem.2013.00022. (Visited on 02/06/2023).

[113]   Maryam Nayebzadeh and Morteza Vahedpour. "A Review on Reactions of Polycyclic Aromatic Hydrocarbons with the Most Abundant Atmospheric Chemical Fragments: Theoretical and Experimental Data". In: *Progress in Reaction Kinetics and Mechanism* 42.3 (2017), pp. 201–220. ISSN: 1468-6783. DOI: 10.3184/146867817X14821527549293. (Visited on 21/01/2022).

[114]   Anders Sørhuus, Vrauke Zeibig, Eivind Holmefjord, Ömer Mercan and Elmar Sturm. "AHEX Full Scale Experiences at TRIMET Aluminium SE". en. In: *Light Metals 2023*. Ed. by Stephan Broek. The Minerals, Metals & Materials Series. Cham: Springer Nature Switzerland, 2023, pp. 1149–1155. ISBN: 978-3-031-22532-1. DOI: 10.1007/978-3-031-22532-1_154.

[115]   Lars Petersen, Casper K. Dahl and Kim H. Esbensen. "Representative mass reduction in sampling—a critical survey of techniques and hardware". en. In: *Chemometrics and Intelligent Laboratory Systems* 74.1 (Nov. 2004), pp. 95–114. ISSN: 01697439. DOI: 10.1016/j.chemolab.2004.03.020. (Visited on 22/06/2021).

[116]   Kamilla Arnesen, Thor Anders Aarhaug, Kristian Etienne Einarsrud and Gabriella M. Tranell. "Influence of Atmosphere and Temperature on Polycyclic Aromatic Hydrocarbon Emissions from Green Anode Paste Baking". In: *ACS Omega* (May 2023). Publisher: American Chemical Society. DOI: 10.1021/acsomega.3c01411. URL: https://doi.org/10.1021/acsomega.3c01411 (visited on 13/05/2023).

[117]   PubChem. *PubChem*. en. URL: https://pubchem.ncbi.nlm.nih.gov/ (visited on 14/03/2022).

[118]   Chamseddine Guizani. "Effects of CO2 on the biomass pyro-gasification in High Heating Rate and Low Heating Rate conditions". en. PhD thesis. Ecole des Mines d'Albi-Carmaux, Sept. 2014. URL: https://theses.hal.science/tel-01146829 (visited on 06/06/2023).

[119]   Isabel Suarez-Ruiz, Fernando Rubiera and Maria Antonia Diez. *New Trends in Coal Conversion: Combustion, Gasification, Emissions, and Coking*. en. Google-Books-ID: bMlaDwAAQBAJ. Woodhead Publishing, Aug. 2018. ISBN: 978-0-08-102202-3.

[120]   Yan Min Zhang, Guo Zhe Guo, La La Zhang and Jun Hong Song. "Synthesis, analysis and application of naphthalene sulfonic acid formaldehyde condensate". In: *IOP Conference Series: Earth and Environmental Science* 237.2 (Feb. 2019). ISSN: 1755-1315. DOI: 10.1088/1755-1315/237/2/022029. (Visited on 15/05/2023).

[121]   Coren Pulleyblank, Sabrina Cipullo, Pablo Campo, Brian Kelleher and Frederic Coulon. "Analytical progress and challenges for the detection of oxygenated polycyclic aromatic hydrocarbon transformation products in aqueous and soil environmental matrices: A review". In: *Critical Reviews in Environmental Science and Technology* 49.5 (Mar. 2019), pp. 357–409. ISSN: 1064-3389. DOI: 10.1080/10643389.2018.1547622. (Visited on 09/06/2023).

Appendix

Paper I

Article

Analysis of Polycyclic Aromatic Hydrocarbon Emissions from a Pilot Scale Silicon Process with Flue Gas Recirculation

Kamilla Arnesen,* Kurian J. Vachaparambil, Vegar Andersen, Balram Panjwani, Katarina Jakovljevic, Ellen Katrin Enge, Heiko Gaertner, Thor Anders Aarhaug, Kristian Etienne Einarsrud, and Gabriella Tranell*

ACCESS | Metrics & More | Article Recommendations | Supporting Information

ABSTRACT: Flue gas recirculation (FGR) is a method used in several industries to control emissions and process conditions, such as NO_x reduction and temperature levels, and increase the CO_2 concentration in the off-gas, to be better suited for methods of carbon capture. In this study, the influence of FGR, varying levels of flue gas flow and oxygen concentration on the emissions of polycyclic aromatic hydrocarbons (PAHs) was investigated during Si alloy production. In addition, computational fluid dynamics (CFD) modeling was performed using OpenFOAM for combustion of C_2H_2 and H_2 with varying O_2 levels to simulate FGR and to gain better insight into the impact of furnace operations on the PAH evolution. Experimental results show that increasing FGR (0−82.5%) and decreasing levels of oxygen (20.7−13.3 vol %) increase the PAH-42 concentration from 14.1 to 559.7 $\mu g/Nm^3$. This is supported by the simulations, where increased formation of all PAHs species was observed at high levels of FGR, especially for the lighter aromatic species (like benzene and naphthalene), due to the lower availability of oxygen and the reduction in temperature. Residence time was identified as another key parameter to promote complete combustion of PAHs. Benzene oxidation can be prevented with temperatures lower than 1000 K and residence times smaller than 1 s, while complete oxidation is found at temperatures of around 1500 K.
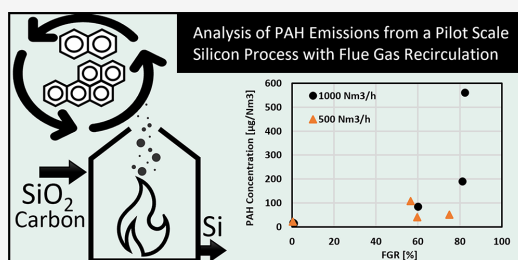
INTRODUCTION

Polycyclic aromatic hydrocarbons (PAHs) are a group of organic molecules consisting of two or more fused aromatic rings. They occur naturally in petroleum and resin products and can be produced by incomplete combustion of organic matter. Natural sources of PAHs are forest fires and volcanic activity, and anthropogenic sources can be burning of biomass and oil, production of coke and the use of carbon in industrial processes. PAHs are classified as persistent organic pollutants, and some species are known to be mutagenic and carcinogenic.[1] The European Union has agreed on a General Union Environment Action Program to reduce exposure and emissions of PAHs in 2013.[2] In 2004 the global emission of PAHs were estimated to be 520 Gg/y, using reported emissions and emission factors, where combustion of biofuel and wildfire account for 56.7% and industrial activity such as coke production is less than 10%.[3] The focus is often on the EPA-16 PAH, which is a list with components consisting solely of aromatic rings. The list was established in the 1970s and has become the standard for measuring and reporting PAH emissions. An upside to this is that keeping track of changes and trends over time has becomes more convenient. Some argue that the EPA-16 list is not optimal when measuring the

exposure of toxic emissions, as some compounds have a short life span and decompose quickly when exposed to sunlight while other more stable compounds are not included, such as alkylated or substituted PAH.[4]

Mixtures of PAHs are often characterized based on ratios to identify suspected emission sources, either by isomer pairings or larger fractions within the mixture.[5] The process and conditions are crucial for which PAHs are formed and destroyed, such as raw material and temperature. A high temperature process such as flame oxidation (e.g., methane combustion at 2000 °C) often produces high molecular weight (HMW) PAHs as the conditions can produce radicals that react and form stable PAHs. This is often called pyrogenic combustion. At lower temperatures (e.g., diesel engine runoff emission) PAHs of low molecular weight (LMW) are formed and can be referred to as petrogenic sources.[6] An example of

A

such a ratio used for separating between pyrogenic and petrogenic sources are the ratios between phenanthrene (Phen) and anthracene (Anth), where Phen is more thermodynamically stable and is therefore a more likely product from a high temperature combustion process. Fluoranthene (Fla) and pyrene (Py) is another such example, and the two ratios are often studied as a pair to better identify source emissions.[7,8] A ratio between LMW and HMW PAHs can also refer to the carbon source. LMW/HMW < 1 indicates a pyrogenic source with incomplete combustion of fossil fuel or wood, and a ratio >1 could indicate a petrogenic source including oil spill and petroleum products.[9]

A semiclosed submerged arc furnace (SAF) is commonly used to produce metallurgical grade silicon (MG-Si) through a carbothermal reduction, using a mix of coal, coke, charcoal and woodchips as the reductants. The carbon materials reduce the quartz to silicon alloy, by the overall reaction shown in eq 1, where σ is the Si yield, which gives the distribution between tapped Si and SiO leaving the furnace to react to SiO_2 (silica fume).[10]
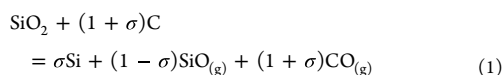
$$SiO_2 + (1 + \sigma)C = \sigma Si + (1 - \sigma)SiO_{(g)} + (1 + \sigma)CO_{(g)} \qquad (1)$$

Silicon oxide (SiO) and carbon monoxide (CO) that reach the top of the furnace react with air to form silica fume and carbon dioxide (CO_2), respectively, in the furnace hood.[10] This affects the temperature at the charge surface in the furnace, which can reach 700 to 1300 °C. Because the SAF is semiclosed, the under pressure in the furnace drives the surrounding air into the furnace hood, diluting the furnace off-gas, which consist mainly of air with small amounts of CO_2 and other greenhouse gases, as well as PAHs. Off-gas temperatures can be 400 to 700 °C above the crust of the charge materials in contact with air, and the silica fume is typically captured using a bag-house filter at moderate temperatures of approximately 60 to 220 °C, depending on the filter type. PAHs are emitted from the furnace, either from the top of the gas permeable furnace charge material or through gas released during the tapping process. Typically these PAHs originate from pyrolysis and combustion of the carbon raw materials, electrodes and carbon paste.[11] Efficient pyrolysis of coal should result in the breakdown of large organic molecules to smaller hydrocarbons, and in efficient combustion the only products would be CO_2, H_2O, CO, etc. However, such complete degradation of coal rarely occurs, and organic compounds, including PAHs, are released during the reduction process. Work is being done to develop PAH reduced or PAH-free binder products to reduce emissions.[12] Apart from the PAH evolution driven by fuel containing PAHs, combustion of aliphatic fuels (like methane or acetylene) can also generate PAHs. To the best knowledge of the authors, the fuel bounded PAHs as well as the aliphatic fuels evolving from the carbon material in the furnaces are not well understood. A study by Gaertner et al.[13] reported EPA-16 PAH emissions from the flue gas stack at a silicon plant in Norway to be 2 μg/Nm³ in the off-gas and 1.81 ng/g EPA16-PAH on the dust (PM). Increased levels of PAH emissions were observed after a furnace restart. Reported emission levels vary between plants, and in 2020 Norwegian silicon and ferro-silicon producers reported between 0.35 kg/year and 296.39 kg/year EPA-16 PAH emissions to air and water from different plants to the Norwegian Environmental Agency.[14]

Flue gas recirculation (FGR) is a method to redirect parts of the process off-gas back to the furnace. It can be done to utilize components in the off-gas, increase energy efficiency by reducing heat losses, aid in process control, and as a way to concentrate off-gas species, such as CO_2, for further processing. The silicon industry is a candidate for carbon capture, and flue gas recirculation could increase the CO_2 concentration in the off-gas, adding to the capture efficiency.[15,16]

Exhaust gas recirculation (EGR) is an established method for reducing NO_x formation in engines by reducing the oxygen levels and the temperature and, with that, slowing down the combustion process.[17] Chen et al.[18] tested the effect of EGR to reduce emissions of persistent organic pollutants from diesel engines. This work show a 9 times increase in PAH by mass emission factors when the EGR was set to 5%. In the work of Abdelaal et al.,[19] FGR is used in an attempt to reduce NO formation from dimethyl ether combusted by temperature decrease. In this case, NO is reduced, but for FGR above 20% a noticeable increase in CO and unburned hydrocarbons (UBHs) occurs from 0 to 0.45% and 0 to 650 ppm, respectively, at 40% FGR and 3% O_2. Liu et al.[20] observed increased combustion efficiency of C_2H_4 in a fuel-rich flame between 1680 and 1820 K with EGR when studying PAH formation. A way to reduce PAH emissions from industrial processes requires its capture and treatment or ensuring a complete combustion.

In order to develop processes to ensure complete combustion of PAHs, an understanding of mechanisms that describe the evolution of PAH is important. Very briefly, PAH evolution can be summarized into formation of the first aromatic ring (C_6H_6) during combustion of aliphatic species, the growth into larger PAH and eventually the soot formation, and oxidation of these species into smaller aromatic rings and carbon dioxide. The main formation mechanisms are based on different reactants, where acetylene additions (e.g., HACA), vinyl acetylene additions (HAVA), and radical reactions with C1–C6 are usually in focus.[21] These are complex mechanisms involving hundreds to thousands of reactions; for example, the C_2H_2 combustion mechanism that includes PAH until $C_{20}H_{12}$ contains 112 species and 939 reactions.[22] For readers interested in understanding the PAH chemistry driving its evolution, it is recommended to refer to other works in literature like the review by Reizer et al.[21] Using computational fluid dynamics (CFD) (with a reaction mechanism treating PAH evolution) to model industrial processes is an ideal way to investigate the impact of furnace operations on the PAH evolution. For example, Panjwani et al.,[23] using a postprocessing technique based on CFD modeling, reported that temperature should exceed 800 °C for optimal combustion of 1-methylnaphthalene in addition to having a longer residence time >2 s (when compared to other process gases).

The objective of this study was to investigate the emissions of an extended list of PAHs, including alkylated and heterocyclic PAHs, from pilot scale silicon production and evaluate the effect of flue gas recirculation on the combustion conditions and resulting levels of PAHs. To gain better insight into the complex PAH evolution from the SAF, CFD modeling was performed using OpenFOAM for C_2H_2 and H_2 combustion with varying O_2 levels to simulate FGR.

■ EXPERIMENTAL AND MODELING METHODOLOGY

Pilot Furnace. A pilot scale one-phase submerged arc furnace was used for silicon production with flue gas
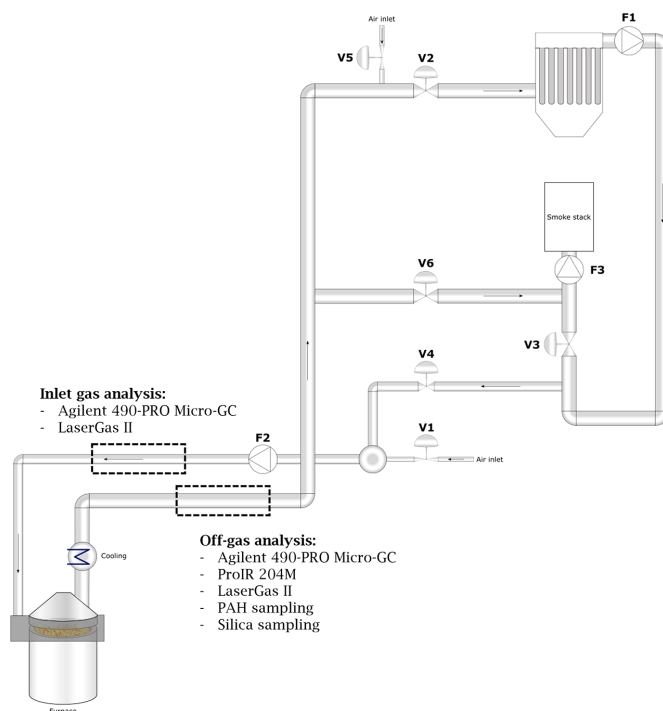
Figure 1. Silicon pilot SAF with a closed off-gas recirculating system. Placement of valves (V), fans (F) and location of various sampling systems are marked. Reprinted with permission from Andersen et al.[24] Copyright 2022 The Minerals, Metals & Materials Society.

recirculation over a 3-day period with continuous operations to investigate how FGR influenced PAH and off-gas composition from the silicon furnace. More details regarding the experiment can be found in the works of Andersen et al.[24,25] The furnace and off-gas system is illustrated in Figure 1. Power was supplied to the furnace thought a 6 in. graphite electrode (EG90, Tanso) at maximum 400 kVA. A mix of coal, coke, charcoal, woodchips and quartz made up the raw materials, which were supplied by an industrial partner. The materials were used as received, except for the woodchips, which were dried at 100 °C for 24 h. More information about the carbon raw materials is found in Table 1.

Table 1. Information about the Carbon Raw Materials Used in the FGR Pilot Experiments[a]

	Coal	Coke	Charcoal	Woodchips
Moisture (wt %)	10.8	11.7	4.7	4.8
Fix C (DB, wt %)	57.6	90.5	79.0	14.6
Ash (DB, wt %)	2.0	2.8	3.3	1.1
Volatiles (DB, wt %)	40.4	6.6	17.7	84.2
Share of C-mix (% Fix C)	40	15	30	15
Carbon (%DW)	78	90.8	83	50.7
Nitrogen (%DW)	1.58	1.68	0.39	0.2
Oxygen (%DW)	12	2.5	9.6	41.4
Hydrogen (%DW)	5.79	1.83	3.71	6.48
Sulfur (%DW)	0.05	0.42	0.05	0.11

[a]Analysis performed by ALS Scandinavia, Luleå, Sweden.

The furnace off-gas system was modified to achieve a closed off-gas system, which included a furnace hood, recycle, and redistribution system. After the off-gas exited the furnace and passed through a bag-house filter, a set of valves was used to determine if the off-gas should exit thought the smoke stack or be recirculated back to the furnace. The FGR ratio was set by the dilution factor between fresh air and recirculated off-gas.

The off-gas composition was analyzed during the experiment using different techniques, on both the furnace outlet and inlet. Gas composition (e.g., H_2, O_2, N_2, CO_2 and CH_4) was analyzed using an Agilent 490-PRO Micro-GC with Soprane II software, TCD detectors, and argon and helium carrier gas. The GC used two columns for separation, where column 1 was a 3m + 10m MS5A, RTS column with Ar carrier gas, and column 2 used a 10 m PPQ column with He carrier gas. In addition, LaserGas II and LaserDust instruments (NEO monitors) were used for measuring CO_2, O_2 and NO_x, as well as for dust analysis. Isokinetic sampling was performed on the off-gas for silica fume[25] and PAH analysis.

PAH Sampling Procedure. A sample collection system for PAH was developed by adapting a standard setup following isokinetic sampling principles to investigate PAH composition in gas and particle phase from the pilot furnace. A nozzle (4.16 mm) and probe (1/2 in., SS) were used to extract the gas from the off-gas duct. Glass fiber thimble filters (22 Ø, Munktell/Ahlstrom, Sweden), followed by cartridges with glass wool and XAD-2 (30.0 g, Supelpak-2, Merck Life Science AS, Germany), were used as absorbents. A rotary vane gas-sampler pump (Paul Gothe GmbH, Germany) was used to maintain stable gas flow. The setup is illustrated in Figure 2. By adjusting the
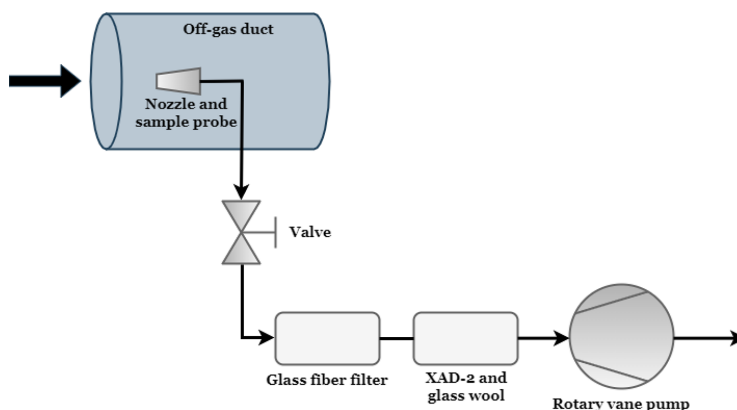
Figure 2. PAH sampling line, including glass fiber filter, XAD-2 cartridge with glass wool and rotary vane pump.

pump extraction velocity to match the gas flow in the off-gas duct, a representative sample extraction was achieved. After sample collection, the filters were removed and the filter holder was cleaned using acetone.

Samples for PAH analysis were obtained at specific experimental steps during the campaign, and process parameters are shown in Table 2. Samples were analyzed to

Table 2. Gas Flow, Recirculation Ratio and Oxygen Set-Points at PAH Sampling in the FGR Pilot Campaign

Sample Number	Flow [Nm^3/h]	FGR [%]	Oxygen [vol%]
1	1000	0	20.7
8	1000	0	20.7
14	1000	0	20.7
5	1000	70	17.2
11	1000	70	17.2
4	1000	88	10.0
13	1000	88	10.0
2	500	0	20.7
9	500	0	20.7
12	500	0	20.7
3	500	60	16.2
7	500	60	16.2
6	500	78	10.1
10	500	78	10.1

investigate how the different process parameters affect concentration, molecular distribution and species of PAH. Glass fiber filters and XAD-2 cartridges were removed before tapping of Si metal. Sampling started when stable furnace conditions were reached, such as at target FGR ratio, off-gas concentration levels, and acceptable temperatures for the bag-house filter, and ended before tapping of the metal. On average, 0.30 Nm^3 off-gas was sampled per hour of silicon production. Sampling was performed at 14 different operation conditions, out of the 27 experimental cycles, and a total of 42 samples were collected (3 samples per experimental cycle). All samples were protected against UV radiation by layers of aluminum foil and stored at 4 °C in a dark location prior to analysis by Norwegian Institute of Air Research (NILU, Kjeller, Norway).

PAH Analysis Methodology. The analytical procedure follows the requirements of NILU's accreditation, according to NS-EN ISO/IEC 17025. Internal standards containing deuterated PAH congeners were added to all samples prior to extraction. Standards are listed in Table S2, found in the Supporting Information. XAD-2 and filter samples were Soxhlet extracted for 8 h in acetone/hexane (1:1), before the fraction was solvent exchanged to cyclohexane prior to liquid−liquid separation between cyclohexane and dimethyl formamide/water (Grimmer method), followed by cleanup using silica gel deactivated with 8% water (adsorption chromatography). After concentration, a recovery standard containing deuterated PAH congeners was added. Acetone samples were treated following the same method, without the Soxhlet extraction and solvent exchange to cyclohexane.

Identification and quantification of native PAHs was carried out using a gas chromatograph coupled to a low-resolution mass spectrometer as detector (GC/LRMS). The analyses were performed in EI mode using SIM. The list of PAH components is shown in Table 3.

Modeling PAH Evolution. A realistic model of the pilot scale submerged arc furnace is extremely complex due to the large uncertainty in the input data needed (like the types and amounts of PAH contained in the carbon materials in the furnace) apart from the transient nature of the flow. Additionally, the computational overhead to simulate such a process is not practical due to the large number of species and reactions that needs to be treated for PAH evolution along with the millions of cells required to mesh a furnace. To gain insight into the PAH evolution in such a complex system, a simplified geometry of a coflow burner is used in this work. The geometry is axisymmetric with a central fuel nozzle of radius equal to around 4 mm. The annulus through which flue gases are added has an inner radius of 4.5 mm and an outer radius of 180 mm, and the radius of the domain is equal to the outer radius of the annulus for the first 20 mm after which it increases to 190 mm for the next 1 m. The flue gases and the fuel are physically separated for the first 20 mm, after which the gases mix and react.

In the present study, only chemistry driven PAH is considered, and the work assumes that the fuel consists of C_2H_2, N_2 and H_2 and that these species are mainly responsible for the chemistry driven PAH.[22] This simplification is mainly

Table 3. List of 42 PAH Components Analyzed in the FGR Off-gas Samples

Compound	MW[g/mol]	$T_b{}^a$ [°C]	# of rings
Naphthalene	128.1	218	2
2-Methylnaphthalene	142.2	241	2
1-Methylnaphthalene	142.2	245	2
Biphenyl	154.2	255	2
Acenaphthylene	152.2	279	3
Acenaphthene	152.2	279	3
Dibenzofuran	168.2		3
Fluorene	166.2	294	3
Dibenzothiophene	184.3		3
Phenanthrene	178.2	338	3
Anthracene	178.2	340	3
3-Methylphenanthrene	192.3	352	3
2-Methylphenanthrene	192.3	355	3
2-Methylanthracene	192.3	359	3
9-Methylphenanthrene	192.3	355	3
1-Methylphenanthrene	192.3	359	3
Retene	234.3		3
Fluoranthene	202.3	383	4
Pyrene	202.3	393	4
Benzo(a)fluorene	216.3	407	4
Benzo(b)fluorene	216.3	402	4
Benz(a)anthracene	228.3	435	4
Triphenylene	228.3	439	4
Chrysene	228.3	448	4
Benzo(ghi)fluoranthene	226.3	432	5
Cyclopenta(cd)pyrene	226.3		5
Benzo(b)fluoranthene	252.3	481	5
Benzo(k)fluoranthene	252.3	481	5
Benzo(j)fluoranthene	252.3	480	5
Benzo(a)fluoranthene	252.3		5
Benzo(e)pyrene	252.3	493	5
Benzo(a)pyrene	252.3	496	5
Perylene	252.3		5
Dibenzo(ac)anthracene	278.3		5
Dibenzo(ah)anthracene	278.3		5
Indeno(1,2,3-cd)pyrene	276.3	536	6
Benzo(ghi)perylene	276.3	550	6
Anthanthrene	276.3		6
Coronene	300.4	430	6
Dibenzo(ae)pyrene	302.4	414	6
Dibenzo(ai)pyrene	302.4		6
Dibenzo(ah)pyrene	302.4		6

^{a}PAH boiling point sources.[26,27]

due to the uncertainty in the type and amount of aromatic species bound to the carbon materials which, if they were known, could be used as fuel instead of the composition used in this work. Additionally, acetylene is reported in literature to be an important species for PAH growth, via HACA (hydrogen abstraction and acetylene or carbon addition mechanism, which involves repetitive abstraction of hydrogen from the aromatic species and addition of acetylene to the radical site) and soot evolution; see Reizer et al.[21] In this study, modeling is aimed at understanding the impact of flue gas recycling on PAH evolution from combustion of a mixture of acetylene (an aliphatic species) and hydrogen and comparing modeling outcomes with PAH emission observed in the furnace experiments. These gases are injected at 42.2 m/s at a constant temperature of 1000 °C with mass fractions (Y) of

C_2H_2, N_2, and H_2 equal to 0.246, 0.708, and 0.046, respectively. The flue gases are assumed to consist (by mass fraction) of N_2 and Ar equal to 0.763 and 0.005 (note that the values are rounded to the third decimal), the mass fraction of O_2 is varied (the values used are 0.232, 0.203, 0.174, 0.145, 0.116 and 0.058), and the remaining fraction is CO_2. The decreasing O_2 content indicates higher levels of FGR. The flue gases are injected at 0.3 m/s at a constant temperature of 300 K. The walls separating the fuel and flue gases for the first 20 mm are set as no-slip walls, the top boundary is set as the outlet, and the remaining wall boundaries are assigned a fixed velocity of 0.3 m/s along the axial direction. The turbulence intensities of the inflow of fuel and coflow of flue gases/air are 8% and 2%, respectively, whereas turbulent mixing length scales (for both boundaries) are set to a value of 0.005 m.

The solver used to simulate the process is reactingFoam, a turbulent reacting flow solver available in the open source CFD framework OpenFOAM that does not treat buoyancy.[28] The solver accounts for conservation equations of mass, momentum, energy and species transport with treatment for species generation/consumption as well as heat released/consumed due to chemical reactions; see works in the literature[29] and S3 in the Supporting Information for details on the governing equations. The reaction kinetics and thermodynamic data for combustion including PAH evolution proposed by Slavinskaya et al.[22] were used in this work. It should be noted that there are more complex reaction mechanisms, which include soot evolution, that are reported in the literature to describe PAH evolution.[30,31] Since the experimental work analyzed PAH species with 2−6 rings, the reaction mechanism proposed by Slavinskaya et al.[22] is used in the model as it considers PAH up to the five ringed species (like benzo(a)pyrene). The reaction mechanism used in this work is based on acetylene combustion comprising 112 species and 939 reactions. It should be pointed out that this reaction mechanism does not distinguish between PAH species with the same chemical composition. The transport of gas species is assumed to be turbulence driven, so the species specific molecular/dynamic viscosity is calculated based on the Sutherland model with coefficients set to a constant value for all species (Sutherland coefficient equal to 1.512×10^{-6} kg/m·s and Sutherland temperature equal to 120 K). The combustion is treated using the Eddy Dissipation Concept (v2005) with turbulence treated using the standard $k−\epsilon$ model. The geometry used for the simulations is meshed using 18226 cells based on grid sensitivity studies, and the solver is run until a pseudo-steady state is reached.

■ RESULTS

Each experimental run lasted about 1.5 h and established the time frame for the test of one set of experimental parameters. An example of how the temperature varies within a cycle is shown in Figure 3. The cycle has a startup period and an end, which are not included when the average process parameters are calculated. At the start of a cycle, the system took some time to stabilize and reach set points for the experiment, and at the end of a cycle, the raw material charge would collapse, causing a blowout, and cause the process parameters to change. A more detailed description of variations within the experiments can be found in the work of Andersen et al.[25]

Flue gas recycling ratios, gas concentrations and flow values were calculated as an average over the stable sampling period. FGR is based on the ratio of inlet and outlet CO_2 concentration measurements by the NEO laser, and ambient
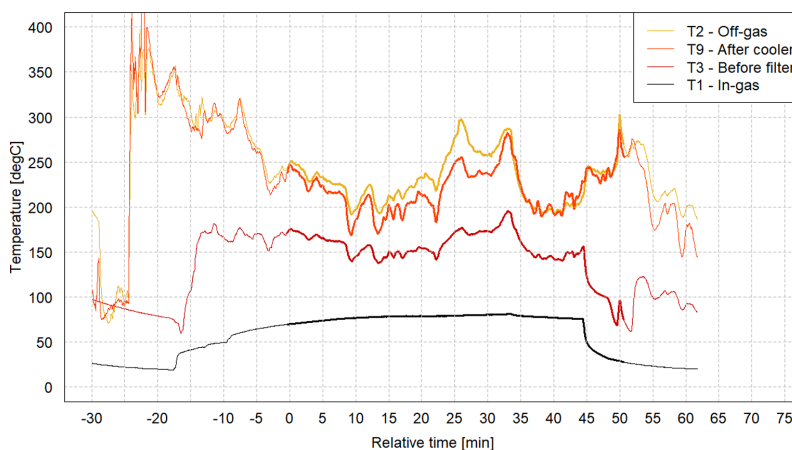
Figure 3. Example of temperature data for one experimental run. Temperature is logged for the off-gas, after the cooler, before the filter, and the inlet gas. The sampling period is highlighted, from 0 to 51 min.

CO_2 was set to 0.06 vol%. The measured flow, FGR and oxygen levels for each PAH sample are presented in Table 4.

Table 4. Measured Gas Flow, Recirculation Ratio and Oxygen Averages from PAH Sampling in the FGR Pilot Campaign, Sorted by Flow and Decreasing Oxygen Levels

Sample Number	Flow [Nm³/h]	FGR [%]	Oxygen [vol %]	Flue Gas Temperature [°C]
1	965	0.6	20.7	208.3
8	914	0.9	20.7	248.6
5	935	60.1	17.6	238.1
4	865	81.3	15.5	231.7
13	919	82.5	13.3	237.1
9	566	0.3	20.4	268.4
3	440	56.6	17.9	275.3
7	497	59.6	17.3	292.9
6	425	75.0	16.4	274.7

After evaluation, results from four tapping cycles were deemed to be unreliable, as no PM was collected in the glass fiber filters even though the sampling pump registered gas flow, indicating a leak in the sampling line with only ambient air being sampled. Results from sample number 2 were determined to be an outlier, as comparing with experiments of similar FGR (0– 1%); the result did not fit within a 90% confidence interval.

PAH Emissions during Si Production. Three experiments were performed as conventional Si production cycles, without flue gas recirculation (samples 1, 8 and 9). One experiment had a gas flow rate at 500 Nm³/h and two had flow rates of 1000 Nm³/h. The total PAH-42 concentrations for these experiments range between 14.1 and 22.0 μg/Nm³. To compare, the PAH EPA-16 concentration range is between 8.5 and 12.9 μg/Nm³ for the same experiments.

Effect of FGR on Flue Gas Composition. Figure 4(a–d) shows how O_2, temperature, CO and CH_4 changes with the level of FGR during the pilot experiments. The FGR levels vary from 0 to 75.0% for experiments at 500 Nm³/h and from 0 to 82.5% for experiments at 1000 Nm³/h (Table 4). Figure 4(a) shows the change in O_2 as an effect of FGR, and similar decreasing trends are present for both 500 and 1000 Nm³/h,

with a significant drop in O_2 concentration occurring at 80% FGR for the 1000 Nm³/h set point. This is also illustrated in panel (c), where the changes in CO levels at 1000 Nm³/h increase from about 500 to 700 ppm when the FGR increases from 81.3 to 82.5%, respectively. The off-gas temperature was measured before the cooler (Figure 1), and the average values are presented in Figure 4(b). All temperature measurements at 500 Nm³/h were at a higher level than for 1000 Nm³/h. Often, the operations were limited by the operational conditions for the bag-house filter (at 185 °C) and were often adjusted by directing gas through the smokestack at the beginning of a cycle and delaying the start of the sampling while waiting for the temperature to stabilize. The levels of methane shown in panel (d) display no significant changes with the varying FGR ratios and oxygen at the experimental steps where PAH were sampled.

Effect of FGR and O_2 Levels on PAH Emissions. Figure 5 shows how the total concentration of PAH-42 changes with varying (a) FGR ratios and (b) oxygen levels for samples at 1000 and 500 Nm³/h. At 1000 Nm³/h, the PAH concentration increases from 16.0 to 559.7 μg/Nm³ with decreasing O_2 levels (20.7–13.3 vol %) and increasing FGR (0–82.5%). Overall, the PAH concentrations are lower for the samples at 500 Nm³/ h conditions than at 1000 Nm³/h, ranging between 22.0 and 107.8 μg/Nm³, when comparing with similar FGR (0–75.0%) and oxygen levels (20.4–16.4 vol %).

A correlation was found between the total PAH-42 concentration and the level of oxygen and FGR, at 99.0% and 89% confidence, respectively. By separating the PAH into fractions of LMW and HMW, the correlation was found to be at 96.0% confidence interval between LMW PAHs and the level of oxygen and 76.0% for FGR and, as well as a 99.0% and 97.0% confidence interval between HMW PAHs and oxygen and FGR, respectively.

Each experiment produced three samples from the sampling line. PAH contents were analyzed from the filter, acetone washing liquid and XAD-2 absorbent. The normalized distribution of total PAH concentration between the elements in the sampling line is presented in Figure 6 for all experiments. The majority of the PAH species are caught in the glass fiber filter. For experiments at 0% FGR, 57% of the

(a)

(b)

(c)

(d)
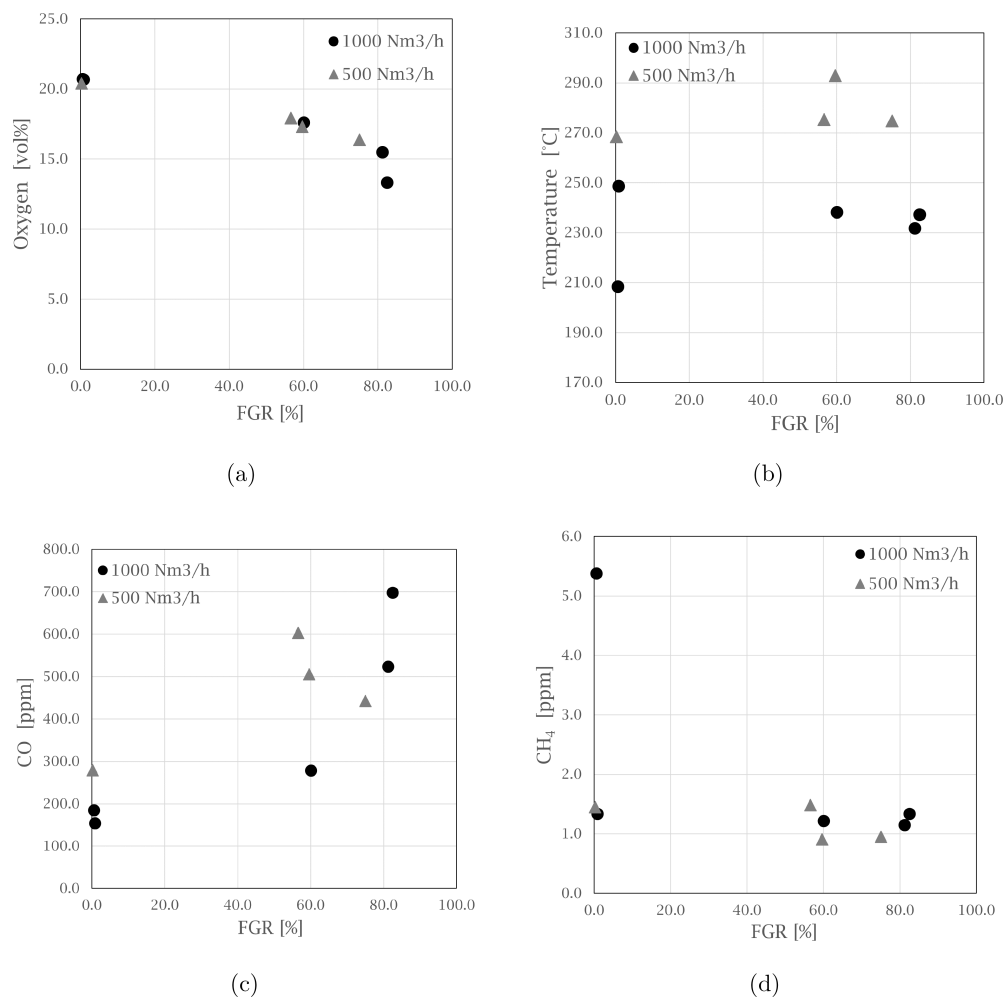
Figure 4. Graphs showing the changes in gas composition and temperature as an effect of FGR for the different flow rates (500 and 1000 Nm^3/h): (a) O_2, (b) temperature, (c) CO, and (d) CH_4.

average amount of the total PAHs was found in the filter. In this fraction, the 4−6 ring high molecular weight (HMW) PAH makes up 71%, and the remaining 29% is the light molecular weight (LMW) PAH with 2 and 3 rings. The experiment at 82.5% FGR is notable, at 1000 Nm^3/h as shown in 6(a), where 77.7% of the PAH passed through the filter and 67.5% were of LMW.

Diagnostic Ratios. As shown in Figure 7, the generally dominating ratio is the fraction of high molecular weight with 4−6 ring PAHs for both 1000 and 500 Nm^3/h experiments, with a pyrogenic ratio of LMW/HMW < 1, and it does not seem to be greatly affected by the FGR rate. This is also supported by the cross-plot in Figure 8, where the ratios of Phen/Anth and Fla/Py show that all of the experiments are placed within the pyrogenic area.

The experiment at 82.5% FGR and 1000 Nm^3/h stands out. Compared with the ratios shown in Figure 6, the PAH levels for this experiment mainly consist of gaseous naphthalene

absorbed on XAD-2, which shifts the LMW/HMW ratio from below or close to 1 to above 1 and toward a petrogenic diagnostic ratio.

PAH EPA-16 and PAH-42. In Figure 9 a comparison between PAH EPA-16 and the 42 PAH components analyzed is shown. The comparison shows that the PAH-16 makes up on average 62% and 58% of the total PAHs for experiments at 1000 and 500 Nm^3/h, respectively. The ratio is stable and is not seemingly affected by the combustion conditions in the furnace and the FGR levels.

PAH Evolution with FGR in the Simplified Simulations. The increase in the flue gas recirculation is observed to decrease temperature as expected, but low oxygen levels in the flue gas (corresponding to mass fraction based % equal to 11.6% and 5.8%) result in no combustion despite the occurrence of some reactions (forming PAHs and water), as seen in Figure 10 and Figure 11. In the simulation where combustion occurs (i.e., mass fraction based oxygen % of

G
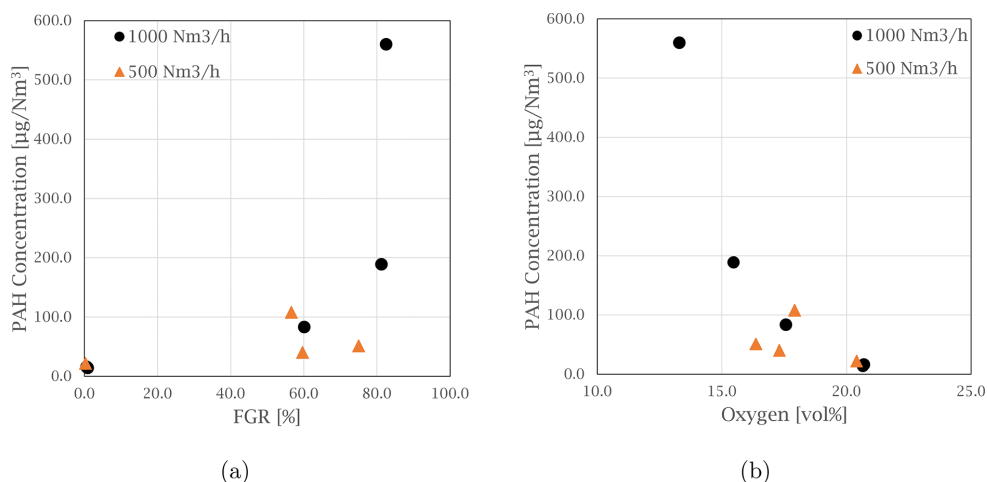
Figure 5. Graphs showing the total PAH-42 concentration in the off-gas at varying (a) FGR ratios and (b) O_2 levels for experiments at 1000 and 500 Nm^3/h.
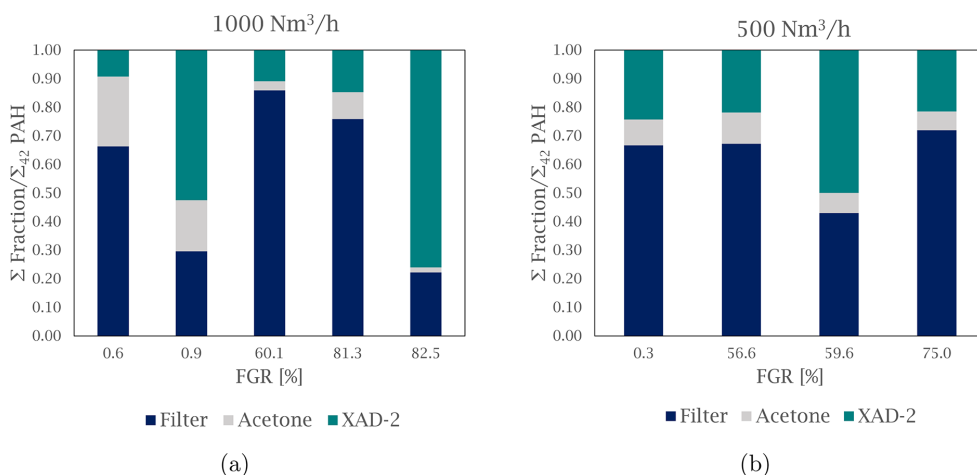

Figure 6. Graphs showing the normalized distribution of PAHs between the filter, washing liquid (acetone), and XAD-2, at varying FGR: (a) experiments at 1000 Nm^3/h and (b) experiments at 500 Nm^3/h.

23.2−14.5%), the PAH generated is observed to get oxidized as these species are convected through the flame front or the region with the high temperature. In the cases with no combustion and FGR with mass fraction based O_2 % of 11.6% and 5.8%, the PAHs generated are transported all the way to the outlet as they never encounter high enough temperature for oxidization. These simulations indicate that the oxidation process of PAH species is dependent on the locally available oxygen, temperature and residence time.

To study the conditions that prevent the oxidation of PAHs, a perfectly stirred reactor (PSR) simulation (see Meeks et al.[32] and S4 in the Supporting Information for further details on the reactor model), in which a mixture of PAH (i.e., A1 or benzene), O_2, CO_2 and N_2 reacts in a 0D reactor at constant temperature until reaching equilibrium, is used. The results from the PSR simulations (see Figure 12) suggest that

temperatures below 1000 K, with residence time smaller than 1 s, and low oxygen can prevent the complete oxidation of benzene.

The PSR simulations show that the main product at equilibrium is carbon dioxide, indicating that oxidization of the benzene is more dominant when compared to benzene's growth into larger PAH species. The composition of larger PAH species at equilibrium predicted by the PSR simulation shows a dependence on temperature, residence time and oxygen levels. So at sufficiently high temperatures (around 1500 K) benzene is observed to be oxidized completely, but at lower temperatures it can partly be oxidized and grow into larger PAHs. If the PAH species are not oxidized, it can evolve into larger/smaller PAH molecules based on the local flow conditions as well as be transported to the off-gas duct of the furnace.
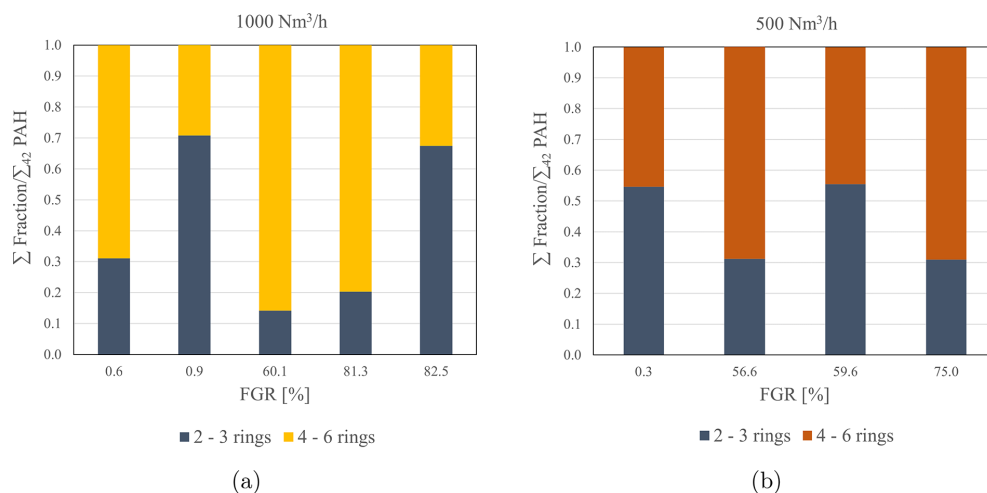
Figure 7. Graphs showing distribution between low molecular weight (2−3 rings) PAHs and high molecular weight (4−6 rings) PAHs in the off-gas at varying FGR: (a) experiments at 1000 Nm^3/h and (b) experiments at 500 Nm^3/h.
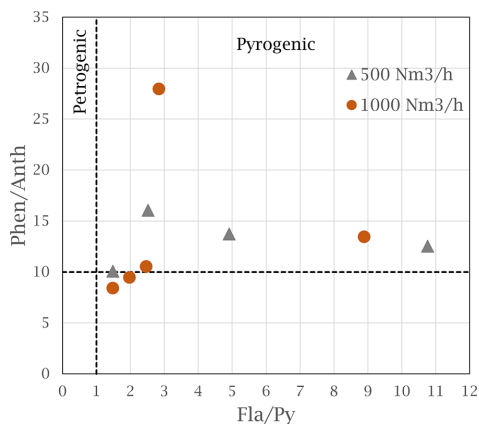

Figure 8. Cross-plot of Phen/Anth and Fla/Py ratios for all experiments in the FGR Si pilot campaign. Lines at $x = 1$ and $y = 10$ suggest the separation of petrogenic and pyrogenic sources for the two ratios, as suggested by Budzinski et al.[7]

As the PAH is oxidized in the simulations with combustion, potential PAH emission from the various scenarios simulated can be understood by simply comparing the maximum mass fraction value of a PAH species in the domain predicted by the model. The maximum amounts of various aromatic species produced for the various flue gas recycling cases are visualized in Figure 13. The reduction in oxygen with increased FGR is generally observed to increase the generation of the aromatic species. The simulations predict that although no combustion is observed in FGR with mass fraction based O_2 % of 11.6% and 5.8%, PAH species formed (especially A1 and A2) are approximately in the same order of magnitude as the other FGR cases. The maximum value of A2 or naphthalene is found to increase up to FGR with a mass fraction based O_2 % of 11.6%. The subsequent increase in FGR is observed to result in a reduction of A2. Comparing the maximum value of the PAH

species formed, smaller PAH species like A1 and A2 tend to be formed in larger amounts when compared to the larger aromatic species (except for BAPYR, which could be due to overestimation as the reaction mechanism does not consider even larger PAH species).

■ DISCUSSION

The three experiments from Si production without FGR have a PAH-42 concentration between 14.1 and 22.0 μg/Nm^3. Comparing these experiments with the emission levels reported by Gaertner et al.[13] of 2 μg/Nm^3, and taking into account the sampling location of Gaertner being after the bag-house filter, which would contribute to decreasing emissions, the results are within a similar range. Sampling by Gaertner was performed during a furnace start-up, and it was noted that the PAH profile changed from bicyclic to heavier compounds, such as phenanthrene and fluoranthene, over time.

At 1000 Nm^3/h, the PAH concentration increased from 16.0 to 559.7 μg/Nm^3 with decreasing O_2 levels (20.7−13.3 vol %) and increasing FGR (0−82.5%), which are parameters that show a strong correlation in this study. This follows the trend presented in other work where the level of unburned hydrocarbons increased with increasing levels of FGR.[18,19] This overall trend, also observed in modeling, is a consequence of the lower availability of oxygen and the reduction in temperature, due to which the extent of oxidation of the PAH is reduced. All eight modeled aromatic species showed a steady increase in concentration, with A1 and A2 (benzene and naphthalene) being the dominating species. This is also observed in the pilot experiment with increasing concentration of naphthalene at low oxygen levels (13.3 vol %). It should also be noted that at very high levels of FGR, the combustion in the furnace hood can also potentially be hindered depending on the flammability limit of SiO and CO gases, similar to the lack of combustion observed in the CFD simulation using FGR with mass fraction based O_2 % of 11.6% and 5.8%. With added FGR, PAH that passes through the bag-house filter could recirculate back to the furnace hood and be oxidized and continue back in the loop as CO_2 or a different PAH (or

1000 Nm³/h

500 Nm³/h

(a)   (b)
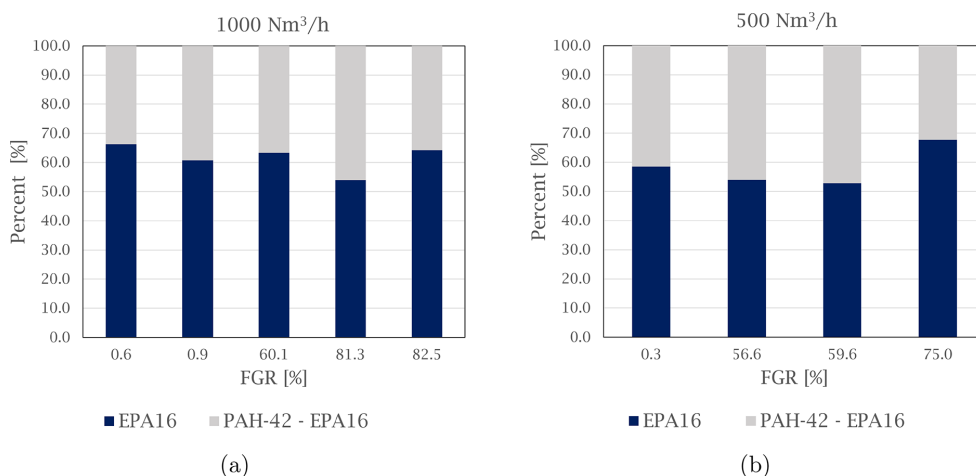
Figure 9. Graphs showing percent distribution between PAH EPA-16 and PAH-42 for all experiments at varying FGR: (a) experiments at 1000 Nm³/h and (b) experiments at 500 Nm³/h.


(a)   (b)   (c)
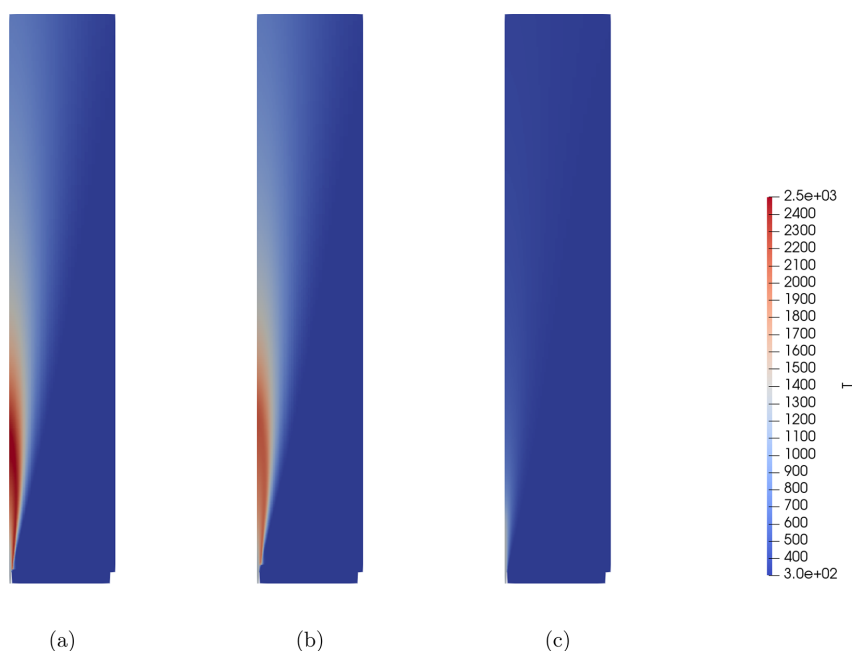
Figure 10. Contour plots of temperature (in K) distribution for varying levels of FGR or O_2 (mass fraction based %) in flue gas: (a) 23.2%, (b) 17.4%, and (c) 11.6%.

hydrocarbon species), or could pass through the combustion zone and increase in concentration if new PAHs are formed in the Si furnace. It should be noted that the CFD simulations in this work assumed that the flue gases are always injected at a constant temperature of 300 K without any PAH, which may not occur in the experiment as the flue gas temperature is often higher than the surrounding air and may contain some PAH species. Numerical modeling to study the impact of PAH in

the recirculated flue gases and at temperatures higher than 300 K should be investigated in future works.

All temperature measurements at 500 Nm³/h were at a higher level than for 1000 Nm³/h, indicating that the temperature could be more affected by the volume of gas and the dilution of heat in a fuel rich environment than the direct effects of FGR. Liu et al.[20] observed increased combustion efficiency of C_2H_4 in a fuel rich flame at elevated temperatures with exhaust gas recirculation (EGR) when
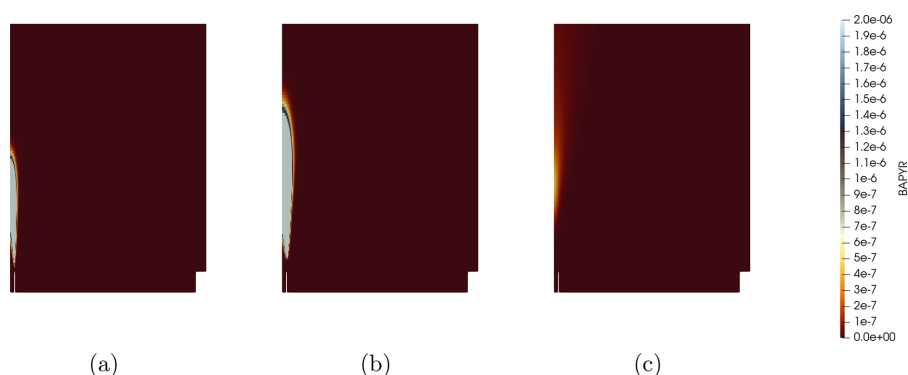
Figure 11. Zoomed-in contour plots of mass fraction of BAPYR ($C_{20}H_{12}$ or benzo(a)pyrene) distribution for varying levels of FGR or O_2 (mass fraction based %) in flue gas: (a) 23.2%, (b) 17.4%, and (c) 11.6%.
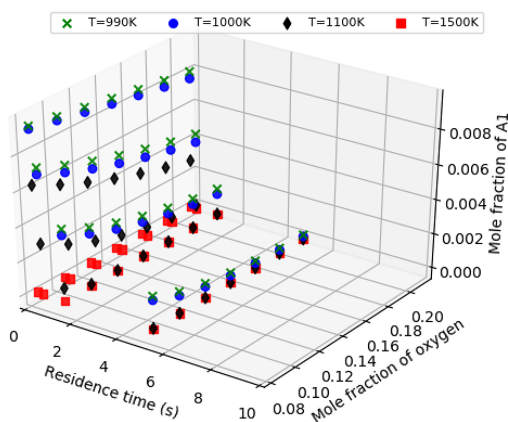

Figure 12. Predicted mole fraction of A1 (or benzene) at equilibrium that did not get oxidized based on PSR simulation. The simulation is run at 1 atm, constant temperature (which is varied as shown in the legend), and mole fractions of N_2 and A1 set to constant values equal to 0.78 and 0.01; the mole fraction of O_2 is varied (on the y-axis), and the remainder is assumed to be CO_2.

studying PAH formation, which could be the explanation for the lower PAH concentrations at lower flow rates. As lower flow of flue gases is observed to increase the temperature in the furnace during experiments, this may increase the overall residence time experienced by PAH species, thus increasing the extent of oxidation of PAH species as observed in Figure 12. It should also be noted that the PSR simulations also indicate that the complete oxidation of A1 or benzene can be prevented if the residence time is lower than 1 s, which agrees roughly with the conclusion of Panjwani et al.,[23] who recommended a residence time larger than 2 s for complete oxidation of 1-methylnaphthalene. Despite lower emission levels in general at lower flow, the HMW fraction dominates the emission profile together with production of the more thermodynamically stable species of phenanthrene and fluoranthene, suggesting that the process remain at high temperature oxidative conditions even at the extreme process conditions tested in the pilot campaign.

To be able to simulate scenarios comparable to experiments, the composition of the process gases emitted from the charge surface needs to be understood well as these gases are assumed to consist of just SiO and CO and details on the in-furnace formed PAH are not known. Another important direction for future investigation is to include PAH species larger than five rings, using an even more detailed reaction mechanism, like the mechanism proposed by Pejpichestakul et al.[31] that treats soot evolution and has around 25000 reactions involving approximately 400 species. Inclusion of larger PAH and soot into the model could aid in accurately capturing the evolution of PAH as the aromatic species considered in this work were observed to get oxidized (see Figure 11), whereas in experiments involving similar flame emission of soot and PAH have been reported.[33] Despite the simplifications in the modeling performed in this work, the overall trends obtained support the experimental observations, indicating the ability of the model to describe complex reactive flow phenomena occurring in the furnace hood.

■ CONCLUSIONS

The influence of FGR on PAH emissions was investigated in this study, through both experimental testing and CFD modeling. The PAH emissions were measured during Si alloy production in a pilot scale furnace with FGR and various levels of O_2 and flue gas flow.

● The concentration of PAH-42 for experiments with no FGR varied between 14.1 and 22.0 $\mu g/Nm^3$. With increasing recycling rate of furnace gas and decreasing O_2 levels, the concentration of PAH increased, independent of the flue gas flow. The PAH-42 concentration increased up to 559.7 $\mu g/Nm^3$, with 13.3 vol % O_2 at 1000 Nm^3/h. A correlation was found between the total PAH-42 concentration and the level of oxygen and FGR, at 99.0% and 89% confidence, respectively.

● High molecular weight PAHs dominated the PAH profile in the experimental samples and made up on average 58% of the total sample. A noticeable shift was observed at low oxygen levels and high FGR, where bicyclic PAHs, such as naphthalene, made up increasing levels of the total sample. Diagnostic ratios suggest the emission profiles fit a pyrogenic high temperature oxidative process, which promotes thermodynamically stable PAH species.

● Simulations showed that an increased level of FGR (without any recycling of PAH) could result in larger amounts
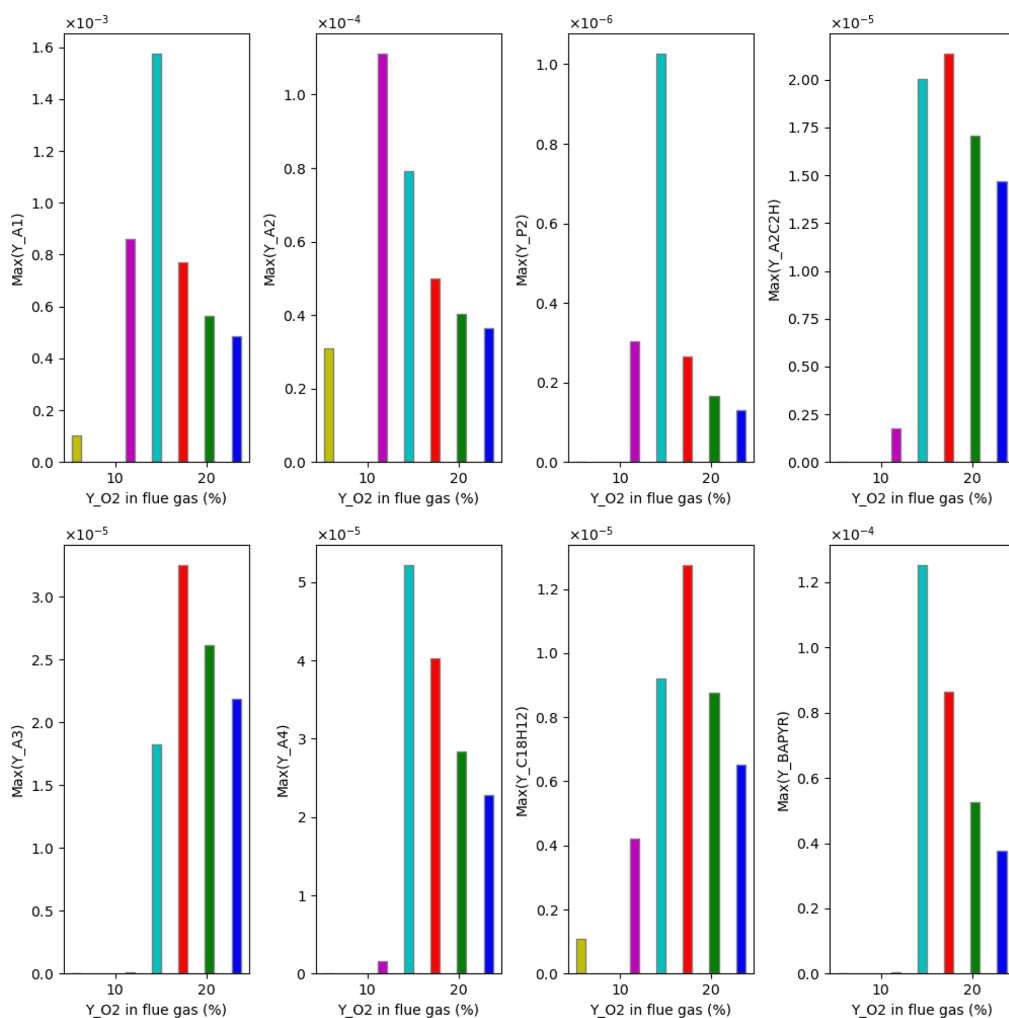
Figure 13. Comparison of the maximum value of mass fraction of 8 aromatic species predicted by the CFD simulations for various flue gas recycling scenarios. The x-axis of the plots represents O_2 (mass fraction based %) in the injected flue gas calculated as the mass fraction of $O_2 \times$ 100. These 8 aromatic species are A1 (C_6H_6 or benzene), A2 ($C_{10}H_8$ or naphthalene), P2 ($C_{12}H_{10}$ or acenaphthene), A2C2H ($C_{12}H_8$ or acenaphthylene), A3 ($C_{14}H_{10}$ or anthracene/phenanthrene), A4 ($C_{16}H_{10}$ or fluoranthene/pyrene), C18H12 ($C_{18}H_{12}$ or benzo(a)anthracene/chrysene), and BAPYR ($C_{20}H_{12}$ or benzo(a)pyrene).

of PAH formed. The simulations predicted a propensity for formation of smaller aromatic species (like benzene and naphthalene) when compared to the larger PAH species with the exception of benzo(a)pyrene (BAPYR), which could be a result of the reaction mechanism treating PAH evolution until BAPYR.

• Investigation of the oxidation of PAH species (represented by benzene) showed that complete oxidation of benzene could be prevented with temperatures lower than 1000 K and residence times smaller than 1 s, while complete oxidation was found at temperatures of around 1500 K.

■ ASSOCIATED CONTENT

ⓢ Supporting Information

The Supporting Information is available free of charge at https://pubs.acs.org/doi/10.1021/acs.iecr.2c04578.

> Full overview of the PAH analysis results, list of the standards used for analysis, and information on the OpenFOAM solver and the perfectly stirred reactor model (PDF)

■ AUTHOR INFORMATION

Corresponding Authors

    Kamilla Arnesen − *Department of Materials Science and Engineering, Norwegian University of Science and Technology*

(NTNU), 7034 Trondheim, Norway; ● orcid.org/0000-0003-2259-1334; Email: kamilla.arnesen@ntnu.no

Gabriella Tranell − *Department of Materials Science and Engineering, Norwegian University of Science and Technology (NTNU), 7034 Trondheim, Norway;*
Email: gabriella.tranell@ntnu.no

Authors

Kurian J. Vachaparambil − *SINTEF Industry, 7034 Trondheim, Norway*

Vegar Andersen − *Department of Materials Science and Engineering, Norwegian University of Science and Technology (NTNU), 7034 Trondheim, Norway;* ● orcid.org/0000-0002-6486-0785

Balram Panjwani − *SINTEF Industry, 7034 Trondheim, Norway;* ● orcid.org/0000-0002-9700-2672

Katarina Jakovljevic − *Department of Materials Science and Engineering, Norwegian University of Science and Technology (NTNU), 7034 Trondheim, Norway*

Ellen Katrin Enge − *Norwegian Institute of Air Research (NILU), 2007 Kjeller, Norway*

Heiko Gaertner − *SINTEF Industry, 7034 Trondheim, Norway*

Thor Anders Aarhaug − *SINTEF Industry, 7034 Trondheim, Norway*

Kristian Etienne Einarsrud − *Department of Materials Science and Engineering, Norwegian University of Science and Technology (NTNU), 7034 Trondheim, Norway*

Complete contact information is available at:
https://pubs.acs.org/10.1021/acs.iecr.2c04578

Notes

The authors declare no competing financial interest.

■ **REFERENCES**

(1) Abdel-Shafy, H. I.; Mansour, M. S. M. A review on polycyclic aromatic hydrocarbons: Source, environmental impact, effect on human health and remediation. *Egyptian Journal of Petroleum* **2016**, *25*, 107−123.

(2) European Union, Decision No. 1386/2013/EU of the European Parliament and of the Council of 20 November 2013 on a General Union Environment Action Program to 2020 'Living well, within the limits of our planet'; 2013.

(3) Zhang, Y.; Tao, S. Global atmospheric emission inventory of polycyclic aromatic hydrocarbons (PAHs) for 2004. *Atmos. Environ.* **2009**, *43*, 812−819.

(4) Andersson, J. T.; Achten, C. Time to Say Goodbye to the 16 EPA PAHs? Toward an Up-to-Date Use of PACs for Environmental Purposes. *Polycyclic Aromatic Compounds* **2015**, *35*, 330−354.

(5) Lima, A. L. C.; Farrington, J. W.; Reddy, C. M. Combustion-Derived Polycyclic Aromatic Hydrocarbons in the Environment—A Review. *Environmental Forensics* **2005**, *6*, 109−131.

(6) Tobiszewski, M.; Namieśnik, J. PAH diagnostic ratios for the identification of pollution emission sources. *Environ. Pollut.* **2012**, *162*, 110−119.

(7) Budzinski, H.; Jones, I.; Bellocq, J.; Piérard, C.; Garrigues, P. Evaluation of sediment contamination by polycyclic aromatic hydrocarbons in the Gironde estuary. *Marine Chemistry* **1997**, *58*, 85−97.

(8) Pies, C.; Hoffmann, B.; Petrowsky, J.; Yang, Y.; Ternes, T. A.; Hofmann, T. Characterization and source identification of polycyclic aromatic hydrocarbons (PAHs) in river bank soils. *Chemosphere* **2008**, *72*, 1594−1601.

(9) Zhang, W.; Zhang, S.; Wan, C.; Yue, D.; Ye, Y.; Wang, X. Source diagnostics of polycyclic aromatic hydrocarbons in urban road runoff, dust, rain and canopy throughfall. *Environ. Pollut.* **2008**, *153*, 594−601.

(10) Schei, A.; Tuset, J.; Tveit, H. *Production of High Silicon Alloys*; Tapir: Trondheim, 1998.

(11) Kero, I.; Grådahl, S.; Tranell, G. Airborne Emissions from Si/FeSi Production. *JOM* **2017**, *69*, 365−380.

(12) Eidet, T.; Mikkelsen, Ø. PAH-free binders in metallurgical carbon pastes. The 15th International Ferroalloys Congress INFACON XV, Cape Town, 2018.

(13) Gaertner, H.; Aarhaug, T. A.; Wittgens, B.; Hunsbedt, L.; Legård, M.; Tranell, G. Measurements of PAH emissions in the ferro-alloy industry. The 15th International Ferroalloys Congress INFACON XV. Cape Town, 2018.

(14) Norwegian Environmental Agency, Norske utslipp - Utslipp til luft og vann og generert avfall, PAH-16-USEPA. https://www.norskeutslipp.no.

(15) Normann, F.; Skafestad, R.; Bierman, M.; Wolf, J.; Mathisen, A. Reducing the Cost of Carbon Capture in Process Industry. 2019; https://www.sintef.no.

(16) Mathisen, A.; Normann, F.; Biermann, M.; Skagestad, R.; Haug, A. T. *CO2 Capture Opportunities in the Norwegian Silicon Industry*; SINTEF Academic Press: 2019.

(17) Henningsen, S. In *Handbook of Air Pollution From Internal Combustion Engines*; Sher, E., Ed.; Academic Press: San Diego, 1998; pp 477−534.

(18) Chen, S.; Cui, K.; Zhu, J.; Zhao, Y.; Wang, L.-C.; Mutuku, J. K. Effect of Exhaust Gas Recirculation Rate on the Emissions of Persistent Organic Pollutants from a Diesel Engine. *Aerosol and Air Quality Research* **2019**, *19*, 812−819.

(19) Abdelaal, M.; El-Riedy, M.; El-Nahas, A. Effect of flue gas recirculation on burner performance and emissions. *Journal of Al-Azhar University Engineering Sector* **2016**, *11*, 1275−1284.

(20) Liu, P.; Zhang, Y.; Wang, L.; Tian, B.; Guan, B.; Han, D.; Huang, Z.; Lin, H. Chemical Mechanism of Exhaust Gas Recirculation on Polycyclic Aromatic Hydrocarbons Formation Based on Laser-Induced Fluorescence Measurement. *Energy Fuels* **2018**, *32*, 7112−7124.

(21) Reizer, E.; Viskolcz, B.; Fiser, B. Formation and growth mechanisms of polycyclic aromatic hydrocarbons: A mini-review. *Chemosphere* **2022**, *291*, 132793.

(22) Slavinskaya, N.; Mirzayeva, A.; Whitside, R.; Starke, J.; Abbasi, M.; Auyelkhankyzy, M.; Chernov, V. A modelling study of acetylene oxidation and pyrolysis. *Combust. Flame* **2019**, *210*, 25−42.

(23) Panjwani, B.; Andersson, S.; Wittgens, B.; Olsen, J. E. *Cleaning of polycyclic aromatic hydrocarbons (PAH) obtained from ferroalloys plant*; SINTEF Academic Press: 2017.

(24) Andersen, V.; Solheim, I.; Gaertner, H.; Sægrov-Sorte, B.; Einarsrud, K. E.; Tranell, G. In *REWAS 2022: Developing Tomorrow's Technical Cycles (Vol. I)*; The Minerals, Metals & Materials Series; Lazou, A., Daehn, K., Fleuriault, C., Gökelma, M., Olivetti, E., Meskers, C., Eds.; Springer International Publishing: Cham, 2022; pp 555−564.

(25) Andersen, V.; Solheim, I.; Gaertner, H.; Sægrov-Sorte, B.; Einarsrud, K. E.; Tranell, G. Pilot-Scale Test of Flue Gas Recirculation for The Silicon Process. *Journal of Sustainable Metallurgy* **2023**, *9*, 81−92.

(26) National Institute of Health. *PubChem*. 2022; https://pubchem.ncbi.nlm.nih.gov/ (accessed 2022−03−14).

(27) Bjørseth, A. *Handbook of polycyclic aromatic hydrocarbons*; Marcel Dekker: New York, 1983.

(28) Greenshields, C. *OpenFOAM v8 User Guide*; The OpenFOAM Foundation: London, U.K., 2020.

(29) Li, T.; Pan, J.; Kong, F.; Xu, B.; Wang, X. A quasi-direct numerical simulation solver for compressible reacting flows. *Computers & Fluids* **2020**, *213*, 104718.

(30) Richter, H.; Granata, S.; Green, W. H.; Howard, J. B. Detailed modeling of PAH and soot formation in a laminar premixed benzene/oxygen/argon low-pressure flame. *Proceedings of the Combustion Institute* **2005**, *30*, 1397−1405.

(31) Pejpichestakul, W.; Ranzi, E.; Pelucchi, M.; Frassoldati, A.; Cuoci, A.; Parente, A.; Faravelli, T. Examination of a soot model in premixed laminar flames at fuel-rich conditions. *Proceedings of the Combustion Institute* **2019**, *37*, 1013−1021.

(32) Meeks, E.; Grcar, J. F.; Kee, R. J.; Moffat, H. K. *AURORA: A FORTRAN program for modeling well stirred plasma and thermal reactors with gas and surface reactions*; U.S. Department of Energy, Office of Scientific and Technical Information: 1996; DOI: 10.2172/206570.

(33) Shaddix, C. R.; Wang, H.; Schefer, R. W.; Oefelein, J. C.; Pickett, L. M. *Predicting the Effects of Fuel Composition and Flame Structure on Soot Generation in Turbulent Non-Premixed Flames*; Defense Technical Information Center: 2011.

Paper II

Analysis of Nitro- and Oxy-PAH Emissions from a Pilot Scale Silicon Process with Flue Gas Recirculation

Kamilla Arnesen,[†] Vegar Andersen,[†] Katarina Jakovljevic,[†] Ellen Katrin Enge,[‡] Heiko Gaertner,[¶] Thor Anders Aarhaug,[¶] Kristian Etienne Einarsrud,[†] and Gabriella Tranell[*,†]

[†]*Department of Materials Science and Engineering, Norwegian University of Science and Technology (NTNU), 7034 Trondheim, Norway*

[‡]*Norwegian Institute of Air Research (NILU), 2007 Kjeller, Norway*

[¶]*SINTEF Industry, 7034 Trondheim, Norway*

E-mail: kamilla.arnesen@ntnu.no

Abstract

Silicon alloys are produced by carbothermic reduction of quartz in a submerged arc furnace. This high-temperature pyrolytic process is a source of polycyclic aromatic hydrocarbons (PAHs), which are a group of aromatic organic molecules with known mutagenic and carcinogenic properties. In this study, the emission of oxy- and nitro-PAHs was investigated from a pilot-scale Si furnace, with varying process conditions such as oxygen level, flue gas recirculation (FGR), and off-gas flow. Analysis shows the presence of both oxy- and nitro-PAH species in all experiments, believed to be formed from radical-induced substitution reactions initiated from SiO combustion and NO_x formation. During Si production without FGR, the level of oxy- and nitro-PAHs range

between 1.1 and 4.4 $\mu g/Nm^3$, independent of the flue gas flow rate. With increasing FGR (0 - 82.5 %) and decreasing oxygen level (20.7 - 13.3 %), concentrations of both oxy- and nitro-PAHs increase to 36.6 and 65.9 $\mu g/Nm^3$, respectively. When levels of substituted PAHs increase, species such as 4-nitropyrene and 1,2-benzanthraquinone are in abundance compared to their parent PAHs. Experiments at lower flue gas flow (500 Nm^3/h versus 1000 Nm^3/h) generally produce less substituted PAHs, as well as SiO$_2$ particulate matter and NO$_x$, where the latter two parameters have a 99 % correlation in this study.

Introduction

Polycyclic aromatic hydrocarbons (PAHs) are a group of organic molecules consisting of two or more fused aromatic rings, with molecules classified as persistent organic pollutants, and some species are known mutagenic and carcinogenic.[1] Primary sources of PAH to the atmosphere are caused by incomplete combustion of organic materials such as coal, oil, petroleum, and wood. PAH is also emitted from natural sources such as forest fires and volcanoes, but anthropogenic activity is the main source of emission. PAH emissions from combustion are formed through two major mechanisms: PAHs produced from pyrosynthesis of carbon and hydrogen sources and emission/evaporation of existing PAHs in the original product, respectively. Both mechanisms are complex interactions affected by fuel type, temperature, oxygen level and combustion conditions.[2]

Metallurgical grade silicon (MG-Si) is typically produced through carbothermal reduction of quartz, using a mix of coal, coke, charcoal and woodchips in a semi-closed submerged arc furnace (SAF). The carbon materials reduce the quartz to silicon alloy by the overall reaction shown in Eq. 1, where σ is the Si-yield, which gives the distribution between tapped Si and gaseous silicon monoxide (SiO) leaving the furnace.[3]

$$SiO_2 + (1 + \sigma)C = \sigma Si + (1 - \sigma)SiO(g) + (1 + \sigma)CO(g) \tag{1}$$
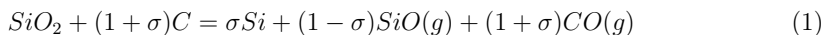
Silicon monoxide and carbon monoxide (CO) that reach the top of the furnace react with air and form silica fume (SiO_2) and carbon dioxide CO_2, respectively, in the furnace hood.[3]

The combustion affects the temperature at the charge surface in the furnace which can reach 700 to 1300 °C. Because the SAF is semi-closed, the under-pressure in the furnace drives the surrounding air into the furnace hood diluting the furnace off-gas, which consist mainly of air. The excess of air combined with the high temperature produce thermal NO_x through combustion, the so called Zeldovich mechanism, of nitrogen and oxygen in the air by radical formation. As described by Kamfjord,[4] the SiO and CO combustion produce high temperature hot spots at the top of the furnace charge, where also VOCs and moisture evaporate, creating conditions for fuel, prompt and thermal NO_x formation.

PAHs are emitted from the furnace, either from the top of the gas-permeable furnace charge material or through gas released during the tapping process. Typically these PAHs originate from pyrolysis, combustion of the carbon raw materials and baking of the electrodes.[5,6] Thomas and Wornat[7] describe the importance of oxygen and temperature in the formation and destruction of PAH in a high temperature reactor using catechol as a model fuel. By investigating the effect of varying oxygen levels and temperatures up to 1000 °C, oxygen is recognized to have an important role both in creating free radicals that lead to increased PAH formation at T < 850 °C, and also increased PAH destruction at T > 850 °C at high levels of oxygen.

In the work by Hrdina et al.,[8] parent PAH transformation through atmospheric oxidation is described, recognizing key atmospheric oxidants of PAHs to include ozone (O_3), hydroxyl radical (OH·), nitrogen dioxide (NO_2), and nitrate radical (NO_3·). Nitrated PAHs (Nitro-PAH) and oxygenated PAHs (oxy-PAH) are two groups of substituted PAH containing at least one nitro group (NO_2) or carbonylic oxygen attached to an aromatic ring.[9] As a result, some of the physiochemical properties change, compared to the parent PAH, which in turn alter their environmental and toxicological effects. The International Agency for Research on Cancer (IARC) classify 1-nitropyrene as "probably carcinogenic to humans", with PAH

3

derivatives recognized as mutagens.[10] These electrophilic aromatic substitution reactions can occur both in gas and solid phase and produce various substituted PAHs, such as nitro- and oxy-PAH species.[11–13] Atkinson et al.,[14] investigated the reactivity of naphthalene in a N_2O_5-NO_3-NO_2-air mixture at troposphere conditions and found naphthalene to form nitro- arenes by initial formation of NO_3-PAH adduct, followed by a reaction with NO_2. The initial reaction to create a PAH adduct is seen to form both oxy and nitro-PAH species, based on the continued reaction of the adduct with available reactants, independent on the initiation of the reaction (by nitrate or hydroxyl radical).[8,15] Oxy- and nitro-PAH compounds are also detected in research on emissions from diesel engines, where NO_x is known to be a considerable part of the exhaust. Heeb et al.,[16] investigated how diesel engine filters influence PAH and nitro-PAH profiles in diesel exhaust and found the filter to promote formation of some nitro-PAH, enhancing the degradation of others depending on the operating conditions of the engine. Hayakawa,[17] investigated the formation of nitro-PAH compared to their parent PAH with increasing combustion temperatures, representing diesel-engines, coal and wood burning stoves. The nitro-PAH/PAH ratio was observed to increase with temperature for compounds such as 1-nitropyrene, 6-nitrochrysene and 7-nitrobenz[a]anthracene. Oxy-PAH have been found in emissions related to diesel exhaust, charcoal and coal production.[18] Drotikova et al.,[19] measured PAH in ambient air in Longyearbyen, Svalbard, and found coal-fired power plants to be one of the main sources of PAHs, with 9-fluorenone and 9,10- anthraquinone to be the dominating oxy-PAH species.

Flue gas recirculation (FGR), or exhaust gas recirculation, is a known method used for emission control by recycling parts of the process off-gas, eg. in diesel engines to reduce oxygen levels, temperature and NO_x formation, and as a way to concentrate off-gas species, such as CO_2, for further processing for CO_2 capture.[20–22] The method has also been found to increase the level of hydrocarbon species (including PAHs), when temperature and oxygen concentration reach a certain level due to reduced oxidation efficiency.[23–25]

While the authors previous work went in depth on an extensive list of native PAHs, this

4

paper has focused specifically on substituted PAHs which within the metallurgical industry is an area still to be explored. The objective of this study was to investigate the emissions of substituted PAH, oxy- and nitro-PAH from pilot scale silicon production and evaluate the effect of flue gas recirculation and furnace conditions on the resulting emission levels.

Experimental methodology

Pilot Furnace

A pilot scale one-phase submerged arc furnace was used for silicon production with flue gas recirculation over a 3-days period with continuous operations. More details regarding the experiment can be found in the works of Andersen et al.[26–28] The furnace and off-gas system is illustrated in Figure S2. The off-gas composition was analyzed during the experiment using different techniques, both on the furnace outlet and inlet. Gas composition (eg. O_2, CO_2, NO_x, CO) and PM was analyzed using an Agilent 490-PRO Micro-GC, LaserGas II and LaserDust instruments (NEO monitors).

A mix of coal, coke, charcoal, woodchips and quartz made up the raw materials and were supplied by an industrial partner. The materials were used as received, except for the woodchips, which were dried at 100 °C for 24 h. Carbon raw material specifications are found in Table S3.

PAH Sampling Procedure

A sample collection system for PAH was developed by adapting a standard set-up following isokinetic sampling principles to investigate PAH composition in gas and particle phase from the pilot furnace. More details regarding the sampling method is described elsewhere.[29] The sampling set-up used glass fiber filters (22 Ø, Munktell/Ahlstrom, Sweden) and XAD-2 (Supelpak-2, Merck Life Science AS, Germany) absorbent with a rotary vane pump (Paul Gothe GmbH, Germany) for sample extraction from the off-gas duct. All samples were

protected against UV radiation by layers of aluminum foil, and stored at 4 °C in a dark location prior to analysis by Norwegian Institute of Air Research (NILU, Kjeller, Norway).

PAH Analysis Methodology

The analytical procedure follows the requirements of NILU's accreditation, according to NS-EN ISO/IEC 17025. Internal standard containing deuterated PAH congeners were added to all samples prior to extraction. Standards are listed in Table S4. XAD-2 and filter samples were Soxhlet extracted for 8 h in acetone/hexane (1:1), concentrated followed by cleanup using silica gel deactivated with 8 % water (adsorption chromatography). After concentration, recovery standards were added. Identification and quantification of a set of nitro- and oxy-PAH analyses were performed by gas chromatography quadrupole time-of-flight (GC-qToF) method in Electron Capture Negative Ion (ECNI) mode. The list of PAH components is shown in Table 1.

Table 1: List of nitro- and oxy-PAH components analyzed for in the FGR off-gas samples.

Compound	MW [g/mol][a]	# of rings	IARC Classification[b]
9-Nitroantheracene	223.2	3	Group 3
2+3-Nitrofluoranthene	247.3	4	Group 3
1-Nitropyrene	247.3	4	Group 2A
4-Nitropyrene	247.3	4	Group 2B
3-Nitrobenzanthrone	275.3	4	Group 2B
7-Nitrobenz[a]Antheracene	273.3	4	Group 3
1,3-DiNitropyrene	292.2	4	Group 2B
1,6-DiNitropyrene	292.2	4	Group 2B
9-Fluorenone	180.2	3	-
9,10-Anthraquinone	208.2	3	-
2-Methyl-9,10-Anthraquinone	222.2	3	-
6H-Benz[de]Anthracen-6-one	230.3	4	-
1,2-Benzanthraquinone	258.3	4	-
6H-Benzo[cd]Pyren-6-one	254.3	5	-

[a] PAH MW[30]
[b] PAH IARC status[10]

Results and discussion

Each sampling period started within a new experimental cycle for the pilot furnace, after stable process conditions were reached. A cycle from feeding raw materials, to charge material collapse and metal tapping lasted about 1.5 hour. Near the end of the cycle was often marked with a blowout in the furnace, which caused the furnace conditions to change, and marked the end of a stable period. A more detailed description of variations within the experiments can be found in the work of Andersen et al.[26]

On average, 0.30 Nm^3 off-gas was sampled per hour of silicon production. Results from 9 different experiments, out of the 27 runs, will be presented in this work, which include a total of 27 samples where the FGR levels vary from 0 to 75.0 % for experiments at 500 Nm^3/h off-gas flow rate and from 0 to 82.5 % for experiments at 1000 Nm^3/h. An overview of the total concentration of PAH-42, oxy- and nitro-PAH from experiments at varying FGR for 1000 and 500 Nm^3/h is presented in Figure 1, and results for all oxy- and nitro-compounds can be found in Table S1 in the supporting information.
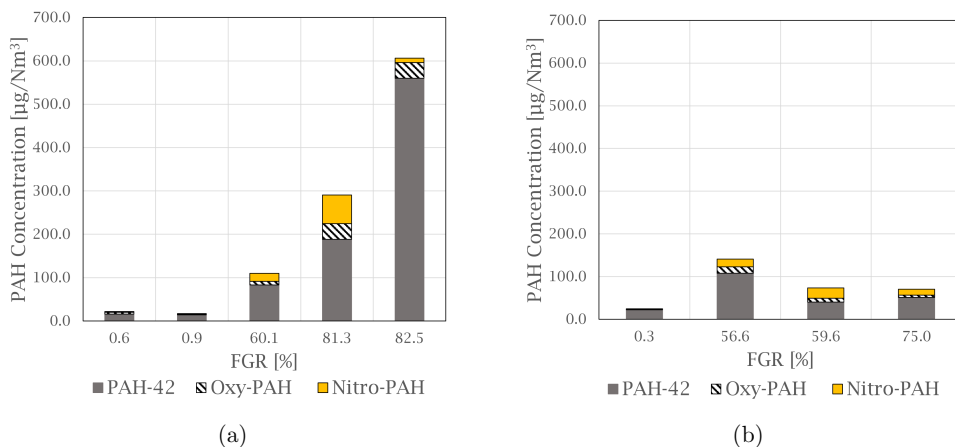

Figure 1: Graphs showing the total PAH-42, oxy- and nitro-PAH concentration in the off-gas at varying FGR levels for experiments at (a) 1000 Nm^3/h and (b) 500 Nm^3/h.

The concentrations are a sum of 8 nitro-species with 3 and 4 rings, 6 oxy-species with 3 to 5 rings, and PAH-42, which is an extended EPA-16 list that also include heterocyclic and alkylated PAHs. Overall, an increase in PAH concentration at higher FGR is observed for both the 1000 and 500 Nm^3/h flow-rates. Higher PAH concentrations were generally observed for the 1000 Nm^3/h experiments as further elaborated by Arnesen et al.,[29] where the increased temperature and residence time at low flow is believed to result in better conditions for combustion. An important note is the number of species being analyzed which represent the different categories, and analyzing 42 species would expect to result in a higher concentration then the 14 substituted PAHs.

Dust and NO$_x$ production

The total amount of particulate matter (PM) and NO$_x$ was measured during the experiments, and the variations are presented in Figure 2. NO$_x$ is the sum of NO and NO$_2$, where NO$_2$ on average make up 13.7±2.0 % of the total amount. A correlation was found between PM and NO$_x$ at 99 %. This correlation is also observed in experimental work performed by Kamfjord,[4] where exothermic SiO combustion to particulate silica fume at the furnace charge surface create local areas with high temperature, and thermal NO$_x$ can form. The level of both dust and NO$_x$ observed in the pilot experiments decrease for experiments at lower flow, 500 Nm^3/h, with amounts below 1.00 kg PM and 0.10 kg NO$_x$. Less ambient air is needed to dilute the off-gas at low flow, and the lower amount of oxygen available for SiO combustion can therefor be a reason for the decreased NO$_x$ levels.

Emission of nitro-PAHs during Si production

The level of measured nitro-PAH in the pilot campaign range between 1.4 and 65.9 $\mu g/Nm^3$. At conditions for Si production without FGR, the level of nitro-PAH are between 1 and 2 $\mu g/Nm^3$. An overview of the total nitro-PAH concentrations and conditions for experiments at 1000 and 500 Nm^3/h together with the average measured values for the experiments,
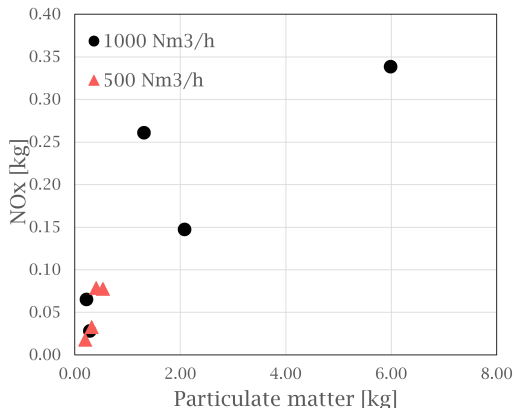
Figure 2: Graph showing the variation in particulate matter and NO_x produced during Si production, for experiments at both 1000 Nm^3/h and 500 Nm^3/h.

flow, FGR level, oxygen level and temperatures, are presented in Table 2.

With some variation a general trend is observed. When combustion conditions change the level of nitro-PAHs increase up to 65.9 $\mu g/Nm^3$ with lower available oxygen, which indicates that higher flue gas recirculation rates that lead to lower oxygen levels in the furnace atmosphere can be a substantial driving force for the generation of nitro-PAHs. Some variation is present between the two flow rates (500 and 1000 Nm^3/h), where the concentration reach higher levels for the increased flow rate. On average, 96.8 % of the measured nitro-PAH species were found in the filter samples. As expected, these species are present as condensed phase based on molecular weight and volatility, combined with the average flue gas temperature.

The compound 4-nitropyrene is the most abundant nitro-PAH specie of those quantified in every sample, accounting for 39.5 to 91.5 % of the total measured nitro-PAH concentration. The second most abundant specie(s) is the combined 2 and 3-nitrofluoranthene, with levels up to 34.0 % of the total concentration in the samples. Figure 3 shows comparisons between the concentration of nitro-PAH species with their parent PAH at different FGR levels (Concentrations of parent PAHs can be found in the supplementary information of

9

Table 2: Nitro-PAH concentrations, measured gas flow, recirculation ratio and oxygen averages from PAH sampling in the FGR Pilot campaign, sorted by flow and decreasing oxygen levels.

Sample nr.	Flow [Nm^3/h]	FGR [%]	Oxygen [vol%]	Flue Gas Temperature [°C]	Nitro-PAH [$\mu g/Nm^3$]
1	965	0.6	20.7	208	1.353
8	914	0.9	20.7	249	1.869
5	935	60.1	17.6	238	18.468
4	865	81.3	15.5	232	65.867
13	919	82.5	13.3	237	9.807
9	566	0.3	20.4	268	1.678
3	440	56.6	17.9	275	18.219
7	497	59.6	17.3	293	24.010
6	425	75.0	16.4	275	14.001

Arnesen et al.[29]). The anthracene species are shown in Figure 3 (a) and (b), where the parent specie is in abundance for most of the experiments, with exception of experiments at 59.6 and 60.1 % FGR, where the distribution is approximately equal. For fluoranthene, in Figures 3 (c) and (d), more 2+3-nitrofluoranthene (separation of 2- and 3-nitrofluoranthene was not achieved with the current analysis technique) than its parent is detected in three of the nine experiments. The opposite is the case for pyrene species in Figure 3 (e) and (f), where regular pyrene is only dominating in one experiment at 82.5 % FGR. Overall, the dominating pyrene species are 4-nitropyrene, followed by 1,3-dinitropyrene, which in some cases exhibit the same concentration levels as pyrene.

Even though the level of NO_x and the concentration of nitro-PAH did not show a direct correlation with the level of flue gas recirculation in this study (5 % correlation) it becomes clear that the formation of PAH species in a pyrolytic system such as the Si furnace is a balance between oxidative combustion, depending on temperature and oxygen, and other competing reactions.

Nitrogen oxides must be present for the nitro-PAHs to form and the NO_x forming reactions are a source of radicals and atmospheric oxidative reactions. Hrdina et al.,[8] describe the necessity of radicals and radical-initiated reactions to create oxidants such as $NO_3^{\cdot}$ and
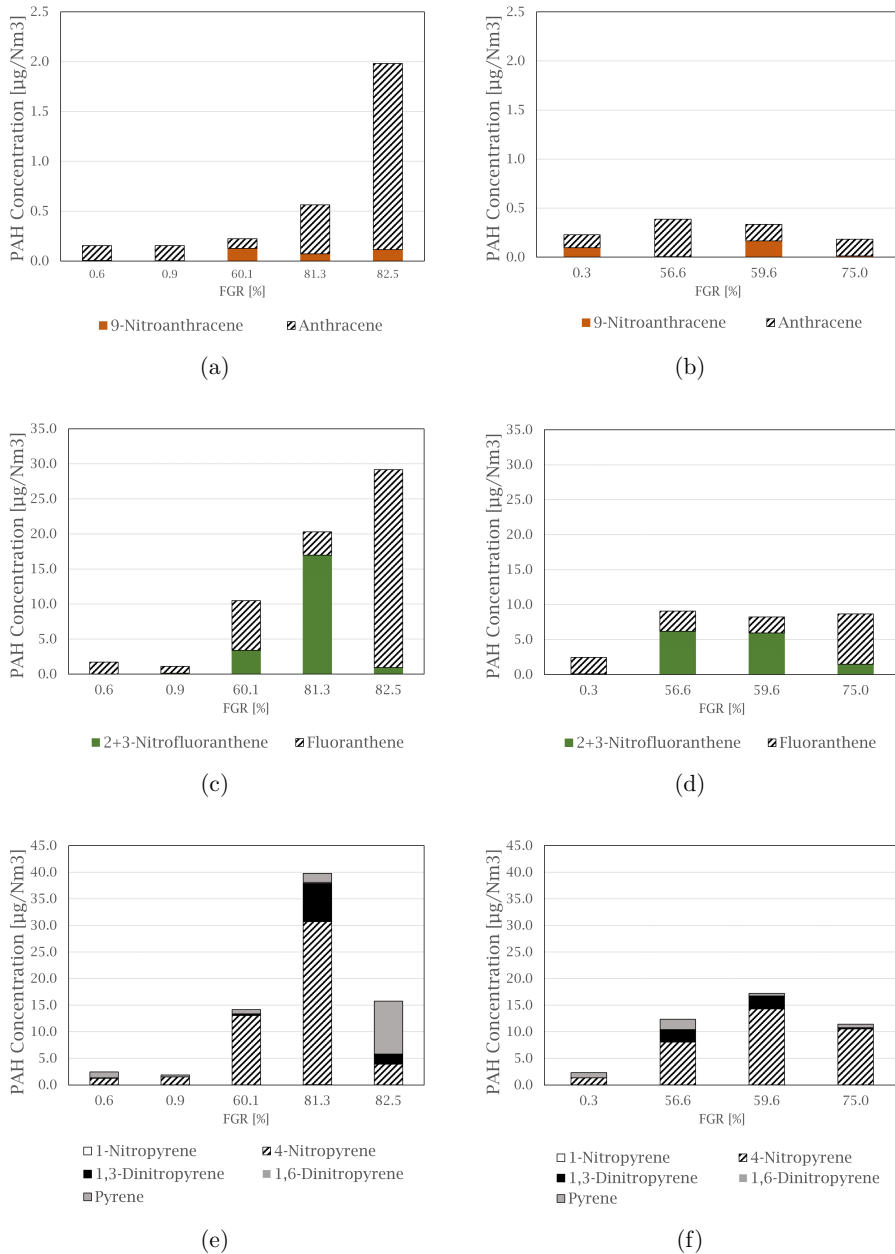
Figure 3: Graphs showing the distribution of nitro-PAH and the corresponding parent PAH for experiments at 1000 Nm^3/h (left) and 500 Nm^3/h (right), (a)+(b): Antheracene species, (c)+(d): Fluoranthene species, (e)+(f): Pyrene species.

OH. which function as activators of the substitution reaction. Katritzky et al.,[11] describe the nature of an aromatic substitution reaction where the initial reaction step produces a temporary positively charged arenium ion. The initial reaction to form the arenium ion is typically the rate-limiting step, and will react further with electron rich molecules. In the case of this study, oxygen or NO_2 are expected to react, and form the final oxy- or nitro-PAH molecule. An example of how nitration of pyrene could occur is presented in Figure 4.
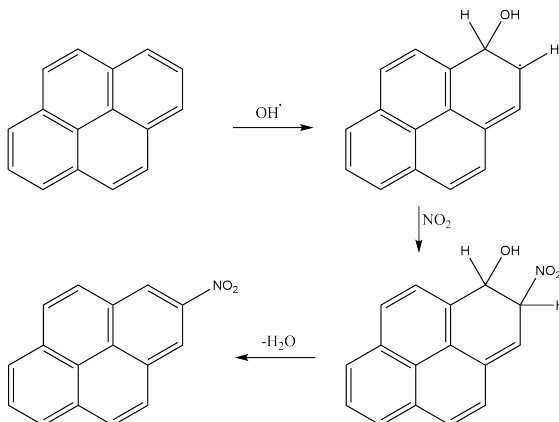

Figure 4: An example of a nitration mechanism of pyrene with OH. initiating the substitution reaction.

The mechanism of the substitution reaction and preferential isomeric formation is often used to characterize PAH emissions. In the studies by Hu et al.,[31] examining nitro-PAH emissions from diesel vehicles and Albinet et al.,[12] studying pollution of substituted PAHs in rural and urban locations in France, where the isomer of 1-nitropyrene is an important and favored pyrene specie. Atkinson et al.,[14] investigated the kinetics of nitro-PAH formation and found 1- and 2-nitropyrene to be favored over 4-nitropyrene in OH radical-initiated reactions with pyrene at ambient conditions. They also determined the rate constants for gas-phase reactions in N_2O_5-NO_3-NO_2-air, and found both 2- and 4-nitropyrene to be a product of the NO_3 radical-initiated reaction. 2-nitropyrene was found to be dependent on the NO_2 concentration, but no such connection was discovered for 4-nitropyrene. In this current

study, 4-nitropyrene was the abundant pyrene specie in all samples, and 4-nitropyrene is thus most likely a product of gas-phase NO_3 radical-initiated reaction directly in the furnace and a result of a primary emission source.

Emission of oxy-PAHs during Si production

The level of oxy-PAHs measured in the pilot campaign range between 1.1 and 36.6 $\mu g/Nm^3$. On average 94.4 % of all the species were found in the filter samples. This is slightly lower than for nitro-PAHs, and is mainly caused by the oxy-PAHs with lower molecular weight (9-fluorenone and 9,10-anthraquinone) passing through the filter. Using bag house filters to clean dust and condensed PAH species from the off-gas is a widely used technique. Off-gas temperature is an important control parameter to protect filter-bag material from degradation and ensure efficient removal of particulate matter. The total concentration of oxy-PAHs for experiments at 1000 and 500 Nm^3/h are given in Table 3, together with the corresponding flow, FGR and O_2 level and off-gas temperature averages for the given experiments. The total concentration of measured oxy-PAHs was found to have a 97 % and 99 % correlation with the average levels of FGR and O_2, respectively, for the various experimental steps. An elevation of the oxy-PAH concentration for experiments at high FGR and high flow is also found here, as for nitro-PAHs.

1,2-benzanthraquinone is the most abundant of the measured oxy-PAH species in 7 out of 9 samples, making up between 41.2 - 69.1 % of the total concentration of the total measured oxy-PAH level, followed by 9,10-anthraquinone, accounting for up to 43.5 % of the total amount in some samples. A comparison between the oxy-PAH concentration and their parent PAH is presented in Figure 5. Fluorene species are shown in Figure 5 (a) and (b), and fluorene is in abundance for all samples but one (the experiment at 59.6 % FGR is the exception where the levels are approximately equal). 9,10-anthraquinone is the dominating specie in the anthracene comparison in Figure 5 (c) and (d), but 2-methyl-9,10-anthraquinoen is also equal to - or exceeding the concentration level of anthracene. Compared to the nitro-PAH

Table 3: Total oxy-PAH concentrations, measured gas flow, recirculation ratio and oxygen averages from PAH sampling in the FGR Pilot campaign, sorted by flow and decreasing oxygen levels.

Sample nr.	Flow [Nm^3/h]	FGR [%]	Oxygen [vol%]	Flue Gas Temperature [°C]	Oxy-PAH [$\mu g/Nm^3$]
1	965	0.6	20.7	208	4.389
8	914	0.9	20.7	249	1.131
5	935	60.1	17.6	238	8.026
4	865	81.3	15.5	232	35.928
13	919	82.5	13.3	237	36.647
9	566	0.3	20.4	268	1.228
3	440	56.6	17.9	275	15.280
7	497	59.6	17.3	293	9.297
6	425	75.0	16.4	275	5.620

species with anthracene as its parent molecule, their oxy-PAHs equivalents are in abundance. In Figure 5 (e) and (f), a oxy- and nitro-PAH specie is compared with their parent PAH, benz[a]anthracene. 7-nitrobenz[a]anthracene is not produced at significant levels for the experiments at 0 % FGR, but increase with increasing FGR, where it exceed its parent molecule. As with the other quinone molecules already mentioned, 1,2-benz[a]anthraquinoen is found in high concentration in all experiments, compared to benz[a]anthracene, especially with increased FGR.

Even though only a small range of substituted PAHs were analyzed, and some PAHs are not investigated, such as bicyclic PAHs, a trend is observed. In general, the oxy-PAHs follow the same trend as the nitro-PAHs and increase at higher levels of FGR. With increasing FGR, the substituted oxy species are equal to or exceed their parent PAH in concentration. These findings are in agreement with the study by Drotikova et al.[19] The 9-fluorenone and 9,10-anthraquinone were found to be the dominating oxy-PAH emissions from a coal power plant in Svalbard. Albinet et al.,[32] also found 9,10-anthraquinone to correlate with emission from diesel engines, and describe the observation as a result of gas-phase formation by ozonation. This coincides with quinones being a result of high temperature combustion processes, as the formation mechanisms that create nitro-PAHs are also applicable to oxy-PAHs. The
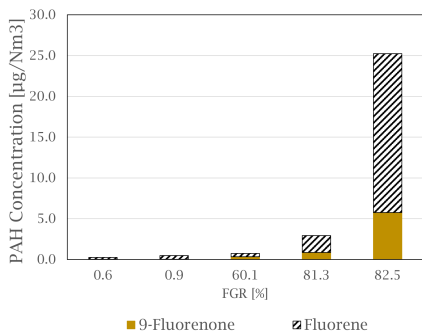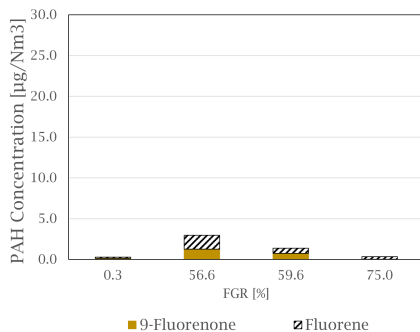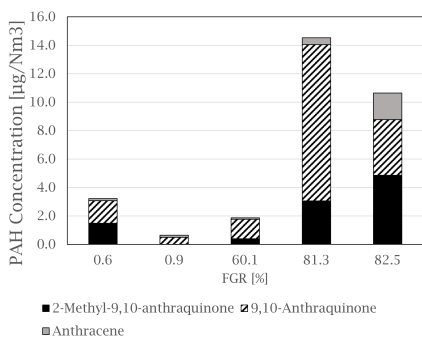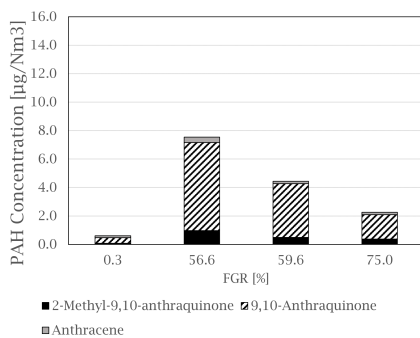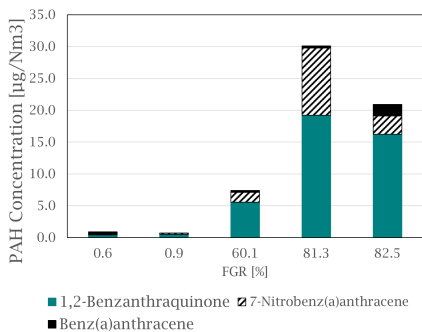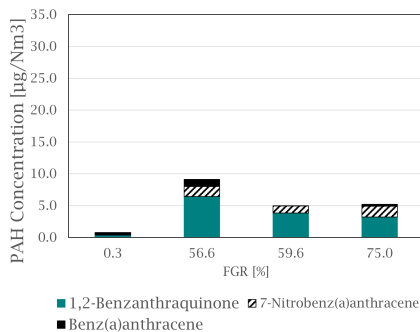
Figure 5: Graphs showing the distribution of oxy-PAH and the corresponding parent PAH for experiments at 1000 Nm^3/h (left) and 500 Nm^3/h (right), (a)+(b): Fluorene species, (c)+(d): Anthracene species, (e)+(f): Benz(a)anthracene species.

observation where some diesel particle filters are seen to facilitate the formation of substituted PAH,[16] is interesting in terms of possible parallels to the Si process, where SiO and SiO_2 PM can have a catalytic effect on radical formation or on formation of PAH-precursors and substituted PAHs.

Estimation of PAH stack emissions

An estimation of the PAH emissions from the FGR pilot experiments is presented in Figure 6. Figure 6 (a) shows the PAH-42 emissions and Figure 6 (b) shows the combined oxy- and nitro-PAH emissions, both at varying FGR levels. The estimation was based on how much of the PAH emissions in each experimental cycle passed through the glass fiber filter used in the sampling set-up and the amount of process gas not being recycled back to the furnace, but exited the stack.
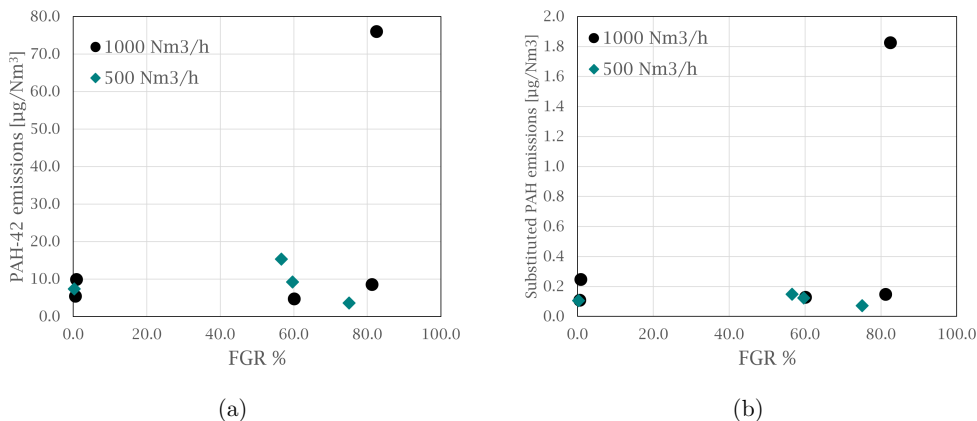

Figure 6: Graphs showing the estimated PAH stack emissions for PAH-42 and substituted PAH (sum of oxy- and nitro-PAHs) for both 1000 Nm^3/h and 500 Nm^3/h at varying FGR levels. (a) PAH-42 and (b) Substituted PAH.

Even though process and temperature variations were not taken into account, an indication towards the PAH emissions, both PAH-42 and substituted PAHs, not being significantly increasing with added FGR is shown, as more of the increased PAHs produced would be re-circulated back to the furnace. The exception is the case at 1000 Nm^3/h and 82.5 % FGR

in both Figure 6 (a) and (b), where the filter efficiency is lower due to the furnace conditions producing more PAH of low molecular weight which can pass through the filter.

Conclusions

In this study, substituted PAH emissions of oxy- and nitro-PAHs, with the size of 3 to 5 rings, were measured from a silicon process. A measurement campaign was performed where Si alloy was produced continuously in a pilot scale submerged arc furnace with FGR and various levels of O_2 and flue gas flow to investigate how FGR influenced furnace operation and off-gas composition. Isokinetic sampling in the off-gas duct was performed to measure PAH levels at varying conditions and analyzed using GC-qToF. The concentration levels for oxy-PAHs were in the range of 1.1 to 4.4 $\mu g/Nm^3$, without FGR, and increased to 36.6 $\mu g/Nm^3$ at 82.5 % FGR. For the nitro-PAHs, the concentration range was between 1.4 and 1.9 $\mu g/Nm^3$, without FGR, and increased to 65.9 $\mu g/Nm^3$ at 81.3 % FGR. With FGR, substituted PAH species, such as 4-nitropyrene and 1,2-benzanthraquinone, were produced in greater amounts than their parent PAHs. Even though the concentration of PAHs measured in the off-gas duct increase with FGR, no significant change is found in the stack emissions with estimations based on the amount of PAHs passing through the filter used for sampling, except for PAHs of low molecular weight. Comparing the two flue gas flows, experiments at 500 Nm^3/h produced overall lower amounts of substituted PAHs, as well as less SiO_2 PM and NO_x, as caused by less oxygen available for combustion, increased temperature in the off-gas and increased residence time in the combustion zone.

Conflicts of interest

There are no conflicts to declare.

Acknowledgement

Supporting Information Available

A full overview of the oxy- and nitro-PAH analysis results, the pilot-scale set-up, details for the raw materials and the PAH standards are provided in the supporting information.

References

(1) Abdel-Shafy, H. I.; Mansour, M. S. M. A review on polycyclic aromatic hydrocarbons: Source, environmental impact, effect on human health and remediation. *Egyptian Journal of Petroleum* **2016**, *25*, 107–123.

(2) Howsam, M.; Jones, K. C. In *PAHs and Related Compounds: Chemistry*; Neilson, A. H., Ed.; The Handbook of Environmental Chemistry; Springer Berlin Heidelberg: Berlin, Heidelberg, 1998; pp 137–174.

(3) Schei, A.; Tuset, J.; Tveit, H. *Production of high silicon alloys*; Tapir: Trondheim, 1998.

(4) Kamfjord, N. E. Mass and energy balances of the silicon process : improved emission standards. Ph.D. thesis, Norwegian University of Science and Technology, Trondheim, 2012.

(5) Kero, I.; Grådahl, S.; Tranell, G. Airborne Emissions from Si/FeSi Production. *JOM* **2017**, *69*, 365–380.

(6) Gaertner, H.; Aarhaug, T. A.; Wittgens, B.; Hunsbedt, L.; Legård, M.; Tranell, G. *The 15th International Ferroalloys Congress INFACON XV*; Southern African Institute of Mining and Metallurgy: Cape Town, 2018.

(7) Thomas, S.; Wornat, M. J. The effects of oxygen on the yields of polycyclic aromatic hydrocarbons formed during the pyrolysis and fuel-rich oxidation of catechol. *Fuel* **2008**, *87*, 768–781.

(8) Hrdina, A. I. H.; Kohale, I. N.; Kaushal, S.; Kelly, J.; Selin, N. E.; Engelward, B. P.; Kroll, J. H. The Parallel Transformations of Polycyclic Aromatic Hydrocarbons in the Body and in the Atmosphere. *Environmental Health Perspectives* **2022**, *130*.

(9) Bandowe, B. A. M.; Meusel, H. Nitrated polycyclic aromatic hydrocarbons (nitro-PAHs) in the environment – A review. *Science of The Total Environment* **2017**, *581-582*, 237–257.

(10) World Health Organization, Agents Classified by the IARC Monographs, Volumes 1–132 – IARC Monographs on the Identification of Carcinogenic Hazards to Humans. 2022; `https://monographs.iarc.who.int/agents-classified-by-the-iarc/`.

(11) Katritzky, A. R.; Kim, M. S.; Fedoseyenko, D.; Widyan, K.; Siskin, M.; Francisco, M. The sulfonation of aromatic and heteroaromatic polycyclic compounds. *Tetrahedron* **2009**, *65*.

(12) Albinet, A.; Leoz-Garziandia, E.; Budzinski, H.; Villenave, E.; Jaffrezo, J. L. Nitrated and oxygenated derivatives of polycyclic aromatic hydrocarbons in the ambient air of two French alpine valleys: Part 1: Concentrations, sources and gas/particle partitioning. *Atmospheric Environment* **2008**, *42*, 43–54.

(13) Carrara, M.; Wolf, J.-C.; Niessner, R. Nitro-PAH formation studied by interacting artificially PAH-coated soot aerosol with NO2 in the temperature range of 295–523K. *Atmospheric Environment* **2010**, *44*, 3878–3885.

(14) Atkinson, R.; Tuazon, E. C.; Arey, J. Reactions of naphthalene in N2O5-NO3-NO2- air mixtures. *International Journal of Chemical Kinetics* **1990**, *22*, 1071–1082.

(15) Keyte, I. J.; Harrison, R. M.; Lammel, G. Chemical reactivity and long-range transport potential of polycyclic aromatic hydrocarbons – a review. *Chemical Society Reviews* **2013**, *42*, 9333–9391.

(16) Heeb, N. V. et al. Secondary Effects of Catalytic Diesel Particulate Filters: Conversion of PAHs versus Formation of Nitro-PAHs. *Environmental Science & Technology* **2008**, *42*, 3773–3779.

(17) Hayakawa, K. Environmental Behaviors and Toxicities of Polycyclic Aromatic Hydrocarbons and Nitropolycyclic Aromatic Hydrocarbons. *Chemical and Pharmaceutical Bulletin* **2016**, *64*, 83–94.

(18) Walgraeve, C.; Demeestere, K.; Dewulf, J.; Zimmermann, R.; Van Langenhove, H. Oxygenated polycyclic aromatic hydrocarbons in atmospheric particulate matter: Molecular characterization and occurrence. *Atmospheric Environment* **2010**, *44*, 1831–1846.

(19) Drotikova, T.; Ali, A. M.; Halse, A. K.; Reinardy, H. C.; Kallenborn, R. Polycyclic aromatic hydrocarbons (PAHs) and oxy- and nitro-PAHs in ambient air of the Arctic town Longyearbyen, Svalbard. *Atmospheric Chemistry and Physics* **2020**, *20*, 9997–10014.

(20) Normann, F.; Skafestad, R.; Bierman, M.; Wolf, J.; Mathisen, A. Reducing the Cost of Carbon Capture in Process Industry. 2019; `https://www.sintef.no`.

(21) Mathisen, A.; Normann, F.; Biermann, M.; Skagestad, R.; Haug, A. T. *CO2 Capture Opportunities in the Norwegian Silicon Industry*; SINTEF Academic Press, 2019.

(22) Sher, E. In *Handbook of Air Pollution From Internal Combustion Engines*; Sher, E., Ed.; Academic Press: San Diego, 1998; pp 27–41.

(23) Chen, S.; Cui, K.; Zhu, J.; Zhao, Y.; Wang, L.-C.; Mutuku, J. K. Effect of Exhaust Gas Recirculation Rate on the Emissions of Persistent Organic Pollutants from a Diesel Engine. *Aerosol and Air Quality Research* **2019**, *19*, 812–819.

(24) Abdelaal, M.; El-Riedy, M.; El-Nahas, A. Effect of flue gas recirculation on burner performance and emissions. *Journal of Al-Azhar University Engineering Sector* **2016**, *11*, 1275–1284.

(25) Liu, P.; Zhang, Y.; Wang, L.; Tian, B.; Guan, B.; Han, D.; Huang, Z.; Lin, H. Chemical Mechanism of Exhaust Gas Recirculation on Polycyclic Aromatic Hydrocarbons Formation Based on Laser-Induced Fluorescence Measurement. *Energy & Fuels* **2018**, *32*, 7112–7124.

(26) Andersen, V.; Solheim, I.; Gaertner, H.; Sægrov-Sorte, B.; Einarsrud, K. E.; Tranell, G. Pilot-Scale Test of Flue Gas Recirculation for The Silicon Process. *Journal of Sustainable Metallurgy* **2022**,

(27) Andersen, V.; Solheim, I.; Gaertner, H.; Sægrov-Sorte, B.; Einarsrud, K. E.; Tranell, G. In *REWAS 2022: Developing Tomorrow's Technical Cycles (Volume I)*; Lazou, A., Daehn, K., Fleuriault, C., Gökelma, M., Olivetti, E., Meskers, C., Eds.; Springer International Publishing: Cham, 2022; pp 555–564.

(28) Andersen, V. Flue Gas Recirculation for the Silicon Process. Ph.D. thesis, Norwegian University of Science and Technology, Trondheim, 2023.

(29) Arnesen, K.; Vachaparambil, K. J.; Andersen, V.; Panjwani, B.; Jakovljevic, K.; Enge, E. K.; Gaertner, H.; Aarhaug, T. A.; Einarsrud, K. E.; Tranell, G. Analysis of Polycyclic Aromatic Hydrocarbon Emissions from a Pilot Scale Silicon Process with Flue Gas Recirculation. *Industrial & Engineering Chemistry Research* **2023**, Publisher: American Chemical Society.

(30) National Institute of Health, PubChem (2022). `https://pubchem.ncbi.nlm.nih.gov/` `(2022-03-14)`.

(31) Hu, S.; Herner, J. D.; Robertson, W.; Kobayashi, R.; Chang, M.-C. O.; Huang, S.-m.; Zielinska, B.; Kado, N.; Collins, J. F.; Rieger, P.; Huai, T.; Ayala, A. Emissions of polycyclic aromatic hydrocarbons (PAHs) and nitro-PAHs from heavy-duty diesel vehicles with DPF and SCR. *Journal of the Air & Waste Management Association* **2013**, *63*, 984–996.

(32) Albinet, A.; Leoz-Garziandia, E.; Budzinski, H.; ViΙlenave, E. Polycyclic aromatic hydrocarbons (PAHs), nitrated PAHs and oxygenated PAHs in ambient air of the Marseilles area (South of France): Concentrations and sources. *Science of The Total Environment* **2007**, *384*, 280–292.
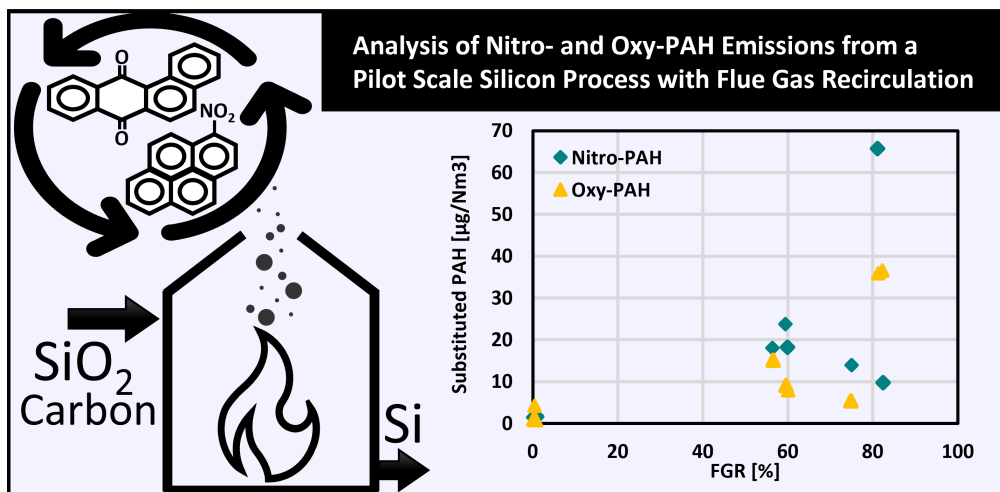
Paper III

Article

Influence of Atmosphere and Temperature on Polycyclic Aromatic Hydrocarbon Emissions from Green Anode Paste Baking

Kamilla Arnesen,* Thor Anders Aarhaug, Kristian Etienne Einarsrud, and Gabriella M. Tranell

Cite This: https://doi.org/10.1021/acsomega.3c01411

Read Online

ACCESS | 📊 Metrics & More | 📰 Article Recommendations

ABSTRACT: Coal tar pitch, a well-known source of polycyclic aromatic hydrocarbons (PAHs), is used as a binder of petroleum coke in prebaked anodes used for electrolysis of aluminum. Anodes are baked up to 1100 °C over a 20-day period, where flue gas containing PAHs and volatile organic compounds (VOCs) are treated using techniques such as regenerative thermal oxidation, quenching, and washing. Conditions during baking facilitate incomplete combustion of PAHs, and due to the various structures and properties of PAHs, the effect of temperature up to 750 °C and various atmospheres during pyrolysis and combustion were tested. PAH emissions from green anode paste (GAP) dominate in the temperature interval of 251−500 °C, where PAH species of 4−

6 rings make up the majority of the emission profile. During pyrolysis in argon atmosphere, a total of 1645 μg EPA-16 PAHs are emitted per gram of GAP. Adding 5 and 10% CO_2 to the inert atmosphere does not seem to affect the PAH emission level significantly, at 1547 and 1666 μg/g, respectively. When adding oxygen, concentrations decreased to 569 μg/g and 417 μg/g for 5% and 10% O_2, respectively, corresponding to a 65% and 75% decrease in emission.
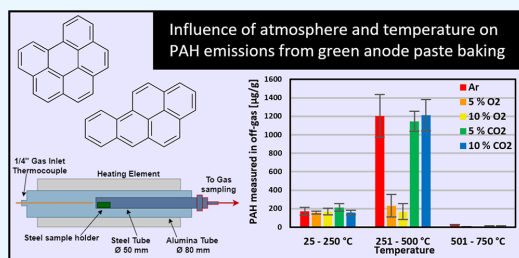
INTRODUCTION

Polycyclic aromatic hydrocarbons (PAHs) are a diverse class of organic compounds, containing two or more fused aromatic rings. Many PAHs are classified as mutagenic, carcinogenic, and persistent organic pollutants, and reduced exposure and emissions are therefore recommended by the Council of the European Union.[1,2] Prebaked carbon anodes for aluminum production are a mix of petroleum coke and coal tar pitch, baked in an anode baking furnace up to 1100 °C over a 20-day cycle. Coal tar pitch is a well-known source of PAHs. The pitch serves as a binder for the coke particles and as an energy source for the baking through combustion of volatile organic compounds (VOCs).[3] In addition, minor elements including sulfur and trace elements such as vanadium, nickel, and iron will be present in the coke and pitch.[4] Flue gas containing PAHs and VOCs from the baking furnace is often treated using regenerative thermal oxidation (RTO) technology, in addition to quenching and washing towers.[5] In the research by Wittgens et al.,[6] a pilot scale combustion chamber with optimized combustion control is presented to facilitate reduced PAH and tar emission in ferroalloy production, finding stoichiometry, gas flow, and temperature to be important conditions.

During anode baking the levels of oxygen in the flue gas have been measured to be between 3 and 11%.[7] Anodes are also reported to be reactive with air and CO_2 during the electrolysis process, at temperatures between 520 and 960 °C. This level of oxygen and thermal conditions may however not be enough to

facilitate complete combustion of PAH. Chevarin et al.[8] tested the O_2 and CO_2 reactivity of baked anodes and its constituents and found the coke to be most reactive with air, while both coke and anode butts showed high reactivity with CO_2 at 960 °C. The coal tar pitch showed the lowest reactivity in all experiments, and this is thought to be influenced by the change in properties of the pitch when baked alone, and with coke particles.

The different structures of PAHs, linear, angular, and cluster, influence the reactivity of the molecules.[9] Angular structures are more stable than linear, as studies show this to be due to better π-interactions, based on Clar's model, and interactions between hydrogen atoms in the bay region.[10] This region is found to increase the molecules' mutagenic and carcinogenic activity.[11] Another influencing factor for PAH stability is the number of rings. Larger PAH molecules have a greater resistance to degradation at ambient conditions, due to increased aromaticity. Degradation mechanisms of large PAH through thermal treatment and chemical oxidation can produce PAH of a smaller size as intermediates if enough energy is not supplied.[12] Sun[13]
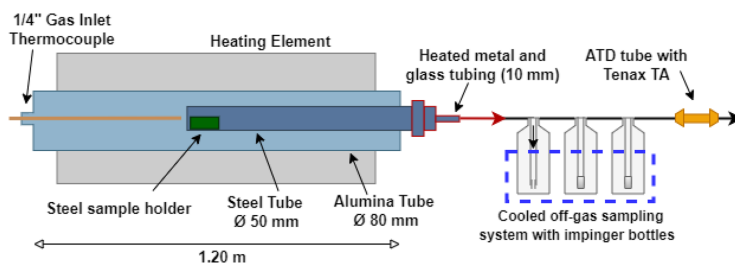
Figure 1. Sketch showing the alumina resistance furnace and off-gas sampling system used for experiments with green anode paste baking.

(a)
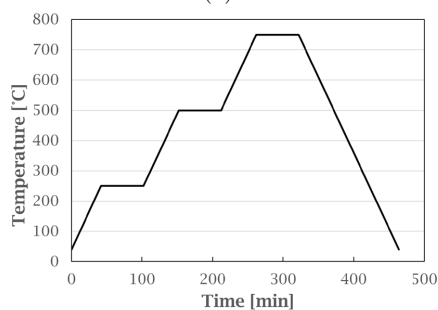
(b)

Figure 2. (a) Bottles with 2-propanol used for collecting PAH species from the off-gas. Bottles with impinger and frits (P0) are used. (b) Temperature ramping program used in the baking of GAP for PAH analysis.

Table 1. Atmospheres and Concentrations Tested for GAP Baking with PAH Analysis

| atmosphere	concentration (%)
Argon	100
O_2	5
O_2	10
CO_2	5
CO_2	10

Figure 3. Average mass loss (%) for GAP samples at varying atmospheres. Error bars show the variation of triplicate experiments.

The main objective of this study has been to investigate the effect of temperature and varying atmospheres on the EPA-16 PAH emissions from green anode paste (GAP) during initial heating of the anode baking process. Conditions at inert pyrolytic and oxidizing conditions were investigated in a controlled laboratory setup to better understand PAH emission profiles from green anode paste.

■ EXPERIMENTAL METHODOLOGY

GAP for the experiments was supplied by an industrial aluminum production partner. The paste contains calcined petroleum coke, anode butts, and coal tar pitch, which was prepared by milling (Herzog Maschinenfabrik, Osnabrück, Germany). Representative sampling was performed following sample splitting and the spoon method, as described by Petersen et al.[16] PAH composition in the off-gas was measured by performing experiments in a laboratory scale alumina tube resistance furnace (Nabertherm, RHTH 120-300/16-18) (Figure 1), where the off-gas was purged, and the organic content was collected in chilled 2-propanol (≥98% Technical, VWR Chemicals), using ice, and further analyzed by GC-MS (CP7462 Agilent column, Xtr EI 350 ion source). Samples were prepared by direct injection of internal standards containing

observed temperature as being a great influence on radical and PAH formation by way of intermolecular reorganization to increase molecular stability and aromaticity, at conditions where complete oxidation is not achieved. Liu et al.[14] investigated PAH emissions from coal combustion in a fluidized bed combustor. In this study, incomplete combustion of PAHs was found at temperatures up to 900 °C, being strongly influenced by the level of excess air in the reactor. Pujro et al.[15] investigated catalytic cracking of heavy aromatic molecules at 450 °C over a fluidized catalytic cracking zeolite catalyst with and without nickel and vanadium. The condensed polyaromatic compounds were found to have an increased activity with the catalysts over the thermal cracking, and this activity was found to increase with the number of aromatic rings.

Figure 4. Off-gas emission of PAH species at various temperature intervals from heating green anode paste in argon atmosphere. Error bars show the standard deviation for each compound based on three experiments.
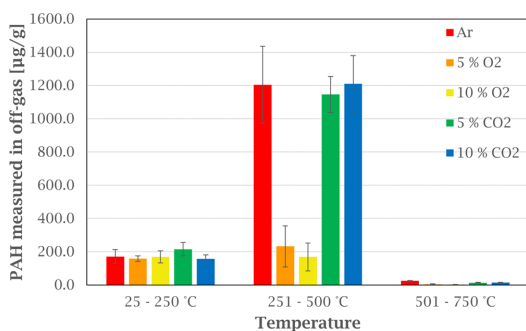

Figure 5. Off-gas emissions of EPA-16 PAHs at different temperature intervals from heating green anode paste in various atmospheres. Error bars show the standard deviation for the PAH concentration for each temperature interval based on three experiments.

deuterated PAH congeners and analyzed using selected ion monitoring (SIM).

For each experiment, 5.00 g GAP was placed in a steel holder and heated in a selected atmosphere with a set temperature ramping program (heating rate 5 °C/h), allowing off-gas sampling and exchange of bottles (Figure 2a) through three temperature intervals, 25−250, 251−500, and 501−750 °C (Figure 2b). The bottles were changed and ice refilled at the end of a hold period, while the gas stream was paused using a ball valve. This temperature range was chosen to study the evaporation of PAH from the raw material and the initial emission mechanism.

Different atmospheres were tested using a gas flow of 0.300 standard liters per minute. The atmosphere details are presented in Table 1. For experiments with different concentration of O_2 and CO_2, air (Technical grade, Linde Gas AS, Trondheim, Norway) and CO_2 (≥99.7%) were diluted in argon (Instrument 5.0) to achieve the correct concentration levels.

Experiments were performed in triplicates, except for 100% Ar, which was performed one additional time to test for

breakthrough of PAH through the three sampling bottles. This test was performed by adding an analytical thermal desorption (ATD) tube filled with the absorbent Tenax TA and glass wool, to the sampling line after the last sampling bottle (Figure 1). The off-gas from the furnace will pass through the bubbling bottles and the ATD tube, where, if present, light PAH will absorb on Tenax TA. The glass wool is present to filter out water and any particles in the stream and shield the absorbent material. The PAH content in the sampling tube was analyzed using thermal desorption and GC-MS.

PAH content in the GAP material was also analyzed using pyrolysis GC-MS. Pyrolysis was performed using a 4 μg sample placed in a tandem μ-reactor (Frontier Lab 3050TR) for 1 min. Analysis was performed once at 400 and 600 °C, and thrice at 750 °C. Compounds were separated and detected using GC-MS (Agilent Technologies; GC 7890B and MSD 5977B), and identified by the NIST Library.

■ RESULTS AND DISCUSSION

GAP Sample Weight Change. All GAP samples used to perform the PAH emissions tests were weighed before and after each experiment at room temperature to investigate sample mass loss. The average mass loss (%) is presented in Figure 3 for all atmospheres. Inert and CO_2 atmosphere show a similar mass loss of 6.5−7.0%, independent of the concentration of CO_2, which could be caused by the thermal evaporation of volatile organic components in the sample. The weight loss increased when oxygen was added, to 20.2% and 34.2% for 5% and 10% O_2, respectively.

Influence of Temperature. All experiments showed a PAH emission profile similar to what is shown in Figure 4, when comparing the effect of temperature. Emission is presented as μg EPA-16 PAH per gram of GAP from experiments in the alumina tube furnace.

Low molecular weight (LMW) PAHs (2 and 3 rings) are the main contributors to the emission at low temperatures, from room temperature to 250 °C. Up to 500 °C, the high molecular weight (HMW) PAHs (4−6 rings) are emitted, at a higher concentration level. Lastly, PAH emissions decrease significantly
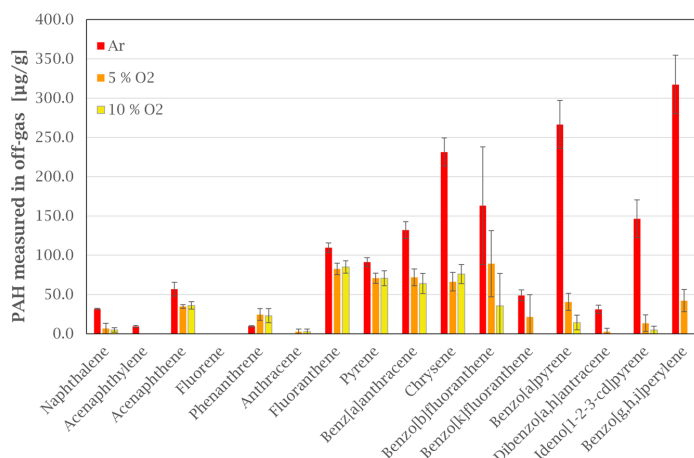
Figure 6. Comparing EPA-16 PAH emissions in off-gas from green anode paste heated in argon and oxygen (5 and 10%) atmospheres. Error bars show the standard deviation for each compound based on three experiments.
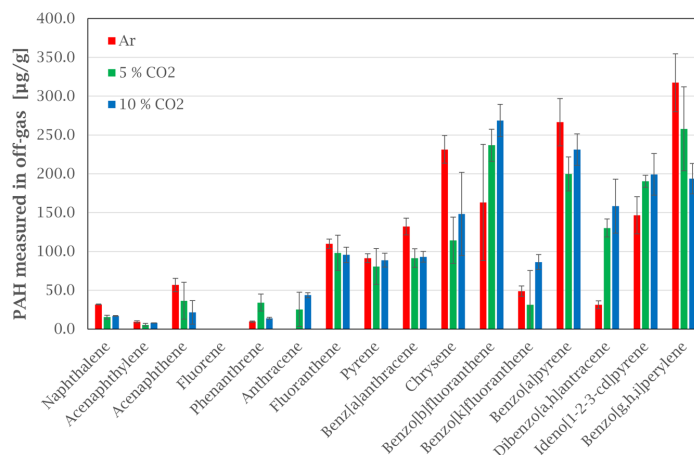
Figure 7. Comparing EPA-16 PAH emissions from green anode paste heated in argon and CO_2 (5 and 10%) atmospheres. Error bars show the standard deviation for each compound based on three experiments.
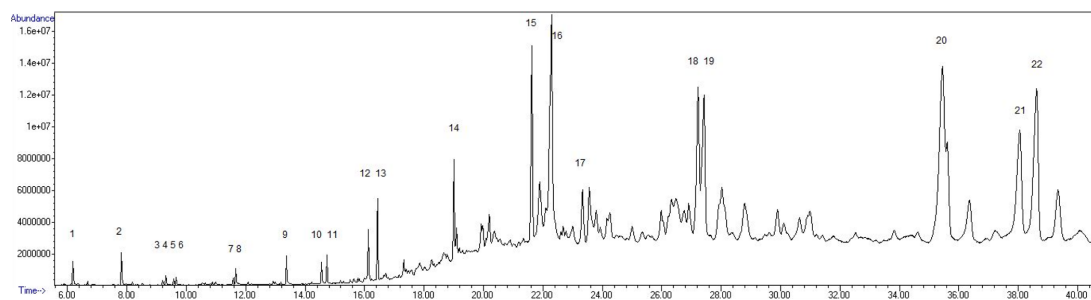

Figure 8. Spectrum showing signals from pyrolysis GC-MS of GAP at 750 °C. Abundance is shown on the *y*-axis and time on the *x*-axis.

for temperatures between 500 and 750 °C. This observation fits with the general range of boiling points for PAH-16 compounds, starting at 218 °C for Naphthalene and reaching 550 °C for Benzo[g,h,i]perylene.[17]

Table 2. Concentration of PAH Species Found in Tubes and 2-Propanol after Experiment with GAP in Argon Atmosphere[a]

PAH species	tube [μg/g]	2-propanol [μg/g]
naphthalene	0.2	31.7
acenaphthene	5.2	56.7
phenanthrene	10.0	9.5
anthracene	2.3	0.0
fluoranthene	22.9	109.7

[a]Values in 2-propanol are an average of three experiments, and results from tubes are from a single experiment.

Table 3. Detected and Identified PAH Species from Pyrolysis GC-MS of GAP at 750 °C

ID no.	species
1	Benzene
2	Toluene
3	Xylene
4	Xylene
5	Styrene
6	Xylene
7	Indane
8	Indane
9	Naphthalene
10	Naphthalene, 1-methyl-
11	Naphthalene, 2-methyl-
12	Biphenyl
13	Acenaphalene
14	Antracene/Phenanthrene
15	Fluoranthene/Pyrene
16	Aromatic, Not identified
17	Pyrene, 1-methyl-
18	Tripenylen/Benz(a)anthracene
19	Tripenylen/Benz(a)anthracene
20	Benzo(e)pyrene/Benzo(k)fluoranthene
21	Benzo(e)pyrene/Perylene/Benzo(a)pyrene
22	Benzo(e)pyrene/Perylene/Benzo(a)pyrene

This is also evident in Figure 5, where the total concentration of PAH from each temperature interval is presented.

Figure 5 also shows that the total PAH emissions level at low temperatures seem to be independent of the atmospheres tested, as the same level of emission within the standard deviation.

Influence of Atmosphere. The effect of the atmosphere on the PAH emissions is shown in more detail in Figures 6 and 7. Compared to inert atmosphere, adding 5% oxygen reduced the total PAH concentration by 65%, from 1645 μg/g to 569 μg/g. At 10% oxygen, the total PAH concentration was reduced with 75%, to 417 μg/g (Figure 6). This, seen together with the increased mass loss for the GAP sample (Figure 3), with increasing oxygen levels, indicate increased combustion of the anode paste.

With the temperatures and residence time of the experiment, 10% O_2 is not enough to achieve complete combustion of PAH emitted from GAP. High molecular weight PAHs seem to be more affected by the oxygen level than lower molecular weight PAHs, as the concentration level of four ring PAHs (fluoranthene to chrysene in Figure 6) does not change significantly when the oxygen level increase. As described by Sun[13] and Liu et al.,[14] complete combustion of PAH depends on several factors such as temperature and oxygen levels. In this

study, the seemingly stable level of four ring PAHs could be the result of combustion products from the decomposition of other HMW PAH compounds, where the insufficient temperature levels and available oxygen could lead to stabilization of the radical combustion products. The majority of the emissions from the experiments occur at temperatures of 500 °C or lower (Figure 4), where the HMW PAHs would be in a condensed state. In this state, the molecules could be susceptible to catalytic degradation in a gas—solid phase initiated by the trace elements nickel, vanadium, and iron in the GAP mixture, as described by Pujro et al.[15]

Adding CO_2 to the atmosphere did not affect the total PAH concentration significantly compared to the argon atmosphere. The total PAH concentration for atmospheres with 5 and 10% CO_2 were 1547 and 1666 μg/g, respectively (Figure 7).

The weight loss of GAP samples in CO_2 was similar to that in argon, indicating that no significant oxidation of the material occurred. This finding is contradictory to that of Chevarin et al.[8] However, in the current study, the maximum temperature was 750 °C as opposed to 960 °C, and the differences in temperature would influence the CO_2 reactivity of the anode materials; in addition the change in the levels of PAH emitted at temperatures above 500 °C could be too low for an effect to be statistically significant.

Breakthrough Test. Overall, the amount of LMW PAHs present was low for all experiments compared to the HMW species. To confirm this, a repetition of the experiment in an argon atmosphere was therefore performed to test for breakthrough of LMW PAHs from the 2-propanol in the sample collection system. It was done by connecting thermal desorption tubes with absorbent media at the end of the sampling line. Table 2 shows the results of PAHs in the tubes, compared to the average of three experiments of PAHs in 2-propanol.

Results show low amounts of the smallest PAHs (naphthalene and acenaphthene) in the tubes. Fluoranthene is detected in the greatest concentration in the tube out of the five PAHs, corresponding to the relative amounts in the 2-propanol bottles. The noticeable amount of fluoranthene in the tubes could hence be explained by evaporation of 2-propanol, containing PAHs, from sampling bottles to the tube, if the solvent was not kept at sufficiently low temperatures during the experiment. If this occurred, all species present in 2-propanol with lower boiling points than fluoranthene would also be transferred to the tube, as illustrated by data in Table 2.

Pyrolysis GC-MS. Pyrolysis of GAP at 400 and 600 °C resulted in similar pyrolytic profiles, both with few identifiable signals. Pyrolysis at 750 °C produced a species profile presented in Figure 8, corresponding to the identified species in Table 3.

Isomer PAH can not be identified as references for these compounds were not analyzed. Components are not quantified using this technique, but looking at signal abundance and area, a similar trend is shown when comparing with results from 2-propanol samples. The strongest signals originate from components antracene/phenanthrene (signal no. 14, Figure 8) and larger MW PAHs. Together, this confirms the low concentration of LMW PAHs in the 2-propanol samples, and in the tube samples, originating from the green anode paste.

Samples pyrolyzed in the alumina tube furnace produced PAH emissions in the temperature range of 400 to 600 °C (Figure 4), in contrast to the pyrolysis GC-MS experiments, and the reason behind the varying results from the two techniques could be the time of heating for the sample, where the pyrolysis

GC-MS use 1 min, while a tube furnace experiment lasts several hours (Figure 2b).

CONCLUSIONS

The effects of temperature and atmosphere on EPA-16 PAH emissions from green anode paste were investigated in a laboratory alumina tube furnace setup with off-line PAH analysis. Atmospheres tested were argon, CO_2, and O_2 with the temperature interval ranging from room temperature to 750 °C. Results show PAH emissions at the level of 1645 $\mu g/g$, and 1547 and 1666 $\mu g/g$, from inert and CO_2 atmospheres (5% and 10%). With added oxygen, concentrations decreased to 569 $\mu g/g$ and 417 $\mu g/g$ for 5% and 10% O_2, respectively, corresponding to a 65% and 75% decrease in emission. For the current setup with the given temperatures, available oxygen and species resident time, complete combustion of PAHs was not achieved. A suggestion for future work is expanding the analysis techniques for the off-gas to include gas components such as CO/CO_2 and H_2 and other VOCs to investigate the formation and destruction mechanisms of PAHs in more detail. PAHs are persistent molecules, and sufficient levels of oxygen, temperature, and residence time are needed to achieve complete combustion.

AUTHOR INFORMATION

Corresponding Author

Kamilla Arnesen — *Department of Materials Science and Engineering, Norwegian University of Science and Technology (NTNU), 7034 Trondheim, Norway;* ⊙ orcid.org/0000-0003-2259-1334; Email: kamilla.arnesen@ntnu.no

Authors

Thor Anders Aarhaug — *SINTEF Industry, 7034 Trondheim, Norway*

Kristian Etienne Einarsrud — *Department of Materials Science and Engineering, Norwegian University of Science and Technology (NTNU), 7034 Trondheim, Norway*

Gabriella M. Tranell — *Department of Materials Science and Engineering, Norwegian University of Science and Technology (NTNU), 7034 Trondheim, Norway*

Complete contact information is available at:
https://pubs.acs.org/10.1021/acsomega.3c01411

Notes

The authors declare no competing financial interest.

ACKNOWLEDGMENTS

REFERENCES

(1) Zhang, Y.; Yan, Q.; Wang, J.; Han, S.; He, R.; Zhao, Q.; Jin, M.; Zhang, R. Emission characteristics and potential toxicity of polycyclic aromatic hydrocarbons in particulate matter from the prebaked anode industry. *Science of the Total Environment* **2020**, *722*, 137546.

(2) *Decision No. 1386/2013/EU of the European Parliament and of the Council of 20 November 2013 on a General Union Environment Action Program to 2020 'Living well, within the limits of our planet' Text with EEA relevance*, 2013; http://data.europa.eu/eli/dec/2013/1386/oj/eng.

(3) Tajik, A. R.; Shamim, T.; Al-Rub, R. K. A.; Zaidani, M. *Performance Analysis of a Horizontal Anode Baking Furnace for Aluminum Production*; Muscat: Oman, 2017.

(4) Edwards, L. The History and Future Challenges of Calcined Petroleum Coke Production and Use in Aluminum Smelting. *JOM* **2015**, *67*, 308.

(5) Behrens, C.; Espeland, O.; Nenseter, B. Emissions of Dioxins and VOC's from the Årdal Carbon Plant. In *Light Metals 2007*; Minerals, Metals & Materials Society, 2007.

(6) Wittgens, B.; Panjwani, B.; Pettersen, T.; Jensen, R.; Ravary, B.; Hjernes, D. O. SCORE: Staged Combustion for Energy Recovery in Ferro-alloy Industries − Experimental Validation. *Infacon XV: International Ferro-Alloy Congress*, Cape Town, 2018.

(7) Brandvik, T.; Gaertner, H.; Ratvik, A. P.; Grande, T.; Aarhaug, T. A. In Situ Monitoring of Pit Gas Composition During Baking of Anodes for Aluminum Electrolysis. *Metallurgical and Materials Transactions B* **2019**, *50*, 950.

(8) Chevarin, F.; Lemieux, L.; Ziegler, D.; Fafard, M.; Alamdari, H. In *Light Metals 2015*; Hyland, M., Ed.; Air and CO_2 Reactivity of Carbon Anode and Its Constituents: An Attempt to Understand Dusting Phenomenon. Wiley: Hoboken, NJ, 2015; pp 1147−1152.

(9) Wilson, S. C.; Jones, K. C. Bioremediation of soil contaminated with polynuclear aromatic hydrocarbons (PAHs): A review. *Environ. Pollut.* **1993**, *81*, 229−249.

(10) Poater, J.; Duran, M.; Solà, M. Aromaticity Determines the Relative Stability of Kinked vs. Straight Topologies in Polycyclic Aromatic Hydrocarbons. *Frontiers in Chemistry* **2018**, *6*, DOI: 10.3389/fchem.2018.00561.

(11) Borosky, G. L. Theoretical Study Related to the Carcinogenic Activity of Polycyclic Aromatic Hydrocarbon Derivatives. *Journal of Organic Chemistry* **1999**, *64*, 7738−7744.

(12) Ukiwe, L.; Egereonu, U.; Njoku, P.; Nwoko, C.; Allinor, J. Polycyclic Aromatic Hydrocarbons Degradation Techniques: A Review. *International Journal of Chemistry* **2013**, *5*, 43.

(13) Sun, P. *Investigation of polycyclic aromatic hydrocarbons (PAHs) on dry flue gas desulfurization (FGD) by-products*. Ph.D. thesis, The Ohio State University, 2004.

(14) Liu, K.; Han, W.; Pan, W.-P.; Riley, J. T. Polycyclic aromatic hydrocarbon (PAH) emissions from a coal-fired pilot FBC system. *Journal of Hazardous Materials* **2001**, *84*, 175−188.

(15) Pujro, R.; Falco, M.; Sedran, U. Catalytic Cracking of Heavy Aromatics and Polycyclic Aromatic Hydrocarbons over Fluidized Catalytic Cracking Catalysts. *Energy Fuels* **2015**, *29*, 1543−1549.

(16) Petersen, L.; Dahl, C. K.; Esbensen, K. H. Representative mass reduction in sampling—a critical survey of techniques and hardware. *Chemometrics and Intelligent Laboratory Systems* **2004**, *74*, 95−114.

(17) *PubChem*; National Institute of Health, https://pubchem.ncbi.nlm.nih.gov/ (2022-03-14).

Paper IV

Characterization of Industrial Hydrocarbon Samples from Anode Baking Furnace Off-Gas Treatment Facility

Kamilla Arnesen, Alexandre Albinet, Claudine Chatellier, Nina Huynh, Thor Anders Aarhaug, Kristian Etienne Einarsrud, and Gabriella Tranell

Abstract

Polycyclic aromatic hydrocarbons (PAHs) are naturally present in raw materials used as a binder in prebaked anodes for electrolysis of aluminum. Green anodes are baked to about 1200 °C through a cycle of 14–17 days where organic hydrocarbon volatiles contribute to the carbonization process. Off-gases contain volatile and semi-volatile organic components, which are further treated to reduce environmental emissions by techniques such as regenerative thermal oxidizers and dry or wet scrubbers. Still, prebaked anode production contributes to a noticeable part of the reported PAH emissions in Norway. Samples of condensed hydrocarbon-based residues have been collected from an off-gas treatment facility and a set of analytical methods applied to determine the presence of different categories of aromatic hydrocarbons in these samples. Based on the results of the characterization, it was determined that the residue contains sulfur-substituted and polar aromatic hydrocarbons in addition to the PAH-16 routinely reported. It was concluded that future research should be dedicated to extending the range of PAHs that can be reliably determined, with particular emphasis on substituted species.

K. Arnesen (✉) · K. E. Einarsrud · G. Tranell
Department of Materials Science and Engineering, Norwegian University of Science and Technology (NTNU), Trondheim, Norway
e-mail: Kamilla.arnesen@ntnu.no

A. Albinet · C. Chatellier · N. Huynh
National Institute for Industrial Environment and Risks (INERIS), Verneuil-en-Halatte, France

T. A. Aarhaug
SINTEF Industry, Trondheim, Norway

Introduction

Primary aluminum is produced by electrolysis of alumina with carbon anodes in the Hall-Héroult process. Most modern pot lines use prebaked anodes which are a mixture of petroleum coke, anode butts, and coal tar pitch [1]. Anodes are baked in an open or closed-top baking furnace, where green anodes are stacked in pits, covered with packing coke and, heated to 1200 °C through a cycle of 14–17 days [2]. Petroleum coke originates from a crude oil refinery feedstock which will define the coke quality and structural properties. A typical anode grade calcined petroleum coke has a "sponge" structure, with up to 60% aromatic structure, containing 1.5–3.5 wt% sulfur, and traces of vanadium, nickel and iron [3, 4]. The sulfur is usually present as organic sulfur, five-membered heterocyclic rings named thiophenes, on their own, or as a part of thiophene-containing polycyclic aromatic hydrocarbons (PAHs) structures, as described by Xiao et al. [5]. Coal tar pitch has a composition of about 97% aromatic and hetero-aromatic compounds, with a great variety of structures from 128 to >2500 Daltons. The presence of derivatives such as phenols, ketones, amides, and amines are also reported, contributing to the complexity of the mixture. The off-gas from a baking furnace has been analyzed and is reported to contain CO_2, CO, CH_4, H_2, SO_X, and other volatile organic compounds, which originate from the coke and the coal tar pitch [6, 7]. Currently, in Norway, emissions from plants to air and water, are reported to the government and the priority EPA-16 PAH emissions in 2019 were 67 metric tons, where pre-baked anodes for aluminum production is one of the main contributors [8]. Off-gas treatment plants clean the gas to reduce emissions. Typical equipment to reduce airborne industry emissions are regenerative thermal oxidizers (RTO), which reduce organic matter using combustion chambers operated at about 900 °C. Other technologies used for volatile organic compounds, particulate matter and SO_2 are bag house filters, wet scrubbers, and electrostatic

precipitators, often in combination [9]. While the reported PAH-16 emissions are effectively reduced in the gas, some condensed hydrocarbon residues from anode baking furnaces build up in the off-gas treatment plants and are observed in the pipes and filters.

As there is reason to believe that these condensed residues contain aromatics soluble in aqueous solution, more specifically polar and/or sulfur-substituted aromatic compounds, a more in-depth analysis of the condensed residues was initiated. In the current work, the aim has been to identify reliable methods to firstly establish the presence of various polyaromatic compounds (PACs), and, secondly, determine the type of specie(s) associated with the solubility in various solvents mixtures and their properties.

Experimental Procedure

Industrial Facility and Sample Collection

In Fig. 1, a picture of the condensed hydrocarbon residue from an anode baking furnace off-gas cleaning facility is presented. The residue is semi-hard and tar-like, and was collected from a filter that is located after an RTO and a wet scrubber. An aqueous sample was also collected from the wet scrubber. The same residue sample was used for all characterization performed using the different techniques described below.

^{13}C-NMR Analysis

To investigate the carbon structure and functional groups present in the hydrocarbon residue nuclear magnetic resonance (^{13}C-NMR) analysis was performed. Samples were dissolved in acetone ($\geq 99.0\%$ Ph.Eur., VWR Chemicals) and methanol ($\geq 99.5\%$ GPR Rectapur, VWR Chemicals), and the extracts were filtered using white ribbon filter paper (Schleicher & Schuell Micro Science, 589/2 grade) before the solvent was removed using a rotavapor. Samples and 1-naphtalenesulfonic acid (≥ 70–<90%, Sigma Aldrich, Germany), used as a standard, were dissolved in deuterated

Fig. 1 Picture of the condensed hydrocarbon residue from an anode baking furnace off-gas cleaning facility

chloroform, and analyzed by a ^{13}C-NMR spectrometer (600 MHz Burker Avance).

ICP-MS

To quantify the sulfur content in the hydrocarbon residue, ICP-MS was used. Triplicates of the residue were prepared together with two samples of coal tar pitch, as a reference material with known sulfur content (0.53 wt%). The precise mass was measured on Sartorius balance (Krugersdorp, South Africa). Ultrapure 50% v/v nitric acid was added using a 5 mL bottle-top dispenser (Seastar Chemicals, Sidney, BC, Canada). The ultrapure nitric acid was produced at NTNU from p.a. grade nitric acid (Merck, Darmstadt, Germany) using a quartz sub-boiling distillation system (Sub-Pur, Milestone, Shelton, CT, USA). The samples were digested using a high-performance microwave reactor (UltraClave, Milestone, Italy). The digested samples were decanted into pre-cleaned 50 mL polypropylene vials (VWR, PA, USA) and diluted to approximately 26.5 mL with ultrapure water to achieve a final acid concentration of 0.6 M. The final weight of the diluted samples was measured with an analytical balance and converted to volume (density 0.6 M HNO$_3$: 1.0167 g/mL). The samples were analyzed on an Agilent 8800 Triple Quadropole ICP-MS (ICP-QQQ) with SPS 4 Autosampler. They are quantified against standards from Inorganic Ventures.

Fluorescence Spectroscopy

Fluorescence spectroscopy is a widely used technique for the detection and quantification of PACs due to the rigid molecular structure and delocalized electrons of aromatic hydrocarbons.

Calibration

1-Naphtalenesulfonic acid standard (≥ 70–<90%, Sigma Aldrich, Germany) was used as a reference material for the fluorescence measurements. The standard was dissolved in water to produce a stock solution with a concentration of 4120 ppm. Further, standards were prepared by dilution (500, 1000, and 2000 ppm). Each standard, including water and the stock solution, was analyzed by laser induced fluorescence (405 nm) using fluorescence spectroscopy (HD-1000, Advanced Sensors, Carrickfergus, UK) at the emission wavelength range between 400 and 1100 nm. The reported fluorescence signal was an average of five measurements.

Sample Preparation and Analysis

To investigate sample solubility and phase affinity of the PACs in different solvents, residue samples of 10–13 mg

were mixed with equal amounts (30 mL) of either of three different organic solvents and aqueous solutions, i.e. combinations of n-hexane, cyclohexane, and dichloromethane (HPLC, Sigma-Aldrich, Germany) and distilled water, with or without sodium hydroxide (Reag.Ph.Eur. VWR Chemicals) (NaOH) at various concentrations (1.0 M, 2.0 M, 3.0 M, and 5.0 M). In Fig. 2, an example of samples dissolved in n-hexane and increasing concentrations of NaOH are presented. Solutions were mixed for 10 or 60 min before being transferred to a separation funnel. The phases were separated, and fluorescence was measured in both phases using the HD-1000 instrument. The sample dissolution time of 10 min was performed in triplicates and 60 min dissolution was performed once.

UHPLC-Fluorescence/UV and UHPLC-HRMS Analysis

Sample Preparation and Analysis

The analysis of 22 PAHs in the residue and wet scrubber samples has been performed by ultra-high-performance liquid chromatography (UHPLC)-fluorescence, while the presence of potential sulfate- or sulfonate-PAHs (SO_3-PAHs) has been evaluated using a non-targeted screening (NTS) approach and based on UHPLC-high-resolution mass spectrometry (HRMS) analyses.

Prior to extraction internal standard (6-methlychrysene) was added to the samples to evaluate the recovery rate of PAHs. Solid samples were extracted by sonication in toluene (HPLC, Aldrich), for PAHs, or methanol (HPLC, Aldrich) for NTS evaluation of SO_3-PAHs. Aqueous samples were filtrated before liquid/liquid extraction by toluene for PAH analyses. An additional pre-concentration step using an HLB (hydrophilic–lipophilic balanced) solid-phase extraction (SPE) cartridge (Waters, Oasis, HLB SPE), eluted in two

steps with methanol and acidified methanol, was applied of SO_3-PAHs. The resulting extracts (Fig. 3) were diluted in acetonitrile (HPLC, Aldrich) before injection on UHPLC-fluorescence (Ultimate 3000, ThermoFisher) for PAH analyses using a C18 UPLC column (Zorbax). Sample extracts were diluted in Milli-Q water (Millipore) before NTS analysis by UHPLC-HRMS of SO_3-PAHs (UHPLC 1290 Infinity coupled to a Quadrupole-Time of Flight, IFunnel 6550 (Agilent)) using electrospray ionization (ESI) in negative mode and acquisition in auto MS/MS. Separation was achieved using an HSS T3 column (C18, Waters). The presence of potential SO_3-PAHs was based on specific fragmentation patterns and characteristic fragments, namely SO_3^- (m/z 79.9559) and HSO_4^- (m/z 96.9607) fragments [10]. Thirteen commercially available sulfate or sulfonate organic analytical standards were analyzed to study their fragmentation patterns. Additional suspect screening analyses were also performed targeting these compounds as well as based on theoretical m/z of sulfates and sulfonates corresponding to the quantified PAHs in the samples.

Results and Discussion

^{13}C-NMR Analysis

Figure 4 shows the ^{13}C-NMR chemical shift for the sample dissolved in acetone. Three areas in the spectra are noticeable, where one coincides with deuterated chloroform, at 77 ppm, used as a solvent for the extract during analysis. The signals between 0 and 40 ppm indicate the presence of aliphatic carbon and signals at 110–150 ppm originate from aromatic carbon species [11]. It is not possible to determine if the aliphatic carbons are separate components or attached as side chains on an aromatic structure.

Fig. 2 A series with sample dissolved in n-hexane and increasing concentration of NaOH (left to right: Water, 1.0 M, 2.0 M, 3.0 M, and 5.0 M). Organic phase is on the top and aqueous is on the bottom of the flask
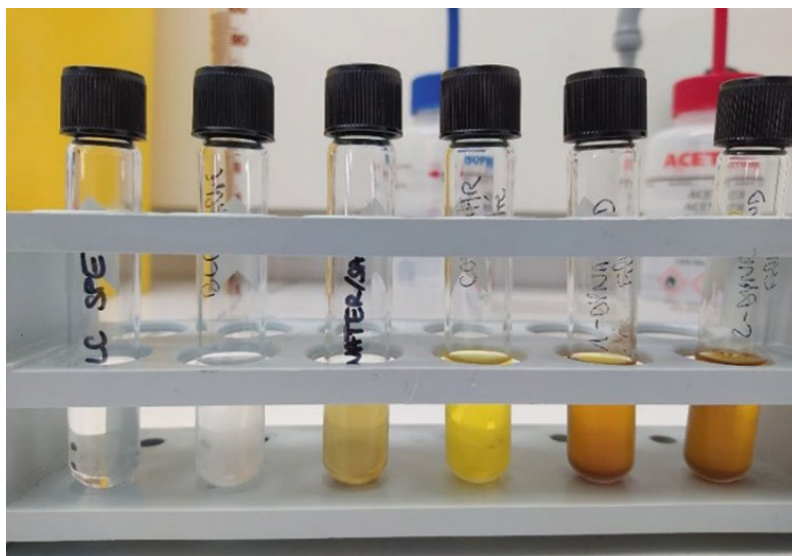
Fig. 3 Extracts for LC-HRMS analyses of the different samples (left to right: solid-phase extraction blank, sonication blank, aqueous, coal tar pitch, Residue-1, Residue-2)
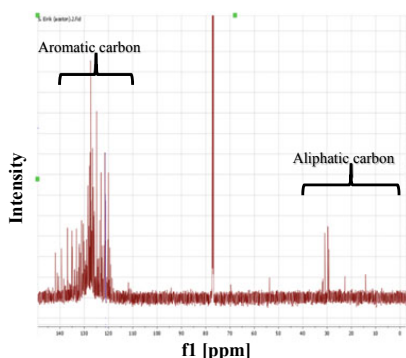

Fig. 4 ^{13}C-NMR chemical shift (ppm) for the condensed sample dissolved in acetone. Deuterated chloroform is used as a solvent during analysis, displayed as the signal at 77 ppm
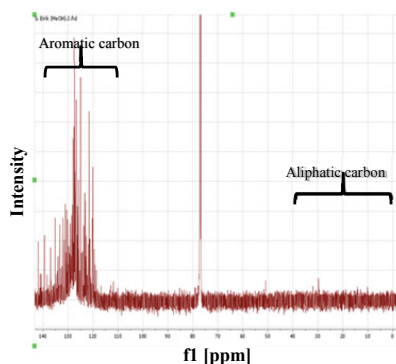

Fig. 5 ^{13}C-NMR chemical shift (ppm) for the condensed sample dissolved in methanol. Deuterated chloroform is used as a solvent during analysis, displayed as the signal at 77 ppm

Figure 5 shows the chemical shift for the sample dissolved in methanol. In addition to the deuterated chloroform at 77 ppm, only the signals from aromatic carbons are present at 110–150 ppm. This may indicate the different properties of the organic solvent influence on which hydrocarbon groups are dissolved. Methanol is a more polar solvent than acetone, which would indicate why the aliphatic carbon is absent from the methanol extract. Aromatic carbon species such as PAH are nonpolar compounds and are generally lipophilic.

Compounds such as benzo[a]pyrene are reported to be sparingly soluble in methanol [12]. This could indicate the presence of other polyaromatic compounds with polar properties, such as heterocycles, alkylated, and substituted PACs [13]. In Fig. 6, the chemical shift from 1-naphtalenesulfonic acid is presented. A signal is visible in the area for aromatic carbon, but as the compound has low solubility in chloroform, the signal is not particularly strong.
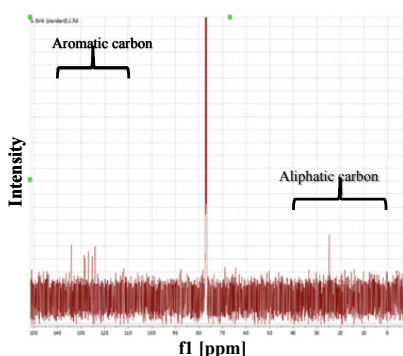
Fig. 6 ^{13}C-NMR chemical shift (ppm) for 1-naphtalenesulfonic acid standard ($\geq$ 70–< 90%). Deuterated chloroform is used as a solvent during analysis, displayed as the signal at 77 ppm

Table 1 Sulfur concentration in residue sample and coal tar pitch from ICP-MS analysis

Sample	S (mg/g)	RDS (%)
CTP 1	4.94	0.9
CTP 2	4.86	1.9
Residue 1	9.42	2.1
Residue 2	9.27	2.0
Residue 3	9.77	1.1
Residue average	9.49	

ICP-MS

Table 1 shows the total concentration of sulfur in the residue sample analyzed by ICP-MS. The average concentration of sulfur is 9.49 mg/g, which is more than in the coal tar pitch raw material used in the anode and could be an indication of an accumulation of sulfur species in the off-gas treatment plant.

Fluorescence Spectroscopy

Calibration

The calibration curve was made using 1-naphtalenesulfonic acid (Fig. 7), as a reference for a possible aromatic species present in the residue sample. The curve is linear in the area between 0 and 4000 ppm, and the fluorescence intensity is between 0.25 and 0.85% based on the pre-programmed calibration of the instrument. In comparison, the intensity of the fluorescence signal from the residue sample could be up to 90 times higher than the concentrations measured for the calibration curve. Not being able to guarantee the continued linearity of the calibration curve, the fluorescence signal was
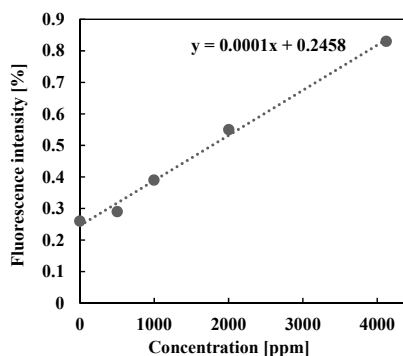

Fig. 7 1-Naphtalenesulfonic acid standard ($\geq$ 70–<90%) fluorescence emission calibration curve. Excitation wavelength at 405 nm and emission wavelengths between 400 and 1100 nm

normalized based on high and low values within the dataset and not reported as an absolute concentration.

Measurements Using the Industrial Residue Sample

The fluorescence spectra were obtained continuously after the aqueous and organic phases were separated for each sample. The fluorescence signal is an average of five measurements in each solution and has been normalized to compare solubility of the residue sample and the interactions of the dissolved PACs with the organic and aqueous solvents. Figure 8 shows the fluorescence signal in the aqueous phase with different concentrations of NaOH after the
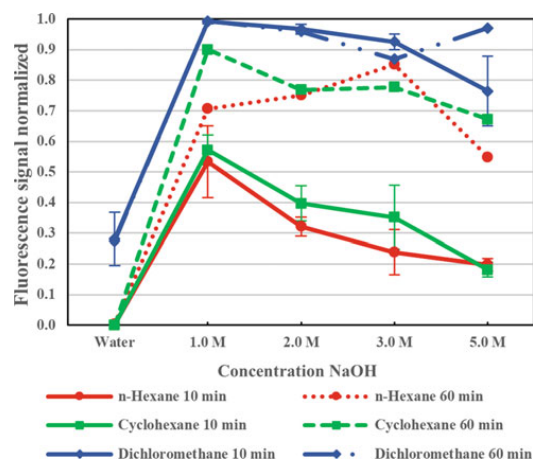

Fig. 8 Normalized fluorescence signal from PACs in the aqueous phase after 10 and 60 min sample dissolution time. Excitation wavelength at 405 nm and emission wavelengths between 400 and 1100 nm. Measurements after 10 min are an average of triplicate tests

sample solution has been mixed for 10 and 60 min.

Both the type of organic solvent and the concentration of sodium hydroxide influence the fluorescence signal from PACs distributed between the two phases. The intensity varies with the type of organic solvent, indicating that the polar dichloromethane is a more effective solvent for the condensed hydrocarbon sample. N-Hexane and cyclohexane have comparable solvent properties, which may result in similar interaction with the dissolved hydrocarbons and explain the overlapping signals for the two solvents. Another overall trend is an increase in fluorescence when the sample is dissolved in an aqueous solution containing NaOH. The addition of hydroxyl ions can react with already dissolved aromatic hydrocarbons, creating aromatic hydrocarbon salts by oxidation, or an acid–base reaction [14]. This reaction would increase the water solubility of the aromatic compounds explaining the increased fluorescence compared to pure water. In addition to being an oxidizing agent, the high-energy vibrations of the hydroxyl ion have been reported to have a quenching effect on the fluorescence emissions, which could explain the decreasing fluorescence signal with increasing NaOH concentration above 1.0 M [15]. Griffiths and Mama also reported on the shift in the fluorescent absorption band when tri-anionic species was produced with increasing pH when looking at the pH-dependency on hydroxyaryl-squarylium dyes [16]. The tests with 60 min dissolution time were performed once, so some uncertainty within the result series may be expected. Overall, the trends are similar to the shorter solubility time, except the signals are somewhat increased. This indicates, especially for n-hexane and cyclohexane, that solubility of the residue could increase with time.

Figure 9 shows the corresponding measurements to Fig. 8, where fluorescence is measured in the organic phase of the sample dissolved in organic solvents and aqueous solutions with varying concentrations of NaOH for 10 and 60 min. Also here, dissolution in dichloromethane results in a stronger fluorescence signal from the aromatic compounds, compared to both cyclohexane and n-hexane. The concentration of NaOH does not seem to affect the distribution of compounds between the two phases.

UHPLC-Fluorescence/UV and UHPLC-HRMS Analysis

Total PAH concentrations (Σ_{22} PAHs) observed were similar in both residue samples (about 160 µg/g) and about 1.6 times higher than in the coal-tar-pitch raw material (about 95 µg/g). The aqueous sample showed concentrations of about 210 ng/ml. Chemical profiles obtained were similar for both residue samples, while higher contributions of heavier PAHs (≥ 5 cycles) were observed for the coal tar
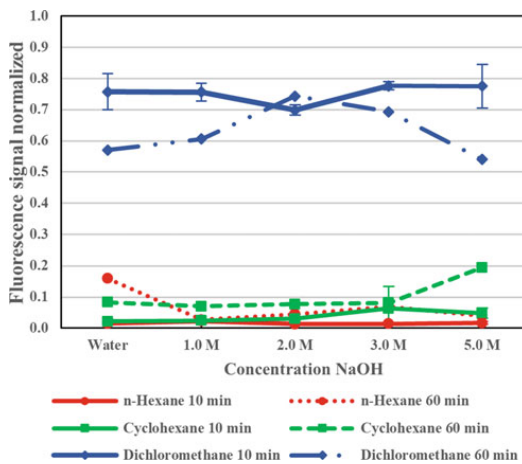

Fig. 9 Normalized fluorescence signal from PACs in the organic phase after 10 and 60 min sample dissolution time. Excitation wavelength at 405 nm and emission wavelengths between 400 and 1100 nm. Measurements after 10 min are an average of triplicate tests

pitch sample. On the opposite, the aqueous sample is dominated by lighter PAH compounds (≤ 4 cycles) which are known to be more water-soluble (Fig. 10).

NTS analyses showed characteristic SO_3^- and/or HSO_4^- fragments highlighting the presence of sulfate or sulfonates organic species in all the samples. The same potential organic sulfate was detected in all the solid samples. For the aqueous sample, two organic sulfonates and one organic sulfate were detected (Fig. 11). Molecular formula calculations (including C, H, O, and S atoms) and confrontation with an in-silico fragmentation tool highlighted potential aromatic sulfonates structures (30/43 and 9/12 of the structures proposed were aromatic sulfonates) [17]. Based on suspect screening analyses, none of the standard sulfate or sulfonate organic compound available was detected in any of the samples. Suspect screening based on theoretical m/z of SO_3-PAHs highlighted the presence of methylnaphthalene sulfate in the aqueous sample.

In summary, the methods used to characterize the industrial residue sample each give different insights into the properties of the condensed off-gas treatment residue. ^{13}C-NMR analysis showed the presence of both aromatic and aliphatic hydrocarbons, in addition to a dependency on solvent properties, as the aliphatic hydrocarbons were only present in the extract using a non-polar solvent. Further characterization using fluorescence spectroscopy confirmed a phase affinity of the aromatic species. The most effective environment for dissolving the sample, both for the aqueous and organic solution with 1.0 M NaOH and dichloromethane, respectively. Dichloromethane is a polar solvent, confirming that the sample contains polar aromatic species,
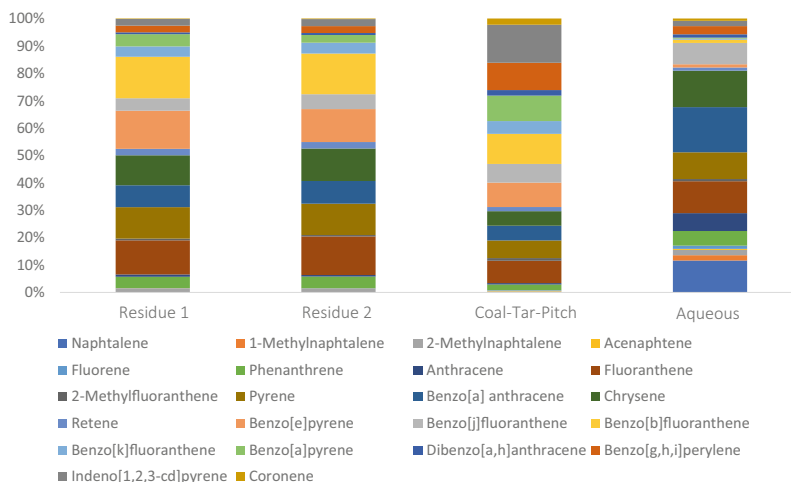
**Fig. 10** Distribution of the quantified parent PAH in the different samples
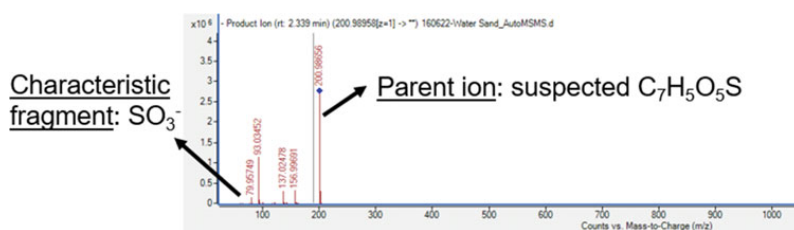
Fig. 11 Example of aromatic sulfonate (probable SO$_3$-PAH) detected in the aqueous sample

which are not present in coal tar pitch and coke, reflecting the complexity of the condensed residue, compared to the raw materials used in the production of pre-baked anodes. The presence of sulfate and sulfonate organic species was confirmed in the hydrocarbon residue and aqueous sample. Polar aromatic hydrocarbons are outside the scope of conventional PAH-16 analysis, but to understand the nature of complex PAH emissions, further research should be dedicated to extending the range of standard methods and techniques to analyze for such species.

Conclusions and Further Work

A multi-method study of condensed hydrocarbon residues from an aluminum anode baking off-gas cleaning facility was carried out in order to determine their content with particular emphasis on polar and/or sulfur-substituted PACs outside the conventional PAH-16 range. The following conclusions were drawn:

- ^{13}C-NMR and fluorescence spectroscopy analysis of the industrial residue confirmed the presence of both polar aromatic and aliphatic compounds in the sample.
- ICP-MS analysis found sulfur species in the residue related to the anode raw materials.
- Substituted PAH (at least aromatic species) with sulfate and/or sulfonate moieties (SO$_3$-PAHs) were highlighted by NTS approach based on ULPC-HRMS analyses.

Given the analytical evidence seen together, it was suggested that the presence of polar aromatic hydrocarbons in the condensed residues, with properties unlike traditional PAH, are due to alkylation and/or substitution reactions occurring during the anode production or in the off-gas cleaning facility. Further experimental work to shed light on their formation, in parallel with analytical method development is suggested.

References

1. E. H. M. Moors, "Technology strategies for sustainable metals production systems: a case study of primary aluminium production in The Netherlands and Norway," *J. Clean. Prod.*, Jan. 2006, doi: https://doi.org/10.1016/j.jclepro.2004.08.005.

2. T. Brandvik, Z. Wang, A. P. Ratvik, and T. Grande, "Autopsy of refractory lining in anode kilns with open and closed design," *Int. J. Appl. Ceram. Technol.*, 2019, doi: https://doi.org/10.1111/ijac.13108.

3. L. Edwards, "The History and Future Challenges of Calcined Petroleum Coke Production and Use in Aluminum Smelting," *JOM*, Feb. 2015, doi: https://doi.org/10.1007/s11837-014-1248-9.

4. M. Legin-Kolar and D. Ugarković, "Petroleum coke structure: Influence of feedstock composition," *Carbon*, Jan. 1993, doi: https://doi.org/10.1016/0008-6223(93)90043-A.

5. J. Xiao, Q. Zhong, F. Li, J. Huang, Y. Zhang, and B. Wang, "Modeling the Change of Green Coke to Calcined Coke Using Qingdao High-Sulfur Petroleum Coke," *Energy Fuels*, May 2015, doi: https://doi.org/10.1021/acs.energyfuels.5b00021.

6. T. Brandvik, H. Gaertner, A. P. Ratvik, T. Grande, and T. A. Aarhaug, "In Situ Monitoring of Pit Gas Composition During Baking of Anodes for Aluminum Electrolysis," *Metall. Mater. Trans. B*, Jan. 2019, doi: https://doi.org/10.1007/s11663-018-1500-8.

7. Q. Zhong, J. Xiao, H. Du, and Z. Yao, "Thiophenic Sulfur Transformation in a Carbon Anode during the Aluminum Electrolysis Process," *Energy Fuels*, Apr. 2017, doi: https://doi.org/10.1021/acs.energyfuels.6b03018.

8. Norwegian Environmental Agency, "Polysykliske aromatiske hydrokarboner (PAH)," *Miljøstatus*. https://miljostatus.miljodirektoratet.no/tema/miljogifter/prioriterte-miljogifter/polysykliske-aromatiske-hydrokarboner-pah/ (accessed Oct. 01, 2021).

9. C. Behrens, O. Espeland, and B. Nenseter, "EMISSIONS OF DIOXINS AND VOC'S FROM THE ÅRDAL CARBON PLANT," p. 7, 2007.

10. M. Riva *et al.*, "Evidence for an Unrecognized Secondary Anthropogenic Source of Organosulfates and Sulfonates: Gas-Phase Oxidation of Polycyclic Aromatic Hydrocarbons in the Presence of Sulfate Aerosol," *Environ. Sci. Technol.*, Jun. 2015, doi: https://doi.org/10.1021/acs.est.5b00836.

11. S. Farmer, T. Soderberg, C. P. Schaller, and L. Morsch, "6.8: Principles of ^{13}C NMR Spectroscopy," *Chemistry LibreTexts*, Jul. 09, 2020. https://chem.libretexts.org/ (accessed Sep. 13, 2022).

12. M. Windholz, S. Budavari, R. F. Blumetti, and E. S. Otterbein, *The Merck index: an encyclopedia of chemicals, drugs, and biologicals*, 10th ed. Rahway, N.J: Merck & Co, 1983.

13. J. T. Andersson and C. Achten, "Time to Say Goodbye to the 16 EPA PAHs? Toward an Up-to-Date Use of PACs for Environmental Purposes," *Polycycl. Aromat. Compd.*, Mar. 2015, doi: https://doi.org/10.1080/10406638.2014.991042.

14. I. J. Keyte, R. M. Harrison, and G. Lammel, "Chemical reactivity and long-range transport potential of polycyclic aromatic hydrocarbons – a review," *Chem. Soc. Rev.*, vol. 42, no. 24, pp. 9333–9391, Nov. 2013, doi: https://doi.org/10.1039/C3CS60147A.

15. J. Maillard, K. Klehs, C. Rumble, E. Vauthey, M. Heilemann, and A. Fürstenberg, "Universal quenching of common fluorescent probes by water and alcohols," *Chem. Sci.*, 2021, doi: https://doi.org/10.1039/D0SC05431C.

16. J. Griffiths and J. Mama, "pH-dependent absorption and fluorescence spectra of hydroxyaryl-squarylium dyes," *Dyes Pigments*, Dec. 1999, doi: https://doi.org/10.1016/S0143-7208(99)00073-X.

17. C. Ruttkies, E. L. Schymanski, S. Wolf, J. Hollender, and S. Neumann, "MetFrag relaunched: incorporating strategies beyond in silico fragmentation," *J. Cheminformatics*, Jan. 2016, doi: https://doi.org/10.1186/s13321-016-0115-9.

NTNU

Norwegian University of
Science and Technology